1

2

TerrainWorks

Wetland Intrinsic Potential: A Screening Tool for Detecting Wetlands in Forested and Non-Forested Environments

Lee Benda, Kevin Andras and Daniel Miller
Mt Shasta, CA/Seattle, WA

1

Contents

List of Figures

List of Tables

Executive Summary

Work reported here is part of Phase 1 of the "Wetlands Mapping Predictive Model Project"; a CMER-WETSAG[1] sponsored study in conjunction with the University of Washington Remote Sensing and Geospatial Analysis Laboratory.

We present a screening tool to detect likely wetland locations in forested and non-forested settings in the Pacific Northwest. Based on understanding of the hydrogeomorphic processes that create wetlands, this tool uses remotely sensed data with a Geographic Information System (ArcGIS) to identify physical conditions potentially conducive for wetland development. These physical conditions may include attributes of topography, geology, soils, vegetation, land cover, and climate. This tool seeks to differentiate those locations that have high intrinsic potential for wetland development from those that have low intrinsic potential. Thus, we refer to it as the 'Wetland Intrinsic Potential' (WIP) tool.

On-the-ground physical conditions are inferred using hydrogeomorphic indicators. For this implementation of the WIP tool, we use five hydrogeomorphic indicators to determine wetland intrinsic potential:

1) depth to water table near streams and rivers,
2) depth to water table near lakes and ponds,
3) relative depth of closed depressions,
4) depth to an impermeable layer, and
5) a climate-topographic wetness index.

These indicators are thought to reflect physical controls on wetland formation. Indicator values are derived from a digital elevation model (DEM), regional climate data (mean annual precipitation), and regional soils or geologic data. Other indices could be incorporated into future versions of WIP, including local relief to delineate poorly-drained areas and models of surface erosion and deposition to detect low-permeability areas associated with sediment accumulation.

The combination of hydrogeomorphic indicators at any location (i.e., a DEM pixel[2]) are used to define a wetland intrinsic potential for that location. This is done by defining suitability curves that link each indicator value to an estimated likelihood of wetland development. These curves vary from zero to one and their shape reflects expectations of how the value of the hydrogeomorphic indicator affects potential for wetland development. For example, low topographic-wetness-index values are associated with dryer soils; high values are associated with wetter soils. So, the suitability curve for the topographic wetness index is near zero for low index values and near one for high index values. Suitability curves are

[1] CMER is the Cooperative Monitoring, Evaluation and Research committee established by the Washington Forest Practices Board. WETSAG is the CMER Wetlands Scientific Advisory Group.

[2] Individual elements in raster data are typically referred to as "cells" for DEMs, and as "pixels" for optical and multispectral imagery. We use the pixel in this report.

defined as piece-wise continuous linear functions with values based on the judgement and experience of the person building the curve.

The suitability-curves are then combined to provide a wetland-intrinsic-potential value that varies from zero to one, with larger values indicating greater potential for wetland formation. Any combination of hydrogeomorphic indicators may be used, ranging from only one (e.g., the climate-topographic wetness index) to all five. A variety of methods may be used to combine the suitability curves; for this study, we used a logistic function.

Within the study area, hydrogeomorphic indicators, suitability curve values, and a wetland intrinsic potential value are calculated pixel-by-pixel over a DEM. Results of the pixel-based intrinsic-potential model are then filtered and aggregated to provide polygons delineating areas with similar WIP values. NAIP[3]-NDVI[4] imagery is used to identify and remove non-vegetated areas, which we assume to be lacking soil, including active alluvial channels, bedrock, talus, and human infrastructure. Other filtering includes removal of: 1) closed depressions that do not meet a minimum size threshold, 2) pixels within active channels, 3) channel-adjacent areas that are too narrow to qualify as a wetland of concern, and 4) groups of pixels in non-channel areas that do not meet a minimum wetland size threshold.

The WIP tool was applied to two U. S. Geological Survey 6th-field Hydrologic Unit Basins[5] (HUC) in the Puyallup River watershed as a demonstration. The tool produces high WIP scores (> 0.6) indicating likely wetlands in several geomorphic settings: 1) adjacent to lakes and ponds, 2) within wide forested riverine corridors, 3) along wide, unconstrained valley floors, 4) at and near large tributary confluences, and 5) along abandoned, historical river valleys. The occurrence of actual wetlands coinciding with high WIP scores was confirmed in many locations where wetlands were visible in NAIP imagery. In some areas, high WIP scores were not included in the National Wetland Inventory[6] (NWI) wetlands. In other cases, WIP identified potential wetland extent considerably larger than NWI polygons. The frequency distribution of WIP scores within NWI polygons (n=253) and outside of NWI polygons were significantly different, indicating that NWI wetlands had hydrogeomorphic features different than non NWI areas. NWI polygons covered 1.6% of the 225 km^2 study watershed, whereas high WIP scores (> 0.6) covered 3.5%. A comparison of the overlap between clumps of high WIP scores (indicating likely wetland formation) and NWI polygons across the upper (forested) and lower (urban and rural farm land) portions of the basin revealed good agreement. However, there appear to be numerous NWI polygons in the lower basin that do not correspond to wetlands on the ground.

---

[3] National Agriculture Imagery Program: https://www.fsa.usda.gov/programs-and-services/aerial-photography/imagery-programs/naip-imagery

[4] Normalized Difference Vegetation Index: see http://www.waurisa.org/conferences/2012/presentations/11%20Chris%20Behee%20Vegetation%20Modeling%20with%20NAIP%20Color%20IR%20Imagery.pdf

[5] See the Watershed Boundary Dataset page: https://nhd.usgs.gov/wbd.html

[6] https://www.fws.gov/wetlands/

WIP could be calibrated to adjust suitability curves and weightings to improve WIP model performance, but would require a comprehensive wetland inventory, particularly under forest canopy. Such a dataset does not currently exist (model calibration is planned for Phase 2).

The eight analytical steps in WIP are contained within a stand-alone ArcMap interface that requires inputs of: 1) DEMs (LiDAR recommended), 2) NHD[7] lakes, 3) mean annual precipitation (PRISM[8]), 4) NAIP-NDVI, and 5) optionally; soils/geology data for soil transmissivity and presence of impermeable layers. Adjustable parameters in the WIP tool include the hydrogeomorphic suitability curves, weighting terms, NDVI filter thresholds, closed-depression size thresholds, and minimum wetland size.

WIP can be used in any watershed with appropriate data layers to develop a remote-sensing-based screening of the probable extent and distribution of wetlands. WIP could be used as a screening tool to inform and prioritize field surveys related to regulatory applications involving land uses, including forestry activities. The tool could also be used to support other wetland research activities. WIP pixels can be combined into provisional wetland polygons using software such as ArcMap or eCognition. WIP can also be integrated within other statistical modeling approaches, with WIP values used as an additional independent variable.

The WIP model identifies areas with conditions conducive to wetland formation. It assumes that areas where wetlands are likely to form can be identified using a suite of hydrogeomorphic indicators derived from digital elevation models and data on soils, geology, vegetation, and climate. An advantage of the WIP approach is that it does not require prior field investigations: it relies solely on remotely sensed digital data. It may also identify areas where wetlands could exist, but do not because, for example, they have been drained or their water source removed. WIP translates conceptual models about how wetlands form to maps showing the (hypothesized) likelihood of finding a wetland. The disadvantage of the WIP approach is that such maps cannot be interpreted as actual wetland locations without verifying data. WIP provides a method to use information we do have (topography, climate), with the knowledge, judgement, and experience of the person using the model, to form a quantitative hypothesis about information we do not have – wetland locations. Once field data on wetland locations is collected, it can be compared to the WIP model outputs to test conceptual models of how wetlands form and to improve WIP model predictions. Field data will also allow use of standard statistical techniques seeking correlations between remotely sensed attributes and wetland locations; the WIP model will help to identify hydrogeomorphic indicators to include in those statistical analyses.

[7] National Hydrography Dataset: https:\\nhd.usgs.gov

[8] PRISM Climate Group: prism.oregonstate.edu

1

2

Wetland Intrinsic Potential: Screening Tool for Detecting Wetlands in Forested and Non-Forested Environments

1. Introduction

Wetlands are an important natural environment providing many ecological functions, including enhanced water storage, flood control, erosion control, water quality, water supply, wildlife habitat, and recreation opportunities. Wetlands go by a variety of names, including 'marshes', 'swamps', 'bogs, 'potholes', and 'fens', and are, by definition, areas where water covers the surface for all or part of a year or is present very near the ground surface, leading to saturated soils and water-tolerant plants. It is estimated that since the 1780s, the lower 48 states of the U.S. have lost over 50% of wetland environments due to land use (Dahl 1990). Hence, there is increasing interest to protect the remaining wetlands and to restore wetland functions in certain locations.

Wetlands are common in watersheds of the Pacific Northwest, with many wetlands occurring in forested areas where they may be mostly obscured by forest canopy. To best manage and protect wetlands during land uses, including urbanization, agriculture, timber harvest and road construction, it is necessary to know where wetlands are located. Although field surveys of wetlands are the best way to detect and map them, such surveys are difficult and expensive to apply across large watersheds with dense forests (Silva et al. 2008).

In the context of forestry activities in Washington, the Cooperative Monitoring, Evaluation and Research (CMER) Committee established a wetland advisory group (WETSAG) to review the science of wetlands in forested landscapes, including the potential impacts from forest practices (Cooke et al. 2005, Adamus 2014). As part of this effort, WETSAG is sponsoring research to detect and map likely wetland areas in forested watersheds in collaboration with the Washington Department of Ecology, Washington Department of Natural Resources, the Remote Sensing and Geospatial Analysis Laboratory at the University of Washington, and TerrainWorks.

The CMER project 'Wetlands Mapping Predictive Model Project', sponsored by WETSAG and described in this report, is designed to be done in two phases. Phase 1 will create a tool for detecting and mapping the hydrological and geomorphological controls on wetland occurrence in Pacific Northwest forested watersheds. The 'Wetlands Intrinsic Potential' (WIP) tool will utilize remote-sensing data, including the highest-resolution digital-elevation models (e.g., LiDAR) and other digital data layers including soils, geology, and multi-spectral aerial imagery. WIP is designed to detect the hydrologic and geomorphic controls on water movement and storage related to 1) topographic depressions, 2) stream/river – depth to water table, 3) lake/pond – depth to water table, 4) topographic, soils, and precipitation controls on subsurface and surface water movement, and 5) impervious layers. In addition, Phase-1 WIP can provide inputs for object-based image analysis, involving image segmentation and classification using software

such as eCognition[9]. Phase 2 of the study is planned to use field data on wetland locations to calibrate WIP to improve model performance and to develop statistical tools for predicting wetland location.

This report presents the results from Phase 1 of WETSAG's development of a wetland-potential screening tool for forested environments. The Puyallup River watershed, located in the Puget Sound of Washington, was chosen to demonstrate the model.

2. Types of Wetlands and their Hydrogeomorphic Controls

Wetlands must have one or more of the following three environmental characteristics: 1) covered by water for all or part of a year (< 6.6 feet), 2) substrate chemistry reflecting frequently saturated conditions (hydric soils), and 3) a plant community dominated by hydrophytes (Cowardin et al. 1976, 1979). Wetlands can also be characterized strictly by their hydrologic and geomorphic controls, referred to as a 'hydrogeomorphic' classification (Brinson 1993, et al. 1997). Hydrogeomorphic wetland classes include (**Figure 1, Table 1**):

1. Riverine
2. Depression
3. Slope
4. Mineral soil flats
5. Organic soil flats
6. Estuarine fringe
7. Lacustrine fringe

Wetlands in forested environments are associated with the full range of channel morphology types, from colluvial channels in headwater areas to low-gradient, alluvial rivers and the transition area in between (**Figure 2**). Riverine wetlands, in larger (non-headwater) channels, can include: closed-depression wetlands (back swamps) and other fluvial-related wetlands, such as abandoned side channels and meanders (oxbows). Headwater-stream-associated wetlands (Creed et al. 2003) may arise due to lateral and vertical subsurface or hyporheic flow, driven by discontinuities in valley gradients and valley widths, and slope–seeps located near channel heads. Subsurface flow along unchanneled valleys or swales that intersect channels can also contribute to wetland formation. Different wetland types may overlap and grade into one another, and wetlands may have multiple hydrogeomorphic controls (Table 1). For example, a riverine backwater may be located near a river water table, adjacent to a hillslope providing concentrated subsurface flow and be situated on top of a shallow impermeable layer.

[9] http://www.ecognition.com/

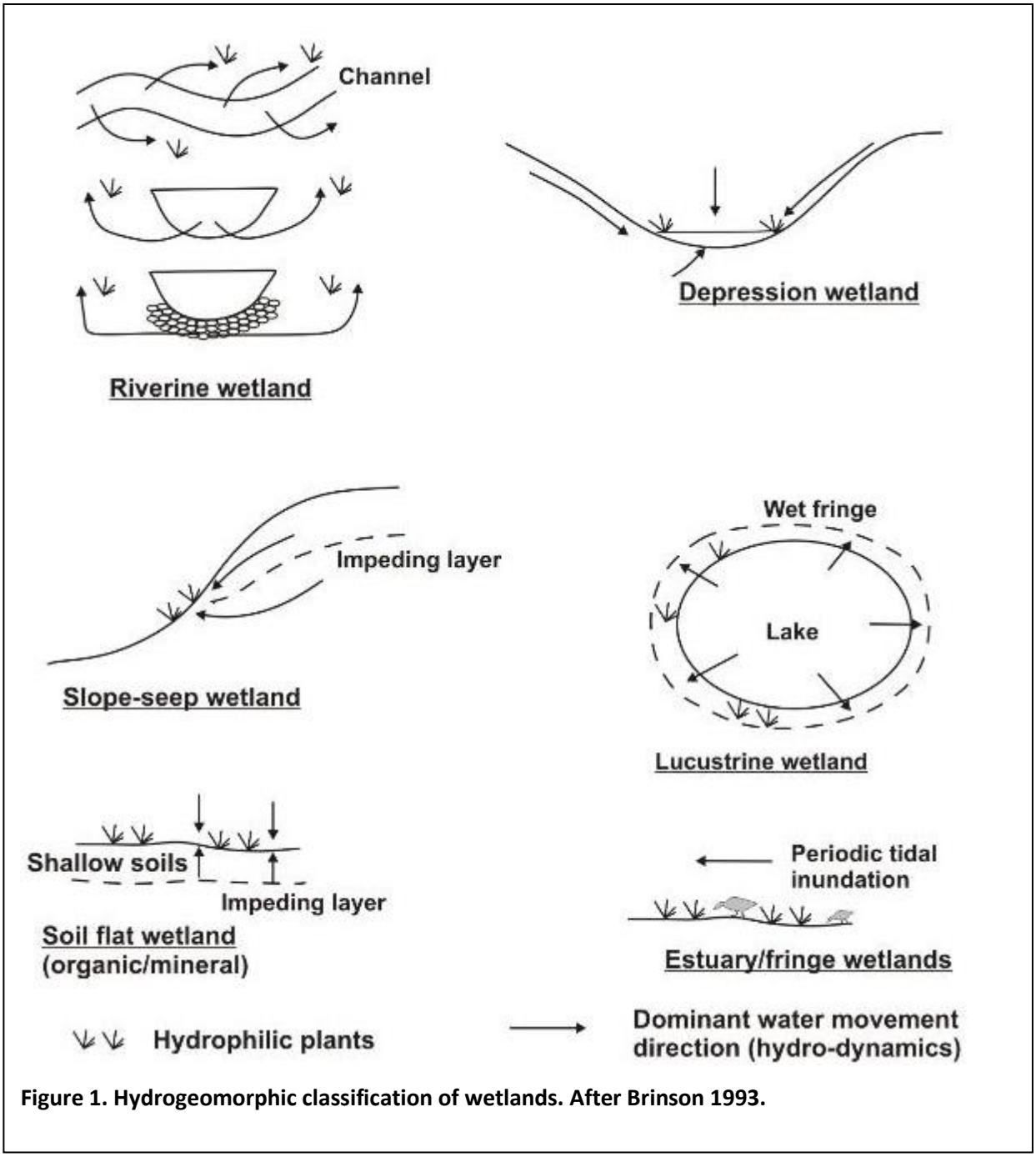

Figure 1. Hydrogeomorphic classification of wetlands. After Brinson 1993.

1

Table 1. Dominant water sources and hydrodynamics of wetland types in WIP.

Wetland Type[1]	Hydrogeomorphic setting	Dominant hydrodynamics[2]
Riverine	Point bar and natural levee deposits within floodplains and low terraces; back swamps; other fluvial depressions, oxbows, abandoned channels	Overbank flow and hyporheic flow
Depression	Abandoned channels (riverine), inverted topography – earthflow terrain- sag ponds; glacial melt features; other	Groundwater, shallow subsurface flow, precipitation
Slope seep	Heads of small streams, permeable/impermeable stratigraphy intersecting ground surface	Groundwater, shallow subsurface flow, permeable/impermeable exposures/outcrops, channel heads
Soil flat	Relatively low-gradient areas with poor drainage due to organic or mineral buildup	Groundwater, precipitation
Lacustrine fringe	Margins of natural and man-made lakes, including adjacent depressions and flats	Lake overbank flow, shallow subsurface flow

[1] After Brinson 1993.

[2] Wilder et al. 2013.

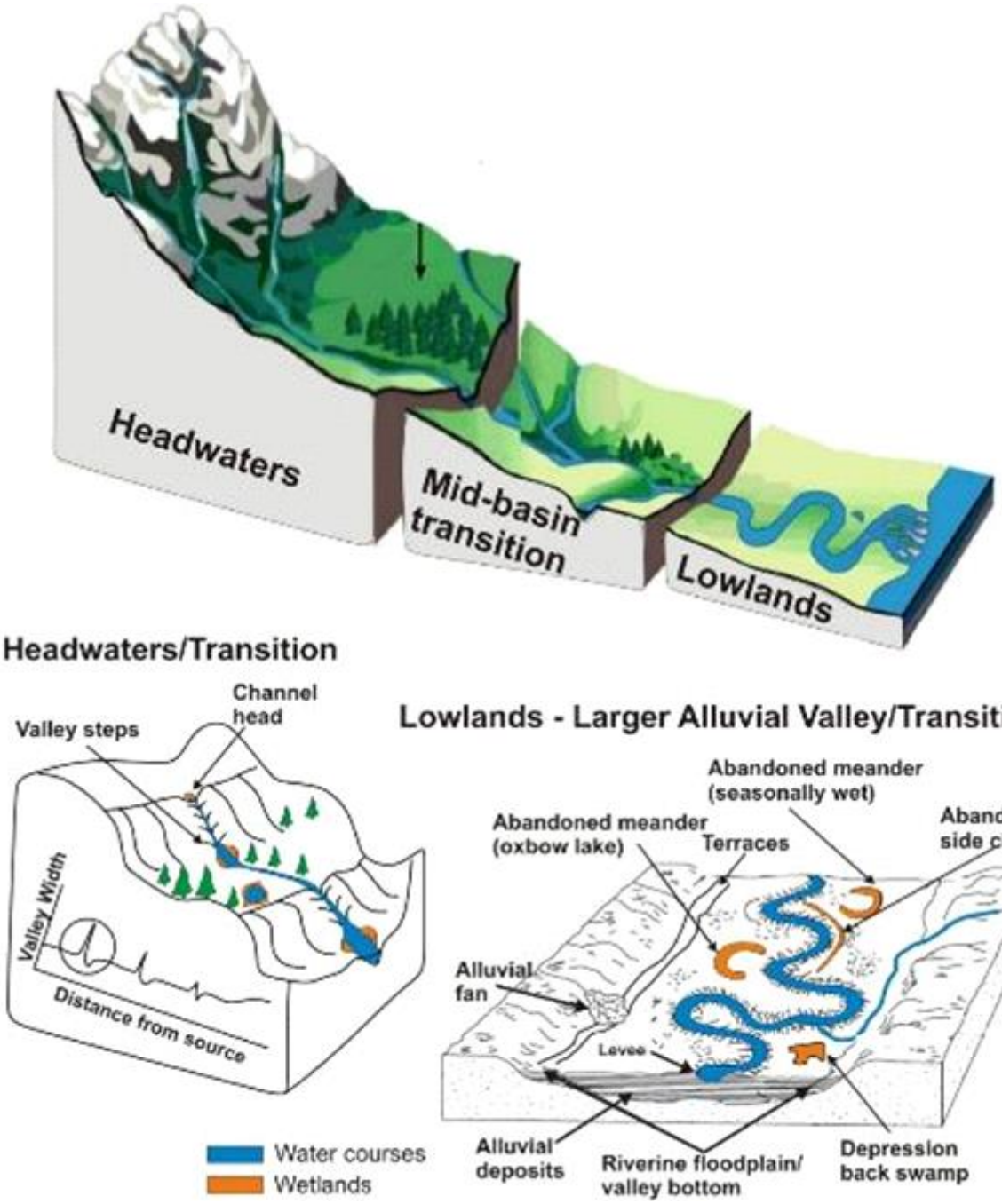

Figure 2 Hydrogeomorphic riverine wetlands span the full range of channel morphological types ranging from colluvial headwaters to alluvial, low-gradient lowlands.

1

3. Previous Work on Remote-Sensing Detection of Wetlands

The literature on wetland science and detection is extensive, dates to the 1960s, and encompasses many hundreds of papers (Tiner et al. 2015). A comprehensive literature review of wetlands is beyond this project scope and unnecessary in the context of project objectives. However, previous work as it relates to the primary task of building a remote-sensing tool for detecting the hydrogeomorphic indictors of wetlands in forested environments is pertinent.

By far the best means to identify wetlands is boots on the ground. The field-based approach, however effective, is expensive to apply across large watersheds and landscapes. Thus, following World War II, aerial photography was the first remote-sensing tool to be used for detecting wetlands over large geographic areas. The U.S. Fish and Wildlife Service employed black-and-white aerial photographs to conduct the first comprehensive mapping of wetlands in the 1950s (Tiner 2015). In the 1960s, color aerial photography was used to detect wetlands in various parts of the U.S. (Olson 1964, Anderson et al. 1968), a technology used to map wetlands for the next 60 years.

Currently, aerial photographs combined with other optical (satellite) imagery constitute the major technologies for identifying and mapping wetlands (Tiner et al. 2015). A new methodology for using remotely sensed information, called object-based image analysis, has been increasing in use since the early 2000s (Knight et al. 2015) and can effectively use optical imagery to detect wetlands where vegetation does not obscure them. In the last decade, availability of high-resolution DEMs, and the need to extend detection of wetlands under forest canopy, led to technologies that focus on the topographic controls on soil moisture, such as the topographic wetness indices (Merot et al. 2003) and wet-areas mapping (White et al. 2012).

A method for identifying potential wetland locations that is particularly well-suited for wetlands that have been obscured by land use or eliminated by land use conversion is historical reconstruction. Collins et al. (2003) used old survey records and historical maps to reconstruct the extent of lower river floodplains and associated marshes. Another method for identifying tidally influenced wetlands is to combine terrestrial DEMs with bathymetry and then apply an annual time series of tidal cycles to predict the proportion of a year coastal areas are inundated with salt water (Benda and Litchert in progress). Using current information on geographic extent of mudflats and salt marshes, areas of likely salt marshes in areas obscured by land use can be identified.

Methods using hydrogeomorphic indicators are best suited for identifying potential wetland conditions under forest canopy. Beginning approximately in 1995, researchers began using the topographic index (TI), first introduced by Beven and Kirkby (1979) in 'TOPMODEL' as an indicator of wetlands. TI can take several forms. The most common is:

$$TI = \ln(\partial / \tan\theta) \qquad \text{Eq. 1}$$

where ∂ is the upslope contributing area per unit contour length and $\tan\theta$ is the local slope (m/m). Topographic convergence acts to concentrate flow and increases contributing-area-per-unit-contour length. Increasing convergence and decreasing slope increase TI and increase the potential for wetland conditions.

A variation on TI is the Soil Topographic Index (STI) (Walter et al. 2002, Lyon et al. 2004) where:

$$STI = \ln(\partial / T \tan\theta) \quad \text{Eq. 2}$$

Here T is the soil transmissivity ($m^2\ d^{-1}$), calculated as the multiple of average hydraulic conductivity (m day^{-1}) and depth to restrictive layer (m) or soil depth.

Numerous researchers have applied TI and STI, the latter also referred to as the 'Topographic Wetness Index' (TWI), between 1995 and present to predict likely areas of high soil saturation and wetland occurrence (Table 2). Merot et al. (2003) added a precipitation term to STI in Europe to account for the large differences in rainfall across the continent. Buchanan et al. (2014) evaluated 400 different versions of TI and TWI with varying parameters of DEM resolution, soil properties (with and without), and flow-accumulation and slope algorithms. They determined that TWI was generally more accurate with higher-resolution DEMs (LiDAR), a D-infinity flow-accumulation algorithm (Tarboton 1997), and the addition of information on soil depth and hydraulic conductivity (Table 2).

A more recent hydrogeomorphic indicator is 'Topographic Depth to Water' (DTW) in which elevations of water bodies, particularly streams and rivers, are used to estimate the closeness of the water table to adjacent land surfaces (Murphy et al. 2007/2008). DTW is used to map wet or saturated soils to identify equipment exclusion zones in Alberta (White et al. 2012) and in Sweden (Agren et al. 2014).

Closed depressions are topographic features that could, when underlain by shallow or low-permeability soils, indicate the potential for wet soils or wetlands to form. Closed depressions identified in DEMS can be real topographic features or artifacts in a DEM. When deriving a synthetic stream network in a DEM using flow routing algorithms, all closed depressions are identified and flow paths through the depressions are defined (a process called 'hydro-conditioning). Closed depressions have been used to detect potential wetlands in Ontario (Creed et al. 2003) and Sweden (Agren et al. 2014). Closed depressions, as part of natural topography, also influence topographic depth to water, creating shallower water depths, and hence areas more likely to contain saturated soils for at least part of the year (Table 1). Depressions may also be sediment-collection areas during wildfires and contain lower-permeability silts and clays.

Subsurface low-permeability layers, such as till or lacustrine deposits, can result in water ponding and formation of saturated soils. Impermeable areas, however, have not been formally incorporated into models for detecting wet areas or wetlands (Table 2). This is likely due to the dearth of detailed subsurface topographic mapping of impermeable layers. As better data becomes available, impermeable areas could be incorporated into wetland detection methods.

Analysis of hydrogeomorphic controls on wetlands could extend to subsurface and surface hydrological models (**Figure 3**). Watershed-scale hydrology is simulated using lumped parameter and spatially distributed models; spatially distributed models have been referred to as 'cell based models' (in the sense of pixels) to parameterize and quantify hydrologic processes at the local scale. They are mostly used to predict surface runoff patterns in watersheds, including the effects of different land uses (Voldseth et al. 2007). In the context of wetlands, physically based hydrology models have been used to study the water balance of known wetlands (Karan et al. 2013). However, spatially distributed hydrology models have not been used to detect wetlands over large watershed areas. This is likely due to the

complexity of wetland occurrences involving multiple factors that are difficult to quantify and parameterize in hydrology models. These factors include variation in soil types, textures and depths, spatial variation in groundwater- and near-surface flow paths, and spatial and temporal variation in evapotranspiration.

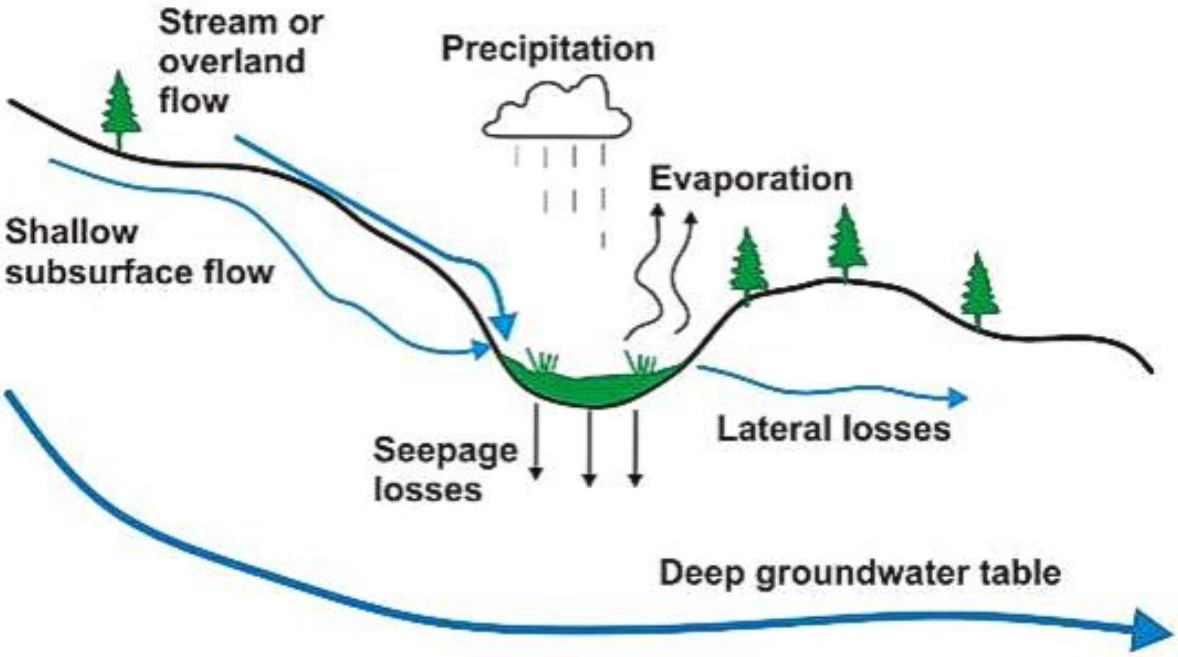

Figure 3. Wetland hydrology components.

Table 2. Studies using hydrogeomorphic indicators to predict soil moisture and wetlands

Location/source	Depressions	Topographic wetness index (TWI)	Topographic depth to water (DTM)	Comments
France/Merot et al. 1995	na	Yes, with 40m DEM	na	One of the earliest use of DEMs, evaluated two different TWI, w/ and w/out soil
Sweden/Rodhe and Seibert 1999	na	Topmodel, TWI index 50m grid	na	Poor results, DEM scale too coarse

Location/source	Depressions	Topographic wetness index (TWI)	Topographic depth to water (DTM)	Comments
Ontario, Canada/Creed et al. 2003	Topographic depressions and also flats (<1.5°)	na	na	Forested ("cryptic") wetlands; used LiDAR; focused on dissolved organic carbon export
Europe/Merot et al. 2003	na	Topmodel, index includes soil transmissivity and annual precipitation	na	Incorporates effective rainfall into TWI index to create 'climato-topo' index
Seine River watershed, France/Curie et al. 2007	na	TWI using 100m DEMs	na	Includes river corridor classification to aid in wetland detection; raises the issue of detecting "missing wetlands" due to land conversion
Alberta, Canada/Murphy et al. 2007/2008	inferred	na	Cartographic depth to water – wet areas mapping	Not necessarily wetlands, but objective is wet areas mapping for equipment exclusion zones near streams
Maryland/Lang and McCarty 2009	na	na, but target is general soil moisture	na	Use LiDAR intensity during 'peak hydrologic expression' (water visible); uses some type of TWI, but unclear for comparison
Olympic Mountains, Washington/Janisch et al. 2011	na	na	na	Provides information on locations and controls of wetlands associated with headwater streams
Alberta, Canada/White et al. 2012	inferred	na	Cartographic depth to water – wet areas mapping	Objective is wet areas mapping for equipment exclusion zones near streams

Location/source	Depressions	Topographic wetness index (TWI)	Topographic depth to water (DTM)	Comments
North Carolina/Leonard et al. 2012	included but also used 'local relief models'	not used, considered unsuitable for low relief terrain	not used	Authors used local relief models that involve predicting land curvature using elevation differences of land pixels within a defined neighborhood
Maryland/Lang et al. 2013	na	Using LiDAR, compared three TWI indices	na	Includes qualitative, professional judgement on TWI thresholds
Sweden/Agren et al. 2014	inferred	Includes TWI index	Uses similar approach to Murphy et al. 2009 and White et al. 2012	Evaluated TWI and DTW, DTW considered more capable
Central New York/Buchanan et al. 2014	na	Evaluated 400 different formations of TWI including DEM resolution, soils, flow accum and other	na	Higher resolution DEMs, adding soils, D-infinity provided the best models

4. Wetland Intrinsic Potential (WIP)

4.1. Approach

Numerous physical factors determine where in a landscape wetlands form. Many of these physical factors can be inferred from hydrogeomorphic indicators that can be identified using remotely sensed data, such as surface topography. Other factors, such as soil transmissivity and presence of underlying impermeable layers, may be estimated using existing soils and geologic mapping. With information on the spatial distribution of these hydrogeomorphic indicators, conceptual models of wetland formation can be used to identify where in the landscape intrinsic physical conditions are conducive to wetland formation.

The 'Wetland Intrinsic Potential' (WIP) tool is designed to identify these locations. The hydrogeomorphic indicators thought to be important for wetland formation are based on conceptual models of water flux

through the landscape, as done with the hydrogeomorphic wetland classification defined by Brinson (1993). For WIP, a set of hydrogeomorphic indicators specific to the environments of interest are identified, and digital data on topography, soils, geology, vegetation, and climate are used within a Geographic Information System (ArcGIS) to map these indicators across a study region.

WIP differs from wetland screening tools that rely on correlations of observed wetland locations with remotely sensed data. For example, wetlands have a distinct appearance in optical and multispectral imagery. A limited set of known wetland locations, based on field surveys, can be used to identify the characteristics that distinguish wetlands from other land-cover types. These characteristics may include differences in color and texture. Wetlands in areas lacking field surveys can then be inferred by identifying in the imagery those areas with characteristics similar to those in the observed wetlands (e.g., Halabisky et al., 2011). Rather than seeking correlations with observed wetland locations, WIP translates conceptual models of wetland formation to maps of expected likelihood of where wetlands exist. Unlike methods that rely on statistical correlations, WIP predictions can be made without any data on actual wetland locations. The resulting maps serve three purposes: 1) they provide an initial screening tool identifying locations potentially conducive to wetland formation, 2) they can be compared to surveyed wetland locations to test conceptual models, and 3) they provide information on hydrogeomorphic indicators that can be used in addition to multispectral imagery in statistical models to seek correlations with observed wetland locations.

An important aspect of WIP is that it seeks to identify locations where conditions conducive to wetland formation exist, not where actual wetlands exist. The presence or absence of a wetland in a location with a high WIP value depends on a variety of factors. Absence may show where a wetland did exist, but has been drained. Absence of wetlands with high WIP values, and presence of wetlands in areas with low WIP values, may demonstrate shortcomings in the conceptual models used to identify the hydrogeomorphic indicators to use, the suitability curves assigned to each indicator, or our implementation of the model. Discrepancies between predicted and observed wetland locations thus provide learning opportunities.

WIP may serve as one component in a suite of wetland screening tools, each of which utilizes different types of information and different ways of using that information. The tools to apply from this suite vary with location within a watershed. In the lower estuarine portions of river valleys, options include historical reconstruction, tidal inundation modeling, and optical detection (**Figure 5**). Above the lower valleys, but in areas lacking forest, optical detection is effective. In forested settings where wetlands are obscured by vegetation, hydrogeomorphic methods are the best option. WIP can be used across all three geographic domains (**Figure 5**), although the appropriate hydrogeomorphic indicators to include may vary with domain.

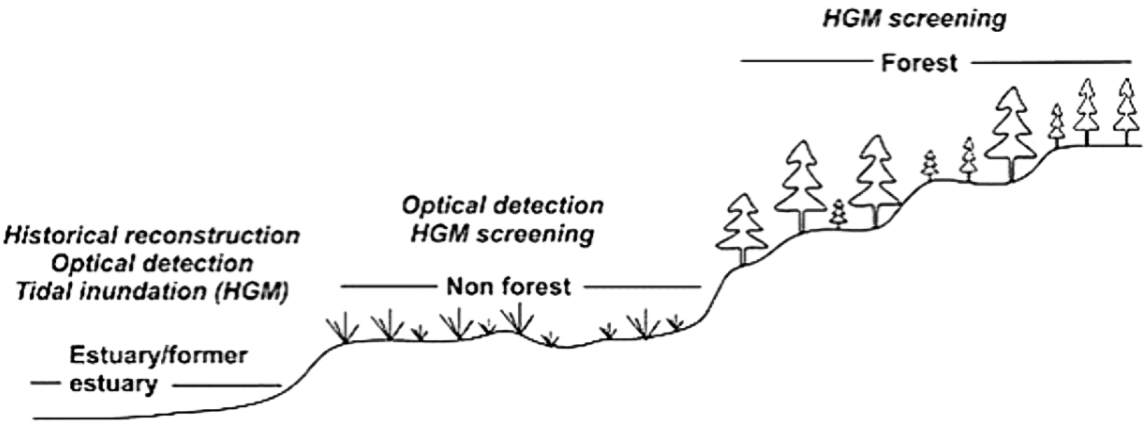

Figure 4. Optional methods for wetland detection vary with geographic location.

The WIP tool uses a Virtual Watershed data structure (Miller et al. 2015, Benda et al. 2015, Barquin et al. 2015), designed to simulate landforms and watershed processes with multiple types of interactions and connectivity, including land uses. It contains flow routing from all DEM pixels, using a multiple-flow-direction algorithm (D-infinity, Tarboton 1997) for unchannalized areas (which allows flow dispersion) and a single-flow-direction algorithm (D-8, which precludes dispersion) once criteria for channel initiation are reached (Clarke et al., 2008; Miller 2015). Flow networks are represented using a linked node data structure, which maintains information at the finest spatial grain, but allows efficient routing and summarization of information across large watersheds. Details on building a virtual watershed are contained in Appendix A. Use of the virtual watershed data structure enables efficient calculation of hydrogeomorphic indicators across large geographic areas.

4.2. Methodology

4.2.1. *Hydrogeomorphic Indicators*

WIP currently incorporates five hydrogeomorphic indicators (**Table 3)**: 1) closed depressions, mapped in terms of their relative depth (depth within the depression divided by maximum depression depth), 2) stream/river - depth to water, 3) lake/pond - water table, depth to water, 4) depth to an impermeable layer, and 5) topographic wetness index**.** Individual wetlands can be influenced by more than one hydrogeomorphic indicator and one indicator may be represented in more than one wetland class (**Figure 1, Table 1**). All five hydrogeomorphic indicators can occur in individual wetland classes.

Table 3. Hydrogeomorphic indicators in WIP.

Hydro-geomorphic wetland indicator in WIP	Units	Influence on wetland potential	Comments	Universal/site specific
1) Closed depression, relative depth	within closed depression polygons, depth (per pixel)/max depth, 0 - 1	Increasing relative depth – increasing wetland potential	Depressions determined by flow routing using DEMs	Site specific
2) Stream/river water table, depth to water	meters, 0 - 1	Decreasing depth to water – increasing wetland potential	Applied only to river corridor, floodplain, low terraces of channel network	Site specific
3) Lake/pond water table, depth to water	meters, 0 - 1	Decreasing depth to water – increasing wetland potential	Applied only to areas adjacent to lakes/ponds	Site specific
4) Depth to impermeable layer; includes where depth goes to zero at outcrops	meters, 0 - 1	Decreasing depth to impermeable layer – increasing wetland potential	Includes soil hydric layers and other impermeable boundaries, including glacial sediments (lacustrine/till); can include micro-topography, such as depressions, that can be sediment deposition areas following disturbances, such as fires	Site specific, but could be universal, depending on data availability
5) Topographic wetness index	dimensionless	Increasing topographic wetness – increasing wetland potential	Modified by soil permeability and climate	Universal-applied to all pixels

4.2.2. *Suitability curves*

WIP relies on "suitability curves" to translate hydrogeomorphic-indicator values to measures of intrinsic potential for wetland formation. Use of suitability curves is a strategy widely used by biologists to deal with physical and biological environments where multiple interacting factors make it difficult to build and parameterize complex quantitative models. A suitability curve provides a simple model that incorporates expressions of process and response (Van Horne and Weins 1991): it specifies a single-valued relationship between the dependent variable, such as animal habitat quality, and the independent variable, such as a landform type or process magnitude. Suitability curves also normalize different parameter-value ranges to a consistent zero-to-one scale (**Figure 5**). Suitability curves have been used extensively to describe habitat potential in terrestrial and aquatic environments (USFW 1981, Morrison et al. 1998, Vadas and Orth 2001, Burnett et al. 2007, Bidlack et al. 2014).

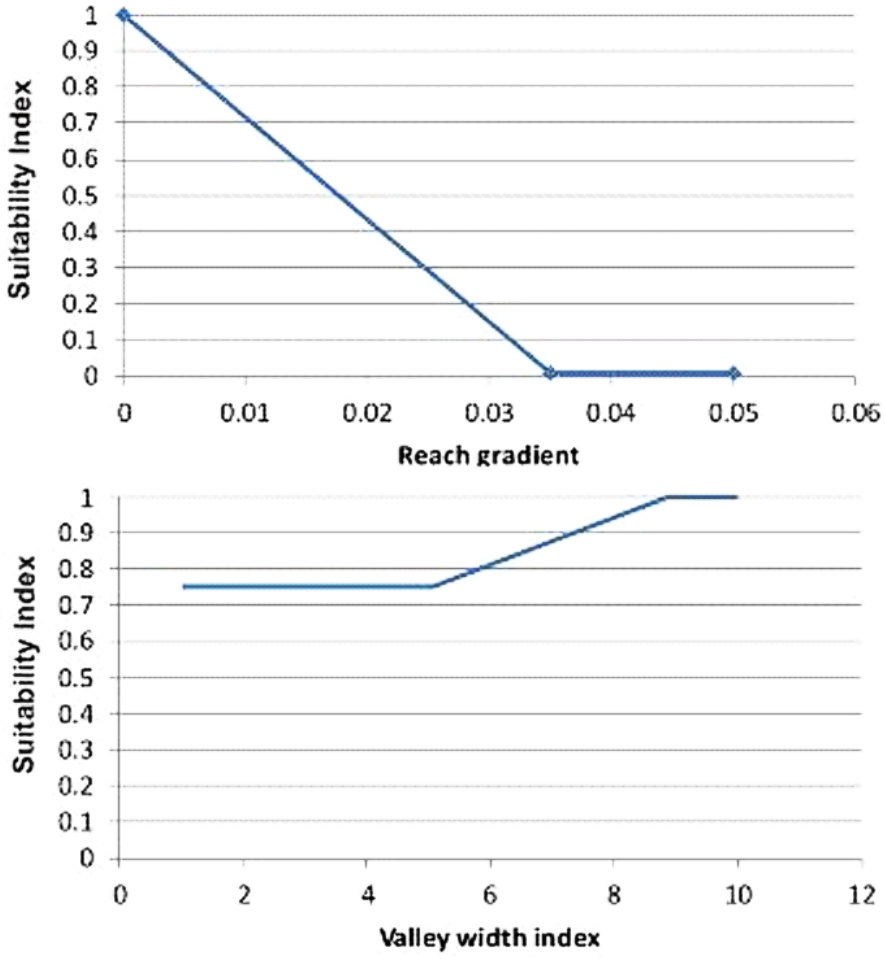

Figure 5. An example of suitability curves indicating the posited relationships between physical conditions and habitat suitability for chinook salmon. From Busch et al., 2011.

There are several ways to treat individual hydrogeomorphic indicators when calculating how they influence wetland formation. Each could be evaluated individually. For instance, riverine wetlands driven by availability of surface and subsurface flow may be most affected by stream/river depth-to-water table. Lacustrine fringe wetlands may be most affected by pond/lake depth-to-water table. Seep wetlands may be most affected by impervious layers that outcrop along hillsides.

Hydrogeomorphic indicators also occur in combination and can reinforce each other in wetland creation. For example, closed depressions are important in wetland development, but only if certain other conditions occur coincidentally, such as a regional or local impermeable layer near the ground surface, a nearby stream/river or lake/pond water table, a high topographic-wetness index, or some combination of all three.

In addition, not all hydrogeomorphic indicators may be equally important. Depth to water table near streams/rivers or lakes/ponds may be more significant, because these indicators are based on vicinity to actual surface-water observations, compared to a shallow impermeable layer, a depression, or a topographic wetness index that only indicate the potential for subsurface flow and increased wetness.

To apply the WIP model using digital data, each hydrogeomorphic indicator is calculated for every DEM pixel and the corresponding suitability curve value for each indicator is determined. This gives up to five suitability-curve values for each pixel. We considered four methods to combine the suitability curve values into a single measure of intrinsic potential: 1) take the maximum suitability curve value, 2) take the arithmetic mean of the curve values, 3) take the geometric mean of the curve values, and 4) apply the curve values in a logistic function. All methods can produce an intrinsic potential value that varies from zero to one (because the suitability curves themselves all vary from zero to one), but they provide different approaches for determining how variation between the curve values influence the final intrinsic potential value. For the maximum, one curve is applied and the rest are ignored. For the arithmetic mean, a zero value for any single curve will reduce the final intrinsic potential value; for the geometric mean, any zero curve value produces an intrinsic potential value of zero, even if the other curves have high values. The logistic function translates the sum of suitability curve values to an S-shaped curve that varies between zero and one; it provides flexibility for weighting each suitability curve differently. Other approaches may also be applied, such as use of fuzzy logic, as has been used to combine multiple landscape attribute values into single measures of landslide susceptibility (Gorsevski et al., 2006; Regmi et al., 2010).

It is not feasible to robustly evaluate these and other methods for combining suitability curves into an estimate of intrinsic potential, in terms of how they affect ability to identify forested wetland locations using hydrogeomorphic indicators, without a validation dataset on actual wetland locations. The validation wetland dataset will be available in Phase 2 of this project and the different options can be evaluated then.

To demonstrate application of the WIP approach, we used a logistic equation to combine suitability curve values[10]:

$$WIP = \exp(g)/(\exp(g) + 1) \quad \text{Eq.3}$$

where WIP is the estimated intrinsic potential (0 to 1) of a wetland occurrence and (g) is a linear combination of individual hydrogeomorphic-suitability-curve values (called the "logit" function):

$$g = b_1(x_1) + b_2(x_2) + b_3(x_3) + b_4(x_4) + \ldots \quad \text{Eq.4}$$

Here, the $x_1 \ldots x_i$ are suitability scores (0 to 1) obtained from individual hydrogeomorphic indicator suitability curves. The $b_1 \ldots b_i$ terms are weighting coefficients that specify the posited relative importance of individual hydrogeomorphic indicators in wetland formation. For example, if the topographic wetness index is thought to be less important than the closed depression and depth-to-water indices, its weight (b value) will be set to a smaller value than weights for the other terms. An intercept of zero is used in Ea. 4, so there is no b_0 term[11].

The logistic equation is also used in logistic regression, for which the weighting terms are adjusted to produce the best match to observations. For example, if a census of wetlands were available for a region, a statistical model based on logistic regression could be built by setting WIP values to zero for DEM pixels where there is no wetland and to one for DEM pixels where there is a wetland. Suitability scores (x_i in Eq. 4) would be replaced with the hydrogeomorphic-indicator values for each pixel, and the weighting terms (b_i in Eq. 4, now including the b_0 term) would then be adjusted to minimize the difference between the predicted and observed WIP values. Here, we are using the logistic model not to fit a curve to observations, but to translate expectations about how hydrogeomorphic factors affect the potential for wetland formation to a map showing where we expect to find wetlands. The suitability curve scores (x_i) and weightings (b_i) in Eq. 4 are hypothetical, based on conceptual models of water flux through a landscape and on user judgement. We could have chosen any of the other previously mentioned methods for combining suitability curves (maximum value, arithmetic mean, or geometric mean); the logistic equation was used to illustrate use of the WIP methodology for this report.

4.2.3. *Wetland Intrinsic Potential Modeling Steps*

There are nine potential modeling steps in WIP, eight of which utilize the Netstream set of Fortran programs, (Miller 2003; Miller et al., 2015; refer to Appendix A for the technical background on the 'Netstream' suite of Fortran programs). The first two steps involve data preparation and running a suite of Fortran programs to create the spatial data needed to run the WIP screening tool, including building

[10] The logistic model has been used to describe certain physical phenomena, such as environmentally limited population growth (e.g., Section 45.3 in Biology, https://openstax.org/details/books/biology), and it is the basis for logistic regression, used for nominal dependent variables. We use it here solely because it provides one method of combining multiple suitability-curve values into a single estimate of intrinsic potential.

[11] This implementation results in WIP values that range from 0.5 to 1.0, and for which additional terms tend to increase the WIP value, even if the additional terms have low suitability scores. That is not an issue for the examples using Eq. 3 in this report, because all examples use the same number of hydrogeomorphic indicators. If a logistic model is used in future implementations of the WIP tool, these shortcomings will be addressed.

the virtual watershed (**Figure 6**). A digital elevation model (DEM) and a mean-annual precipitation grid (e.g., from PRISM) must be provided in Step 2. Step 3 delineates closed depressions, with an option to select a minimum depression area to include in the analysis (0.04 ha or 0.1 ac is the minimum). Step 4

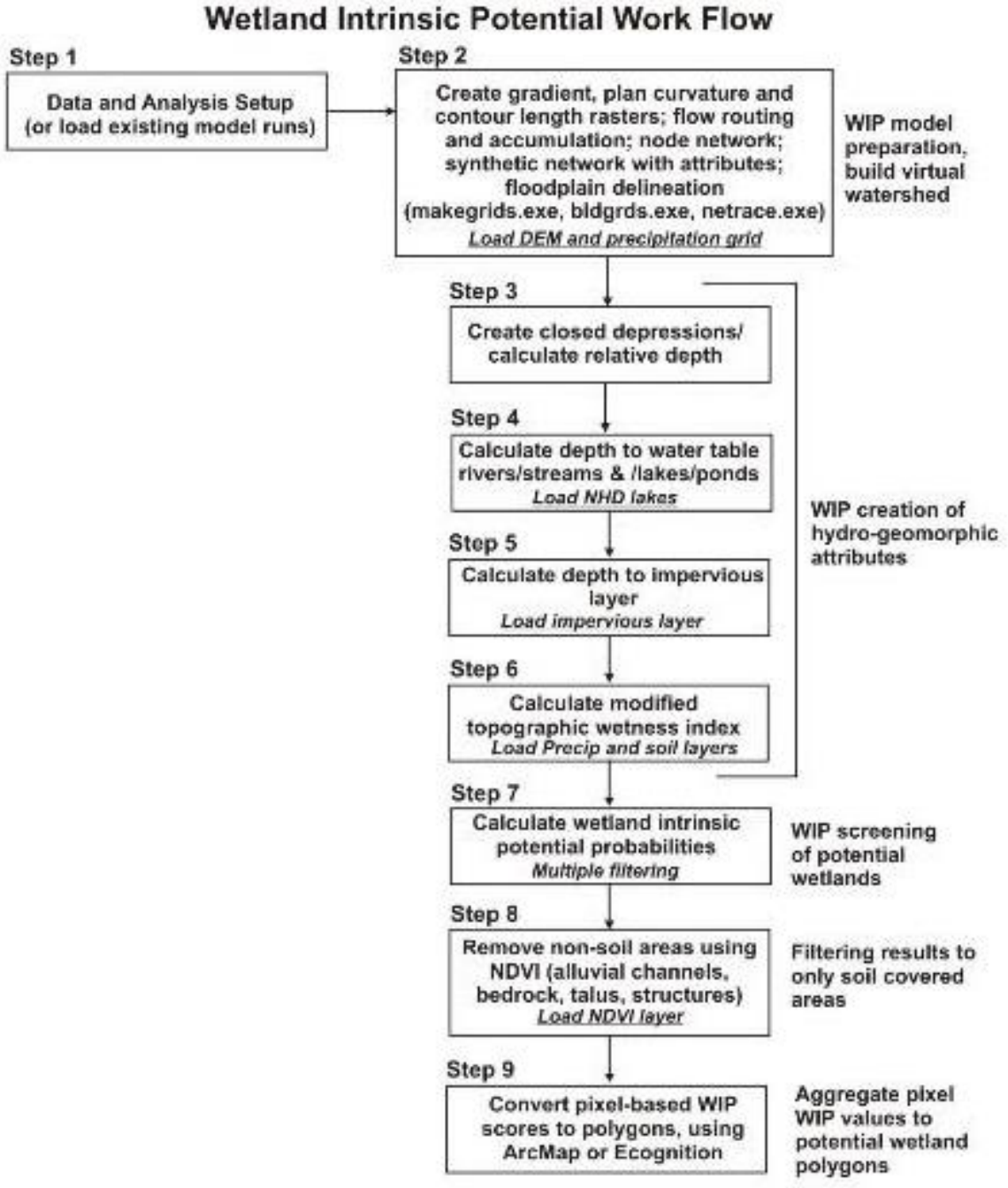

Figure 6. The Wetland Intrinsic Potential workflow requires eight to nine steps.

calculates stream/river and lake/pond depth-to-water and requires NHD lake polygons[12]. Step 6 calculates the topographic-wetness index and, in addition to the DEM, requires mean-annual precipitation (e.g., from PRISM) and (optionally) soil transmissivity (e.g., soil depth times average saturated hydraulic conductivity from SSURGO[13]). Step 7 uses the results from Steps one through six and creates pixel-scale wetland intrinsic potential scores (0 – 1).

Step 7 also applies (optionally) filters to exclude DEM pixels representing open water (channels[14]) and potential wetland areas (defined as contiguous pixels exceeding a minimum WIP score) below a specified size threshold. For example, potential wetland areas, defined by contiguous pixels with a WIP score exceeding 0.8 that together cover less than 400 m^2 (0.1 acre), the lower limit of regulatory oversight in Washington State, can be ignored. Step 8 removes areas that are likely to have no vegetation. We infer that a lack of vegetation is equivalent to a lack of soil and, thus, a lack of wetlands. These areas include bedrock, talus, alluvial channels and anthropogenic structures (e.g., roads, buildings), and requires an NDVI raster derived from NAIP imagery. Step 9 (optionally) converts the pixel scores to polygons of potential wetlands using methods available in ArcMap or E-Cognition. All modeling steps (except #9, included in Phase 2) are included as part of the WIP ArcMap Add-in tool.

LiDAR DEMs are recommended in WIP, because higher-resolution DEMs greatly improve ability to resolve topographic indicators, such as closed depressions and the topographic wetness index. LiDAR DEMs may need to be merged to create seamless, watershed-wide coverage (prior to Step 1, **Figure 6**). If LiDAR DEMs do not fully cover a watershed, 10 m DEMS will need to be merged with LiDAR (using 'Mosaic Tool' in ArcMap 10.x or another program, such as the Merge program in the Netstream Suite).

Each of the five hydrogeomorphic indicators are described in more detail below.

4.2.4. *Hydrogeomorphic Indicator: Closed Depression/Relative Depth*

When building a virtual watershed, a flow direction is defined for each pixel of a DEM, consistent with surface-water flow paths (for additional information about determining flow accumulation and direction, and creation of a synthetic river network, see Appendix A). This requires that flow traced from every pixel eventually reaches an outlet from the DEM. Within a DEM, closed depressions occur for a variety of reasons. When elevation data are of sufficient detail to resolve road surfaces, as with the LiDAR bare-earth DEMs, road prisms at stream crossings can appear as dams blocking downstream flow. Thus, flow through culverts or other drainage structures must be accounted for. Closed depressions may also occur as artifacts in the DEM. Topographic closed depressions also exist on the ground surface and these are the ones of interest in WIP.

[12] https://nhd.usgs.gov/NHD_High_Resolution.html

[13] https://www.nrcs.usda.gov/wps/portal/nrcs/main/soils/survey/

[14] Channel width is estimated using regional regressions to mean annual flow; mean annual flow is estimated using regional regression equations to contributing area and mean annual precipitation. Equations are provided in section 5.2.

Non-road-related closed depressions are identified by flagging DEM pixels that drain to outlets (low points) along the DEM edge. Starting from these drained pixels, adjacent pixels with elevations equal to or greater than the drained pixel are flagged as drained. This process is repeated from the newly flagged pixels until no more pixels can be drained, at which point unflagged pixels delineate closed depressions. Low points along the boundaries of the closed depressions are then located. These locations are the "pour points"; if the closed depression were filled with water, the pour points indicate where the water would spill over to drain out of the DEM. The depth of the closed-depression pixels is then calculated as the difference between the elevation of DEM pixels within the depression and that of the pour point. Each delineated closed depression then has an associated area, average depth, and maximum depth (**Figure 7**). A filter can be applied to exclude closed depressions below a specified size limit.

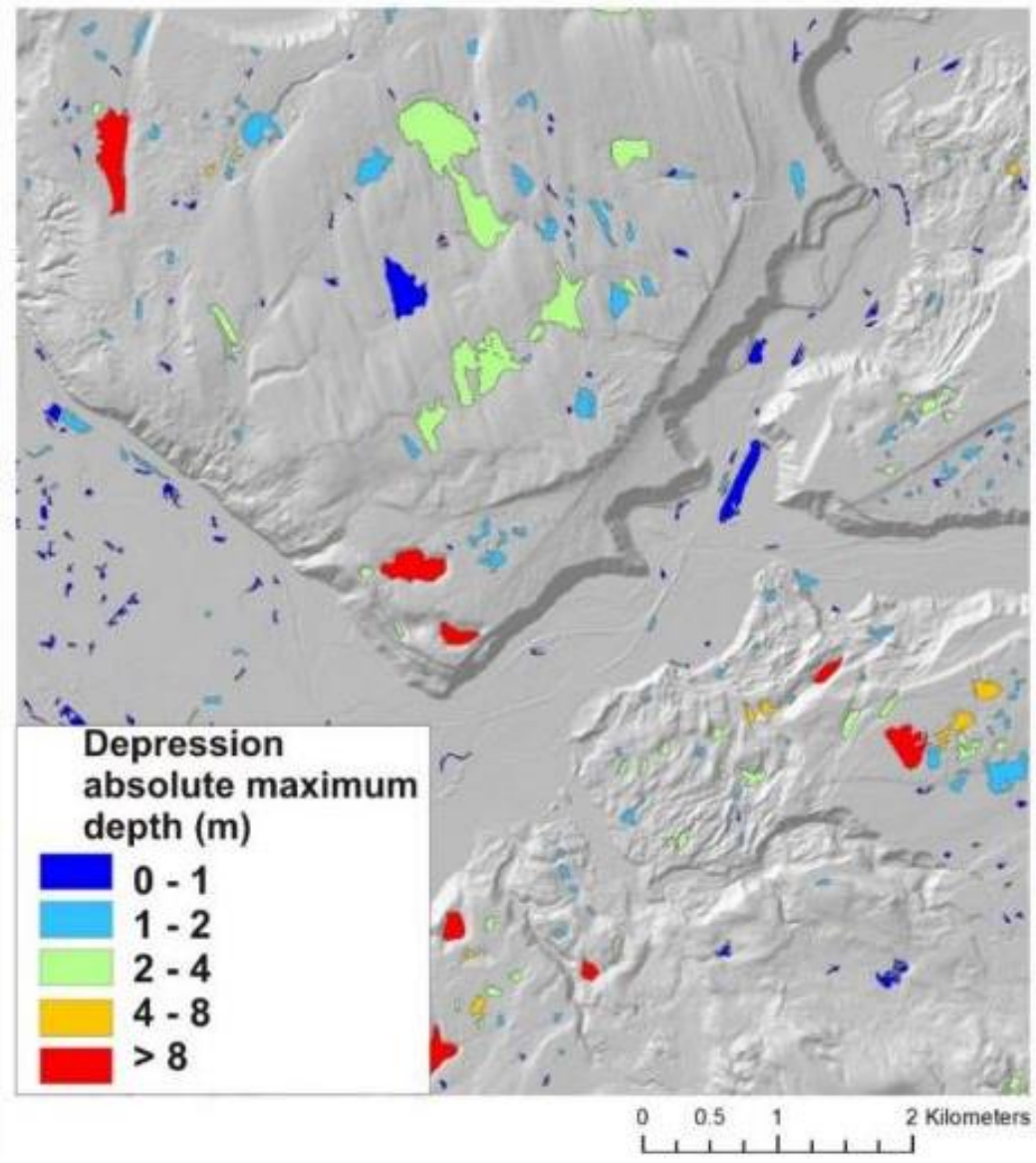

Figure 7. Absolute values of the maximum depression depths. Minimum size shown is 100 m^2.

To determine locations within a depression that might be the most likely to have higher wetness or wet soils, each DEM-pixel depression depth is divided by the maximum depression depth, resulting in a relative depth (0 to 1, **Figure 8**). Larger relative depths are equivalent to being deeper and lower in a closed depression. Hence, the suitability index for closed depressions is designed so the largest relative depths (>0.8) are associated with the largest potential for wet soils and wetland formation.

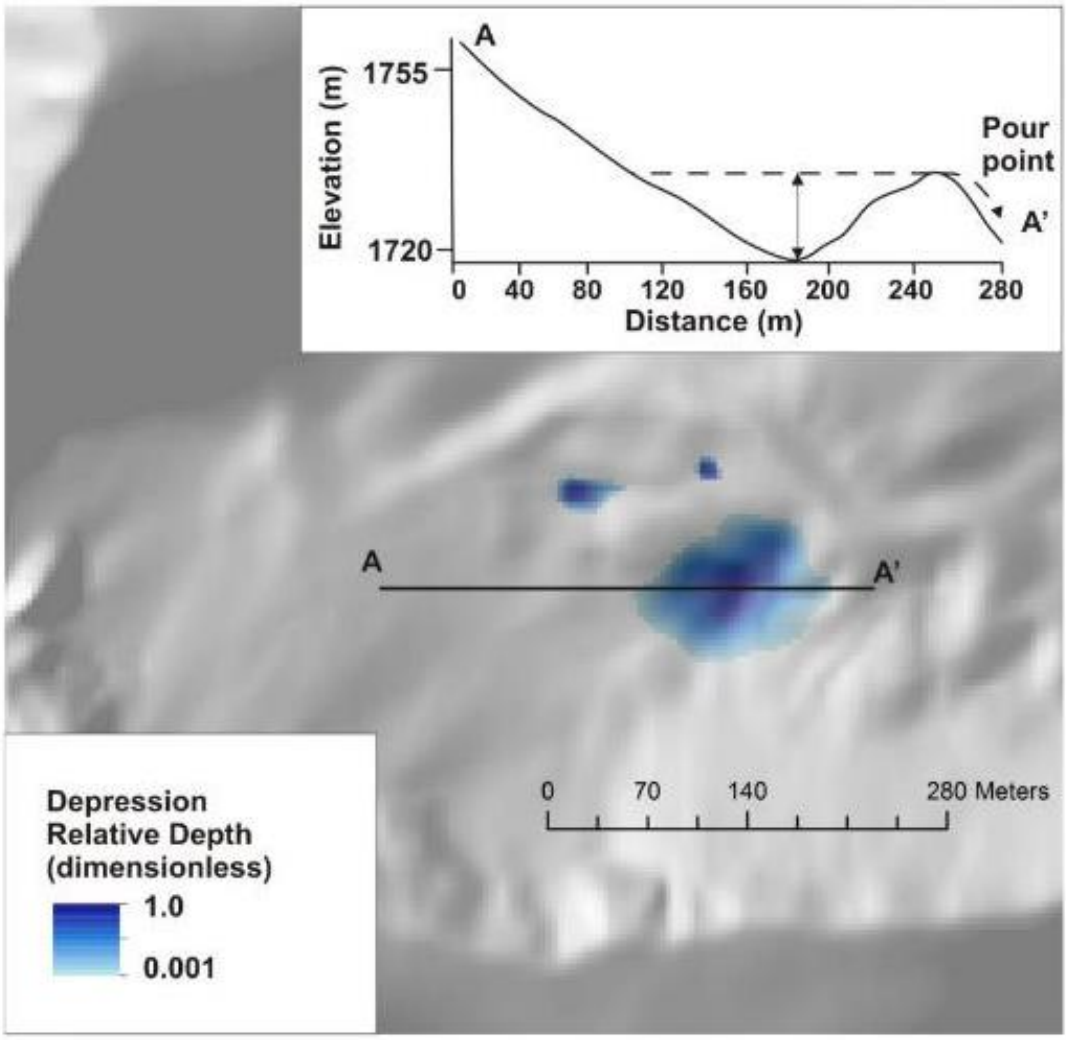

Figure 8. Closed depression relative depth.

In watersheds of the Pacific Northwest, closed depressions commonly form due to mass wasting processes, such as earthflows. Closed depressions in alpine areas also form due to glacial and peri-glacial processes, including moraines disrupting drainage (**Figure 9**).

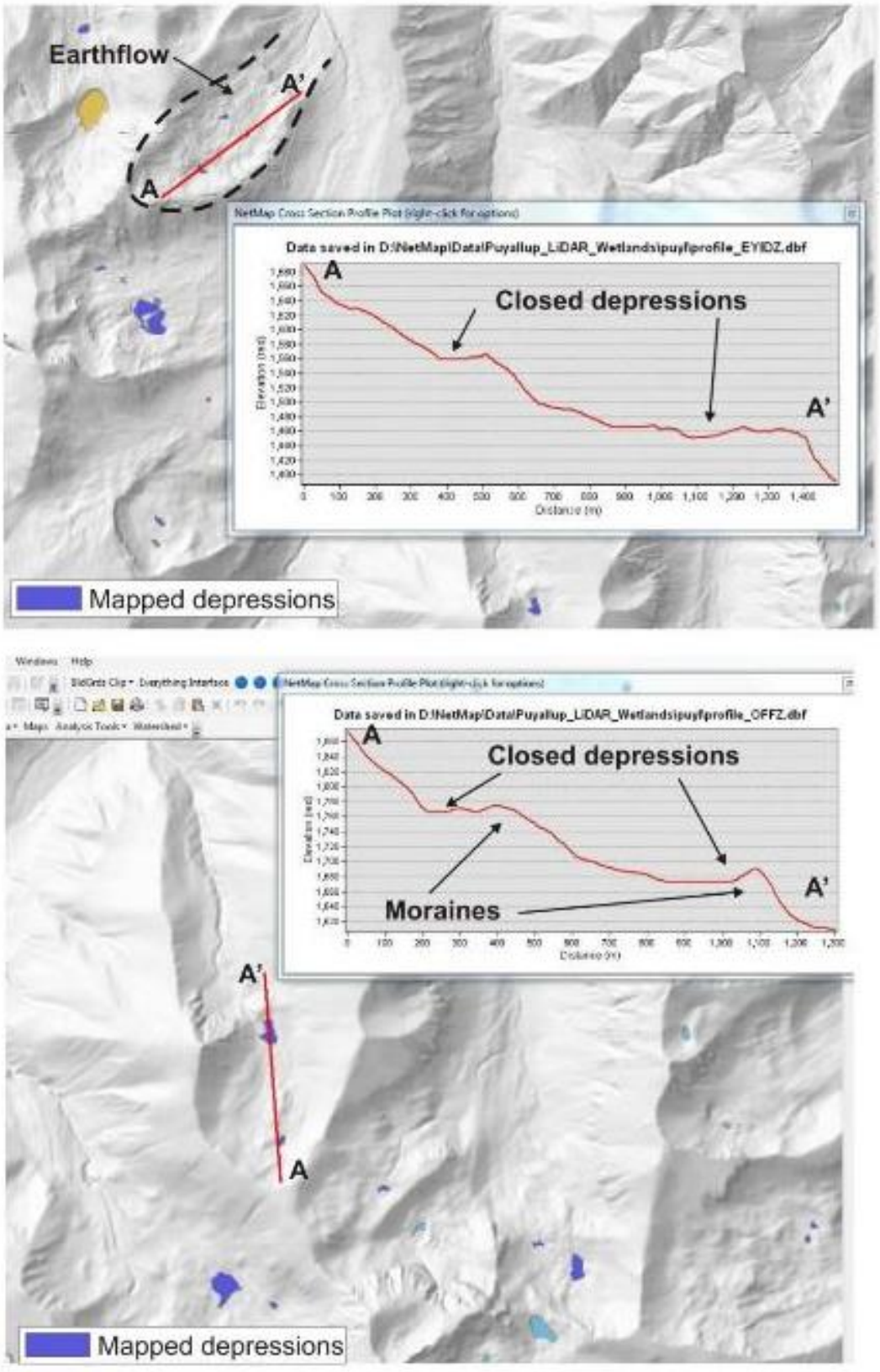

Figure 9. Depressions associated with an earthflow and with alpine glacial activity.

4.2.5. *Hydrogeomorphic Indicator: Stream/River Water Table - Depth to Water*

In valleys that contain alluvial deposits, streamflow elevation is often similar to the elevation of the saturated zone or groundwater table in the vicinity of the active channel in the floodplain and adjacent valley floors (Busch et al. 1992, Stromberg and Patten 1996). Estimated floodplain inundation is used to predict height above the channel for a range of flood levels, in terms of absolute elevations or in bankfull depths (Benda et al. 2011) (**Figure 10**). Height above channel predictions are used in WIP to estimate its inverse - depth to the water table (Chambers et al. 2004), but in streams with widely varying high to low flows, it may underestimate depth to water table. Modeling depth to stream/river water table identifies numerous fluvial features that could support wetlands, including side channels, abandoned meanders, and oxbow lakes and ponds (**Figure 11**).

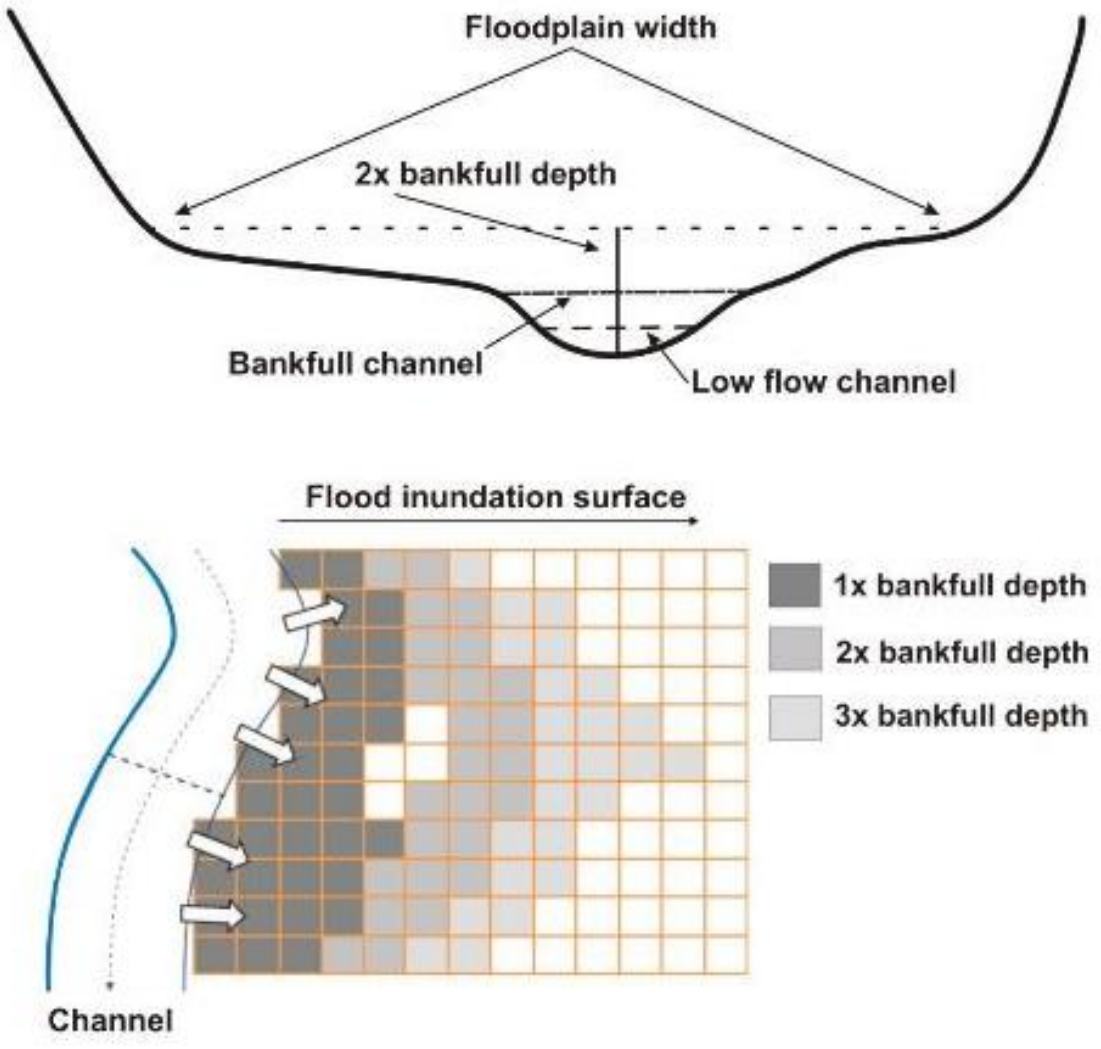

Figure 10. Floodplain mapping tool in WIP is used to identify the likely flood prone portions of the valley floor.

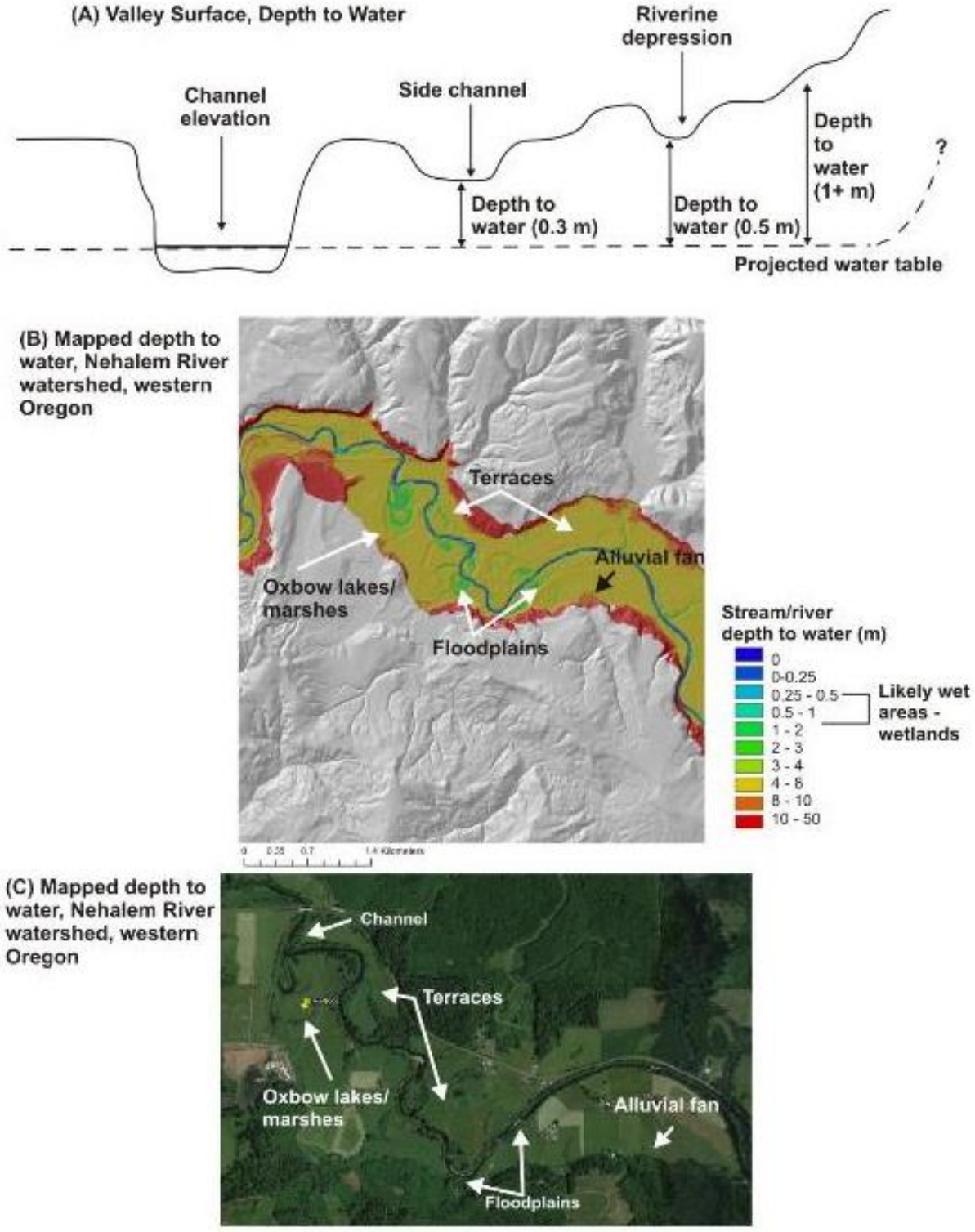

Figure 11. Floodplain inundation modeling is used to infer depth-to-water on floodplains and low terraces along all channels.

1

Smaller depths to water are assumed to lead to wetter surface conditions and support wetland development. A depth of less than or equal to 0.3 m is considered a requirement for wetland development (USCE 1987). A maximum effective depth to water likely tails off above 1 m.

4.2.6. *Hydrogeomorphic Indicator: Lakes/Ponds Water Table - Depth to Water*

Lacustrine wetlands, adjacent to lakes by definition, are handled similarly to depth-to-water associated with streams and rivers. The average elevation of the lake or pond is compared to the surrounding land-surface elevations to estimate depth to water. The lake area in the NHD is reduced by three meters along the contiguous shore lines to account for inaccurate lake boundaries. An average lake elevation is obtained from that area. Then, the local contributing area to each lake and pond is determined. Circumscribed by the lake drainage area, a buffer is employed within to calculate depth to water. Lakes with areas less than 1,000 m^2 are given a buffer radius (around the lake) of 20 m; lakes with areas greater than 10,000 m^2 are given a buffer radius of 200 m. Between these endpoints, the buffer distance is calculated as 0.02 of lake area.

Within lake/pond local drainage areas, the average lake elevation is subtracted from lake-adjacent areas (**Figure 12**). The difference in elevation, per DEM pixel, between the lake-adjacent ground surface and the lake level (projected horizontally under the ground surface) is the depth-to-water hydrogeomorphic indicator (**Figure 13**).

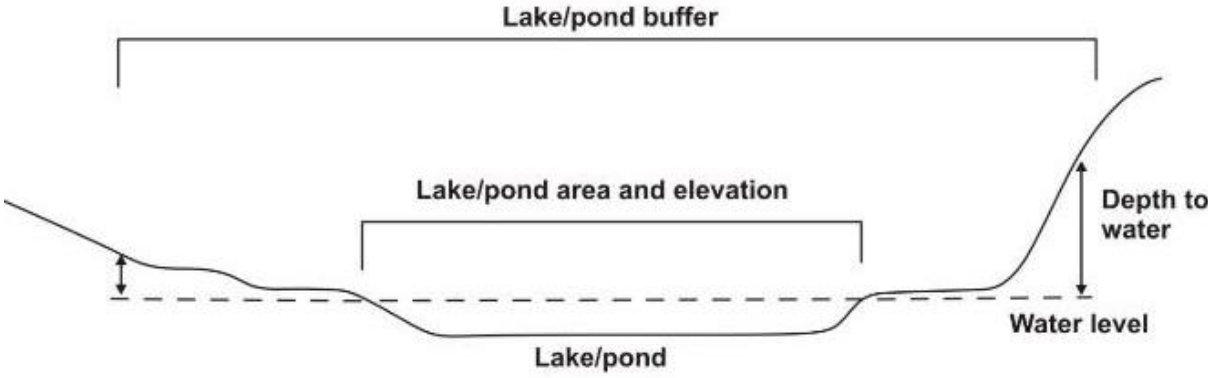

Figure 12. Elevation of land surfaces within the local drainage area of lakes and ponds.

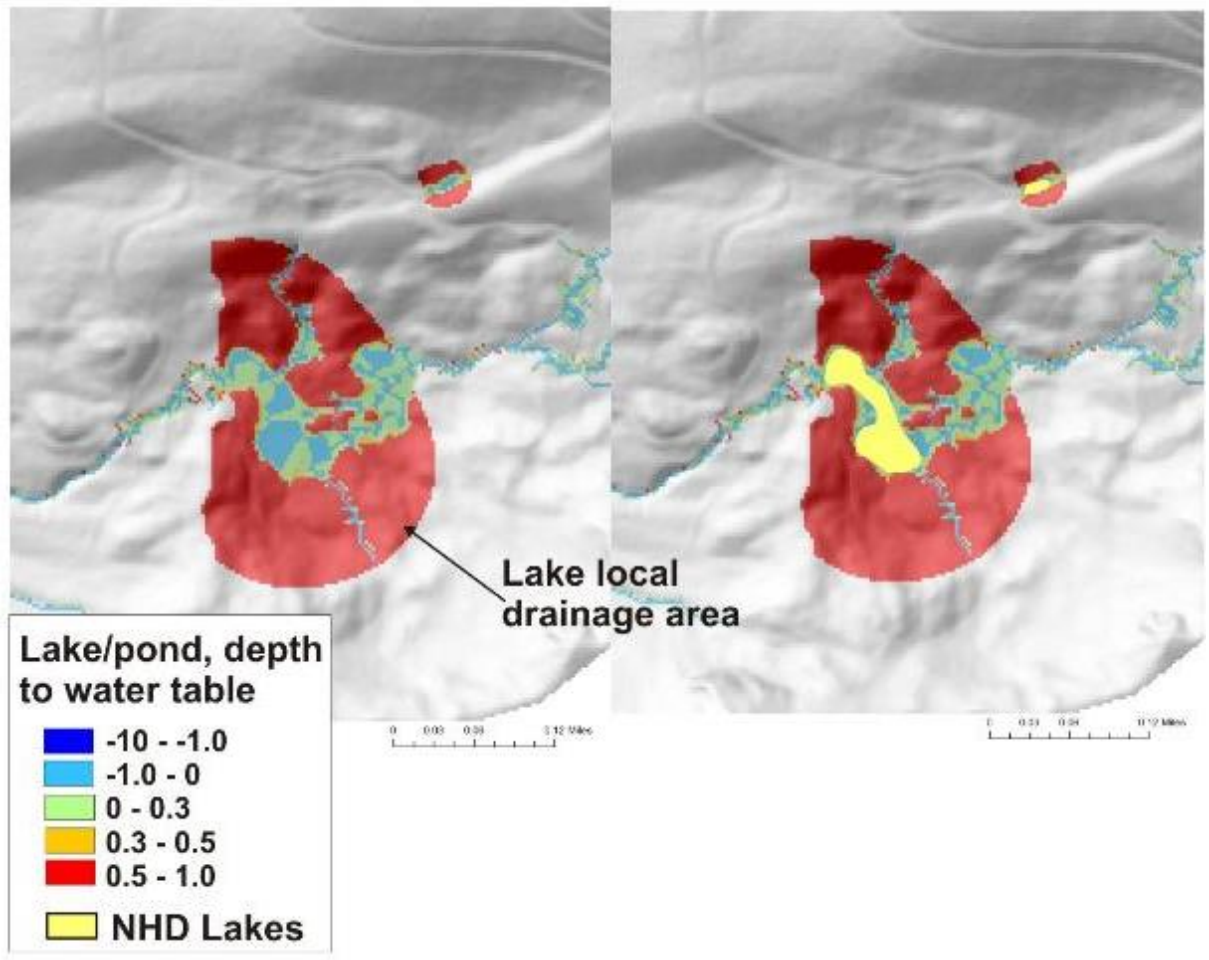

Figure 13. Predicted Lake/Pond depth to water.

4.2.7. *Hydrogeomorphic Indicator: Topographic Wetness Index, Modified by Soil Permeability and Climate*

Spatial variation in mean annual precipitation can exceed 100% and commonly exceeds 200% from the coast to the inland mountains in the Pacific Northwest. Hence, a topographic wetness index should be affected by variation in precipitation. We adopt the approach of Merot et al. (2003) and include a precipitation term in STI, creating a climate-topographic index (CTI):

$$CTI = \ln(\partial Vr / T \tan\theta) \quad \text{Eq. 5}$$

where Vr is the mean annual precipitation taken from PRISM climate data (using the 30-year normal, 1981-2010, interpolated to about an 800-m grid spacing: http://prism.oregonstate.edu/normals). Higher values of Vr yield higher values of CTI. Transmissivity (T) is included if such soil data are available and at appropriate spatial scales. If not, T can be set to one. Application of the CTI in the Puyallup River

watershed produced values that ranged from a low of 12 to a high of 33, with the higher values corresponding to swales and low-gradient areas below them (**Figure 14**).

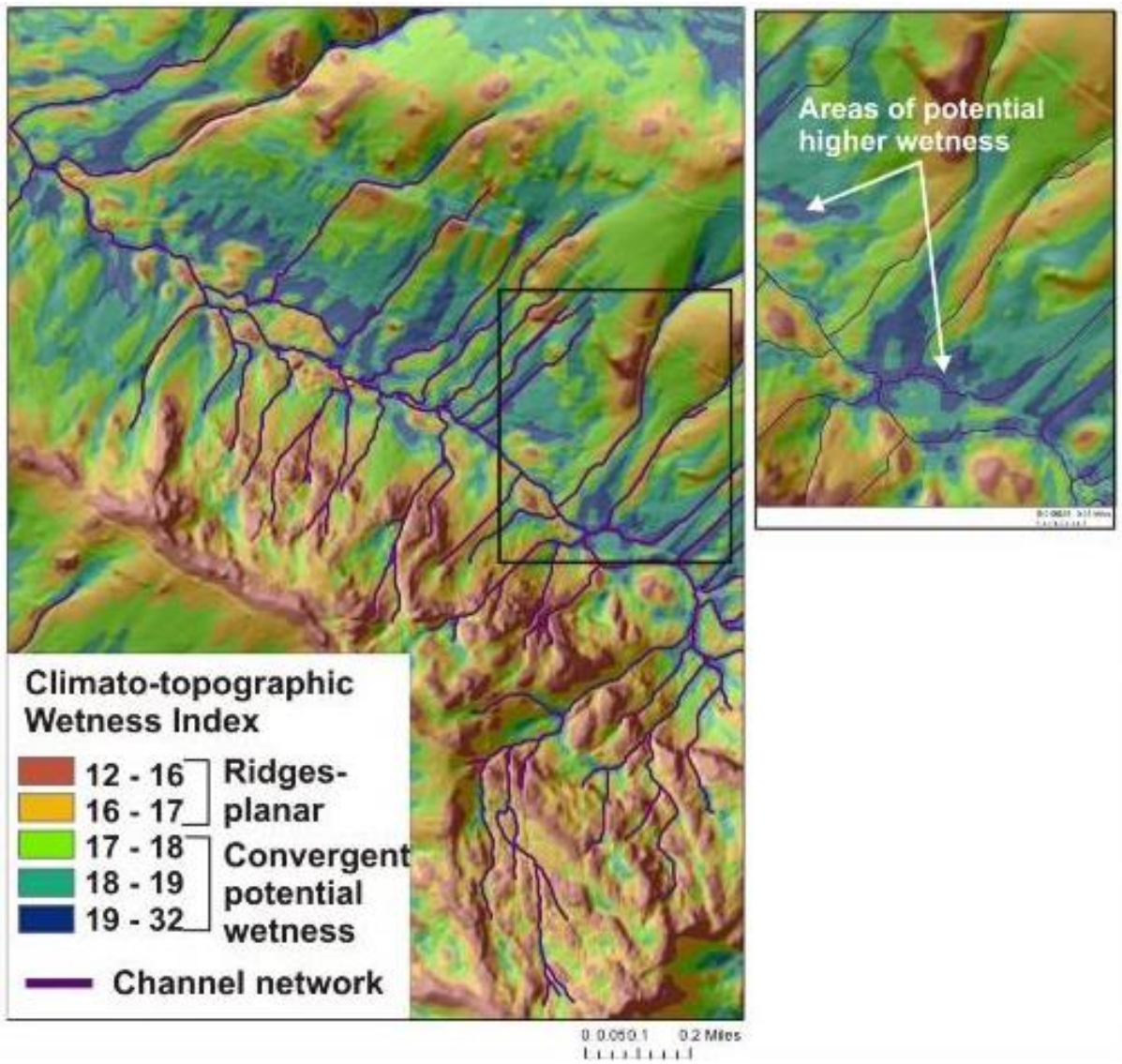

Figure 14. The climate-topographic wetness index in a portion of the Puyallup River watershed.

4.2.8. *Hydrogeomorphic Indicator: Depth to Impermeable Layer*

Low-permeability materials that can impede the downward movement of water include bedrock, glacial sediments such as till and lake beds, and mineral precipitates. Information on the location and extent of impermeable layers will vary significantly across watersheds, depending on the type and quality of geologic and soils mapping available (**Figure 15**).

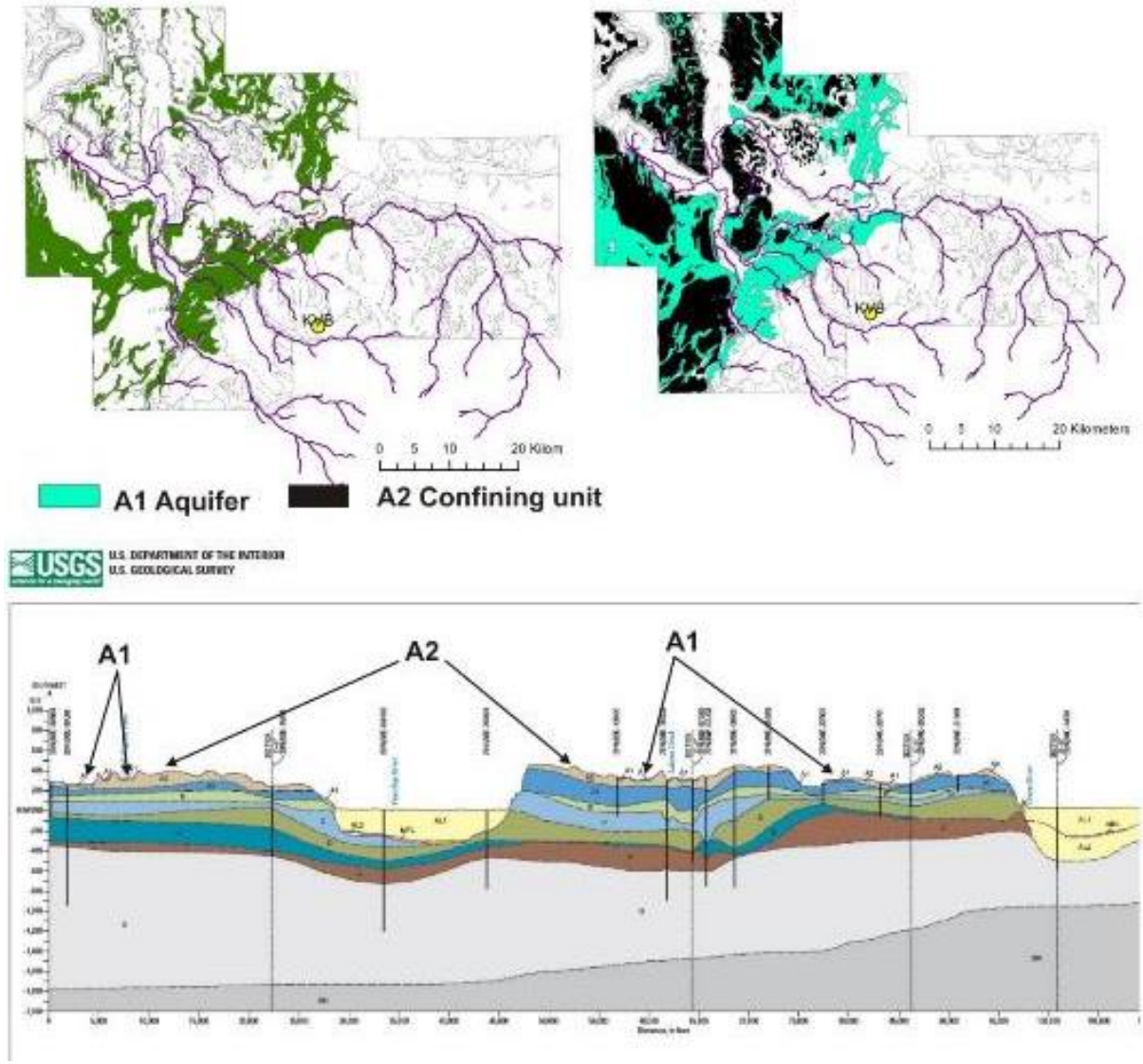

Figure 15. An example of impermeable strata in the Puyallup River watershed.

Low-permeability layers within the geological strata, like lacustrine sediments or tills (Figure 15), are one type of hydrogeomorphic control in WIP. For example, in the figures above (adapted from Welch et al. 2015), unit A2 (till and lacustrine deposits) forms a low-permeability layer underlying unit A1, a high-permeability layer composed of gravel and recessional outwash. Low-permeability strata may also form due to watershed disturbances, such as fires, that lead to erosion and downslope deposition of fine sediments. Local low-gradient areas, particularly closed depressions, have a higher likelihood of accumulating fine sediments, leading to lower-permeability soils. However, conventional soil mapping is unlikely to identify these areas, given the micro-topographic controls on hillslope erosion and deposition. We do not include an impermeable soil component in depressions as a hydrogeomorphic indicator. Future versions of WIP could include one and it could be linked to the erosion potential of the closed-depression drainage area.

4.2.9. *Suitability Curves and Weightings*

Proposed suitability curves for each of the five hydrogeomorphic indicators are shown in **Figure 16**. We used professional judgement to define the provisional suitability curves, because we did not find wetland suitability curves in the literature. The Depression Relative Depth curve is designed to reflect wetness concentrated in the lower portions of the depressions. Index values approach one as relative depth approaches one meter. The Depth to Stream/River water table and Depth to Lake/Pond water table are the same, with a maximum suitability score (1.0) associated with a threshold depth to water of less than or equal to 0.3 m (NRC 1995). Depth-to-water-table thresholds typically are associated with time-duration thresholds (Skaggs et al. 1994). We do not include that in the WIP model, because it is not

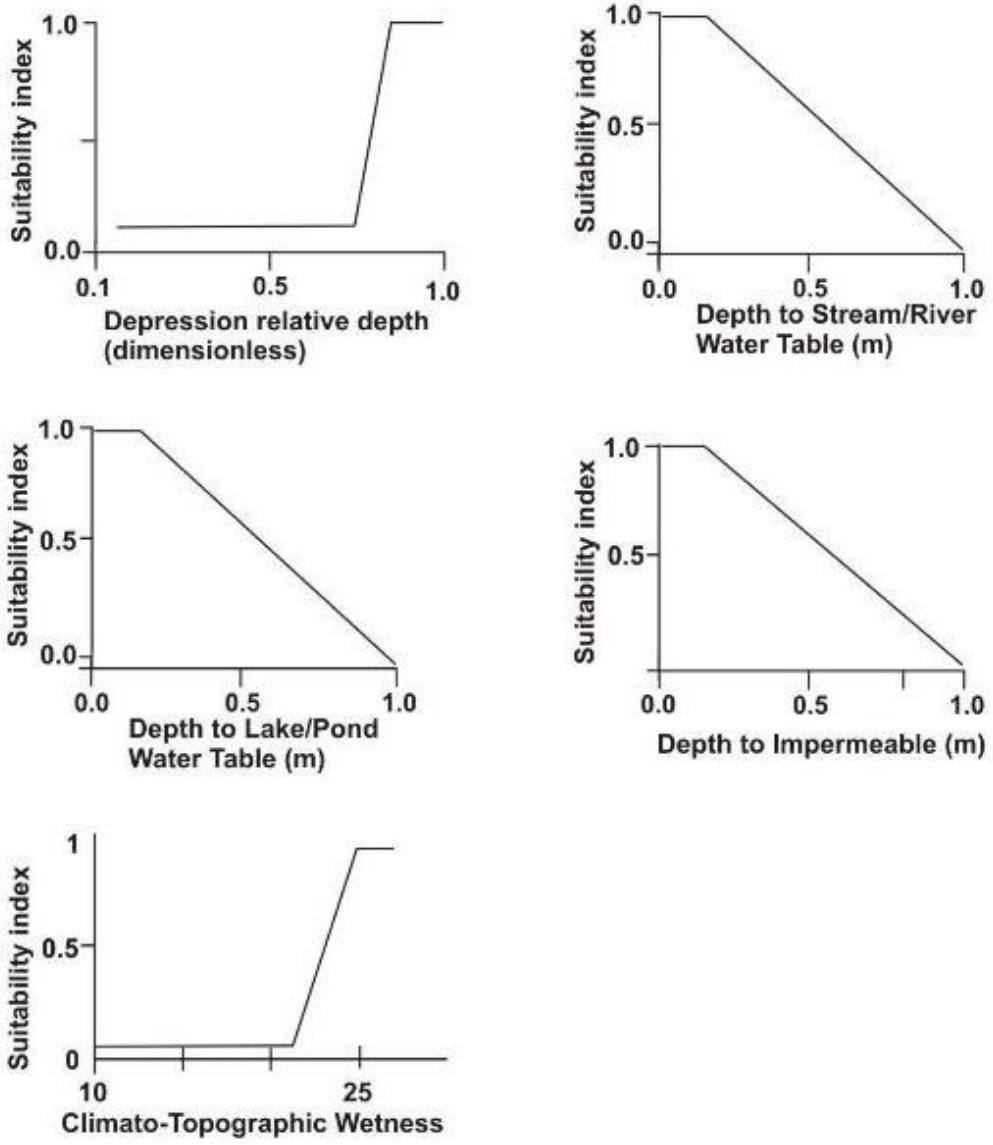

Figure 16. The provisional suitability curves for the five hydrogeomorphic indicators in WIP.

necessary, given our aim of identifying semi-permanent wetland formation conditions. The curve linearly drops off for depths greater than 0.3 m and goes to zero at a depth of one meter. Depth-to-impermeable layer has the same suitability curve. The range of the climate-topographic wetness index is about 12 to 35. Ridges have values of 10 to 15. Areas of convergence produce values above 16. The break point on the suitability curve, estimated using professional judgement, is at a CTI value of 16 and attains the maximum of suitability index = 1 at a CTI of >=25. Hydrogeomorphic indicator suitability curves are adjustable in the WIP ArcMap tool.

Not all hydrogeomorphic indicators may have the same influence on the inferred likelihood of wetland occurrence. For example, the depth-to-water table in streams/rivers and lakes/ponds might represent a more robust hydrogeomorphic indicator in certain areas, with greater predictive power, compared to depth to impermeable layer, topographic wetness index, and closed-depression relative depth. This is because depth to water can be based on observed locations with surface water, whereas the other indicators represent the inferred potential for shallow depth to water. Hence, the five hydro-geomorphic indicators can be given different weightings (b1…bi, Equation 4) ranging from 1.0 to less than 1.0 (**Table 5**) based on professional judgement. Weightings are adjustable in the WIP ArcMap tool.

Table 4. Provisional weighting values used in calculating the logit (Eq. 4).

Hydrogeomorphic wetland indicators in WIP	**Weighting (b_1…b_5) in Eq. 4[1]**	**Comment**
1) Closed depression, relative depth	0.6	Third highest because closed depressions generally require the inclusion of other hydrogeomorphic indicators
2) Stream/river water table, depth to water	1.0	Highest weighting because of confirmed water table near ground surface
3) Lake/pond water table, depth to water	1.0	Highest weighting because of confirmed water table near ground surface
4) Depth to impermeable layer; includes where depth goes to zero at outcrops	0.8	Next highest weighting because impermeable should promote ponded water tables, but mostly unverified
5) Climo-topographic wetness index	0.5	Fourth highest because CTI is only an indicator of concentration of subsurface flow. However, could be locally higher in depressions

[1] Weightings are adjustable in the WIP ArcMap tool. Alternatively, all weightings could be set to 1.0. Weightings could be adjusted by calibrating Eq. 4 using a comprehensive wetland inventory (Phase 2 study).

Individual wetlands can be associated with more than one and often several hydrogeomorphic indicators. For instance, a depression may abut a hillside with a high topographic wetness index, an environment that may also be underlaid by an impermeable (glacial deposit) layer (**Figure 17**). The five hydrogeomorphic indicators can lead to a maximum of ten unique combinations of wetland indicators, per pixel, involving from one to four indicators (**Table 6**).

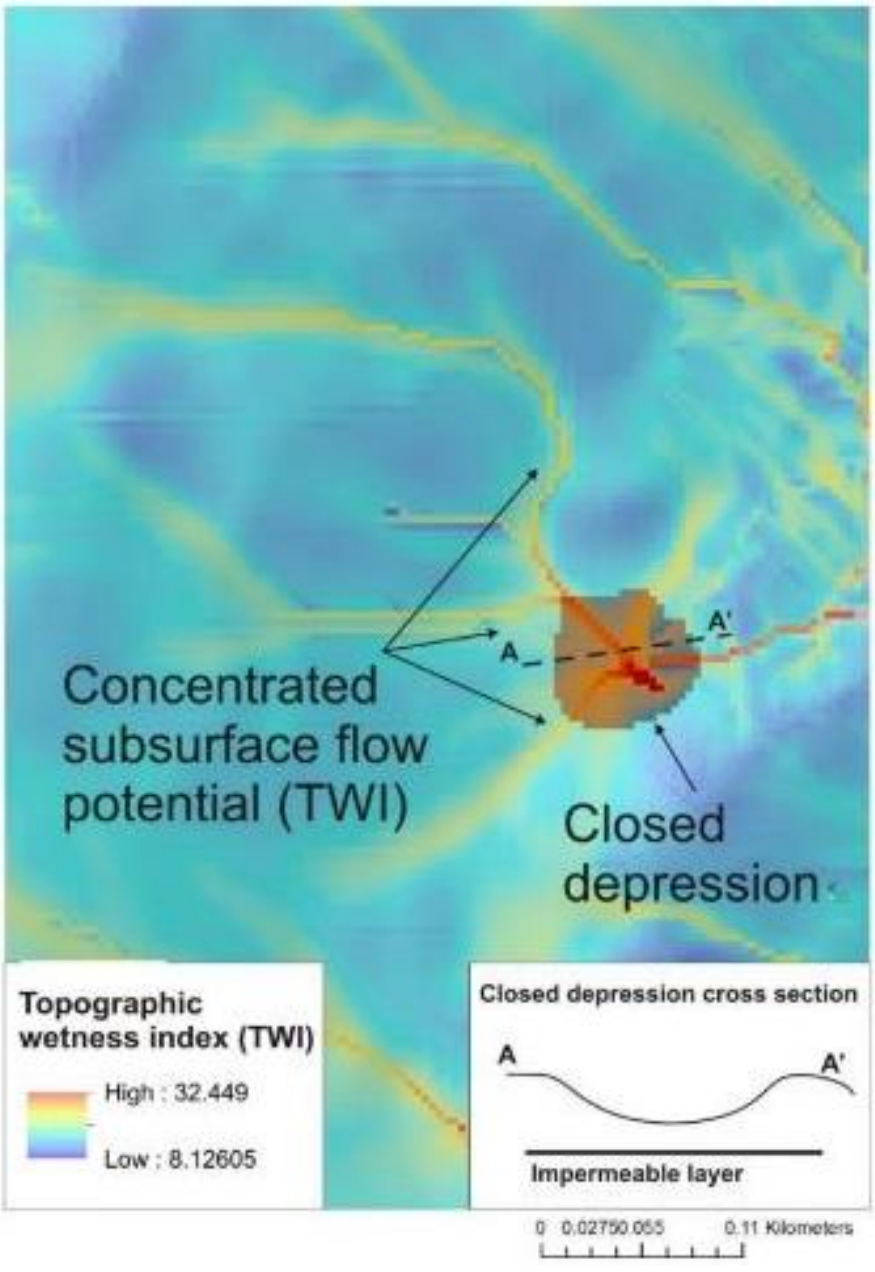

Figure 17. Multiple hydrogeomorphic processes can be associated with individual wetlands

Table 5. Combinations of pixel based hydrogeomorphic indicators and the processes they represent.

Number	Hydrogeomorphic indicators[1]	Processes
1	CWI	Subsurface flow concentration
2	CWI + D_d	Subsurface flow concentration; relative depression depth (potentially higher deposition – higher fines)
3	CWI + d_R	Subsurface flow concentration; close depth to river/stream water table
4	CWI + d_L	Subsurface flow concentration; close depth to lake/pond water table
5	CWI + d_i	Subsurface flow concentration; close to mapped impermeable layer
6	CWI + D_d + d_R	Subsurface flow concentration; relative depression depth (higher deposition – higher fines); close depth to river/stream water table
7	CWI + D_d + d_L	Subsurface flow concentration; relative depression depth (higher deposition – higher fines); close depth to lake/pond water table
8	CWI + D_d + D_i	Subsurface flow concentration; relative depression depth (higher deposition – higher fines); close to mapped impermeable layer
9	CWI + D_d + d_R + D_i	Subsurface flow concentration; relative depression depth (higher deposition – higher fines); close to mapped river/stream water table; close to mapped impermeable layer
10	CWI + D_d + d_L + D_i	Subsurface flow concentration; relative depression depth (higher deposition – higher fines); close to mapped lake/pond water table; close to mapped impermeable layer

[1] CWI – climate-topographic wetness index; D_d – closed depression; d_R – stream/river, depth to water table; d_L – lake/pond, depth to water table; d_i – depth to impermeable layer. In pixels with both d_R and d_L (areas of overlap between lake adjacent areas and river adjacent areas), the shallowest depth to water is selected and thus they are not combined. d_R or d_L and d_i can occur coincidentally.

4.2.10. *Removing Non-Soil Areas from WIP*

Soils are required to create a wetland. WIP's logistic equation and the five hydrogeomorphic indicators do not address the presence or absence of soil. Lakes can be bordered by areas that lack soil, such as talus and bedrock. Wide alluvial river valleys will lack soils. Thus, during application of WIP, soil-free areas are removed. These include areas with active alluvial channels, bedrock, talus, lakes and human infrastructure (Step 8 in WIP workflow, **Figure 6**).

The National Agriculture Imagery Program (NAIP) acquires aerial imagery (4 band digital orthophotos)) during growing seasons across the U.S. The Normalized Difference Vegetation Index (NDVI) is used to identify the absence of vegetation, and hence soil free areas in WIP. NDVI is calculated as:

$$NDVI = (NIR - Red)/(NIR + Red) \quad \text{Eq. 6}$$

where NIR is the spectral reflectance measurements acquired in the red (visible) and near-infrared (NIR) wavelengths. Following application of WIP values, NDVI values (approximately less than 0.4) are used to identify and exclude soil-free areas (**Figures 18 and 19**).

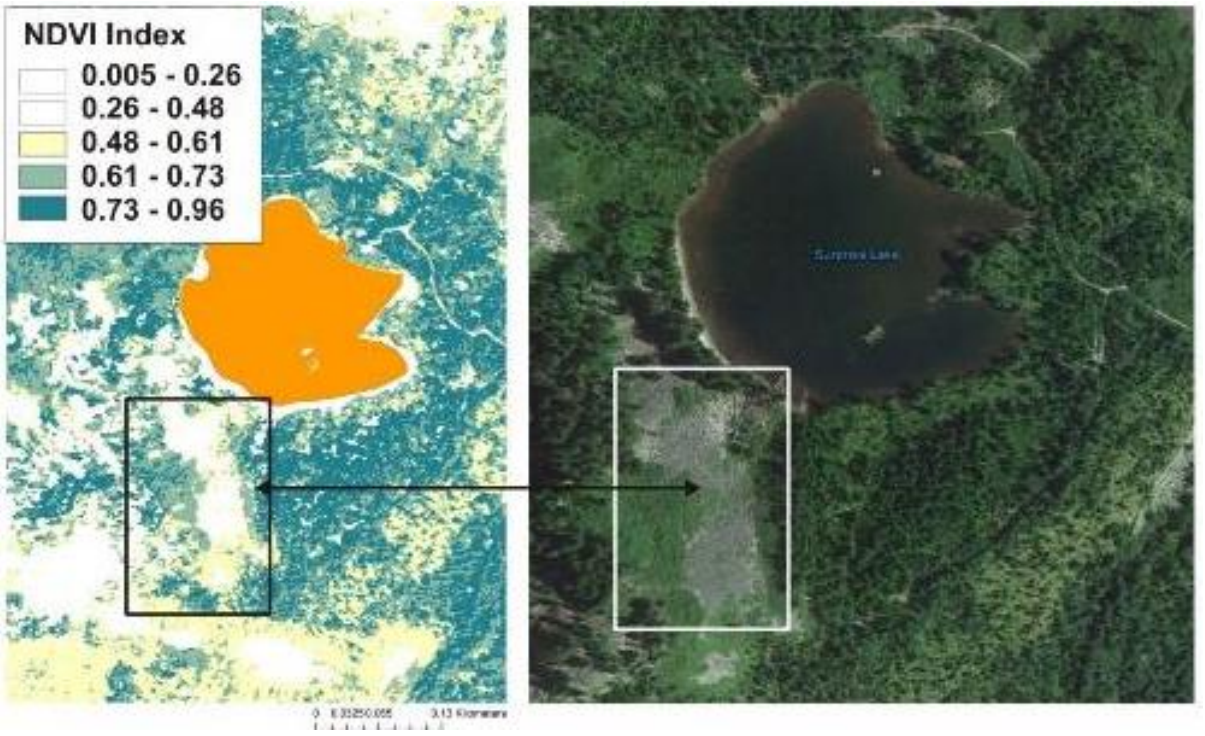

Figure 18. An NDVI threshold is used in WIP to identify soil-free talus and bedrock that cannot support wetland development.

Lakes can be omitted from the NDVI-based removal of non-soil pixels, because lake borders may be drawn poorly (in the NHD) and WIP scores near lake boundaries may indicate wetlands. In ArcMap, an analyst can simply place the lake layer above the WIP score raster shapefile to visually eliminate WIP scores in mapped lakes.

4.2.11. *Aggregation of Pixels to Polygons of Potential Wetlands*

WIP produces pixel-scale scores with a spatial resolution (pixel size) dictated by the DEM resolution (**Figure 20**). Wetlands extend beyond individual pixels on a map; they are generally shown as polygons in a GIS (e.g., NWI datasbase). From a policy perspective, wetlands less than 0.1 ha (31.6 m x 31.6 m) are the minimum for surveying and managing in the Pacific Northwest (Janisch et al. 2011). However, smaller wetlands (to 0.1 acre) may also be of interest to analysts. Selection of a size minimum can be set by the analyst in the WIP ArcMap tool.

Depending on the threshold WIP score that is used to identify potential wetland areas, the pixel-based wetland index may be aggregated into polygons. This can be done using tools in ArcMap or using software like eCognition. This component of WIP is part of the Phase 2 project.

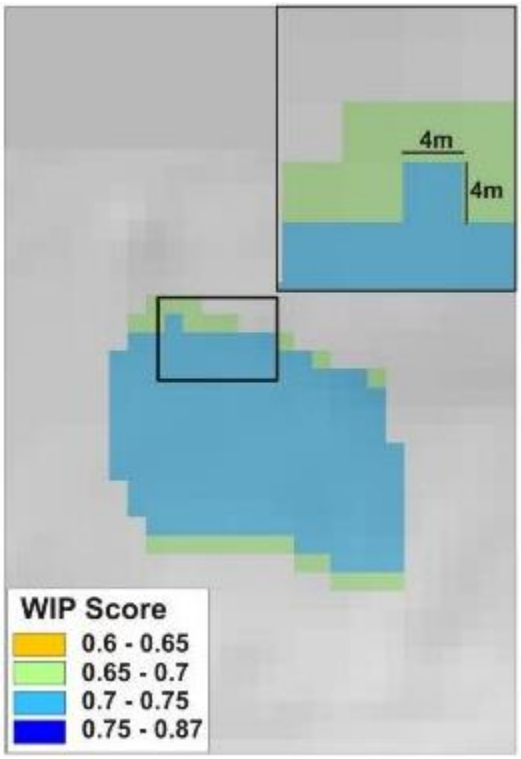

Figure 20. Pixel scale WIP scores.

4.3. Wetland Intrinsic Potential – ArcMap Interface

WIP is designed as a stand-alone tool in ArcMap (as an ArcMap add-in). The WIP ArcMap tool is organized according to the first eight modeling steps (**Figure 6**). Each step within the ArcMap add-in are illustrated in **Figures 21** through **24**.

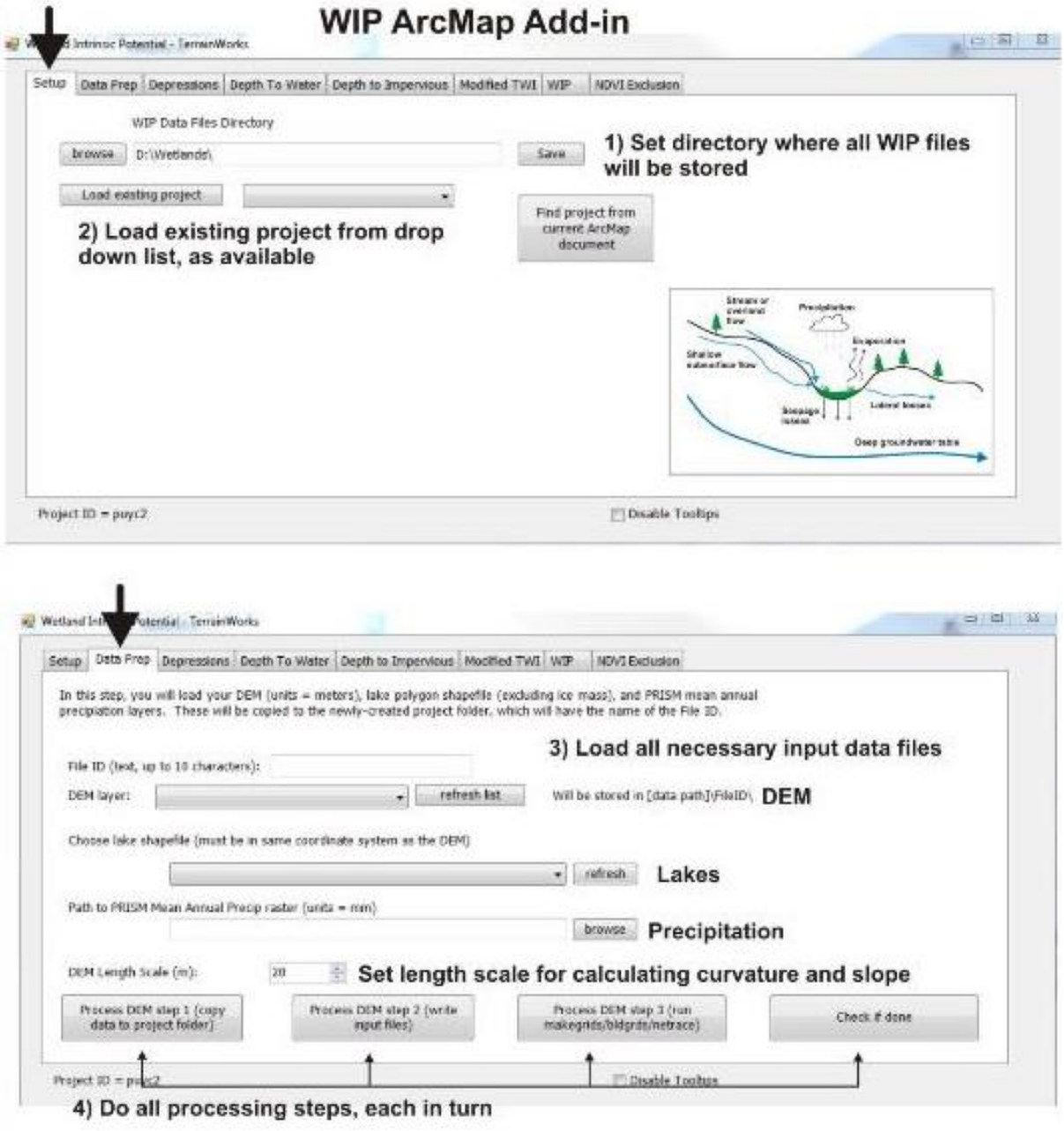

Figure 21. WIP's ArcMap tool interface, steps one and two.

Figure 22. WIP's ArcMap tool interface, steps three and four.

Figure 23. WIP's ArcMap tool interface, steps five and six.

1

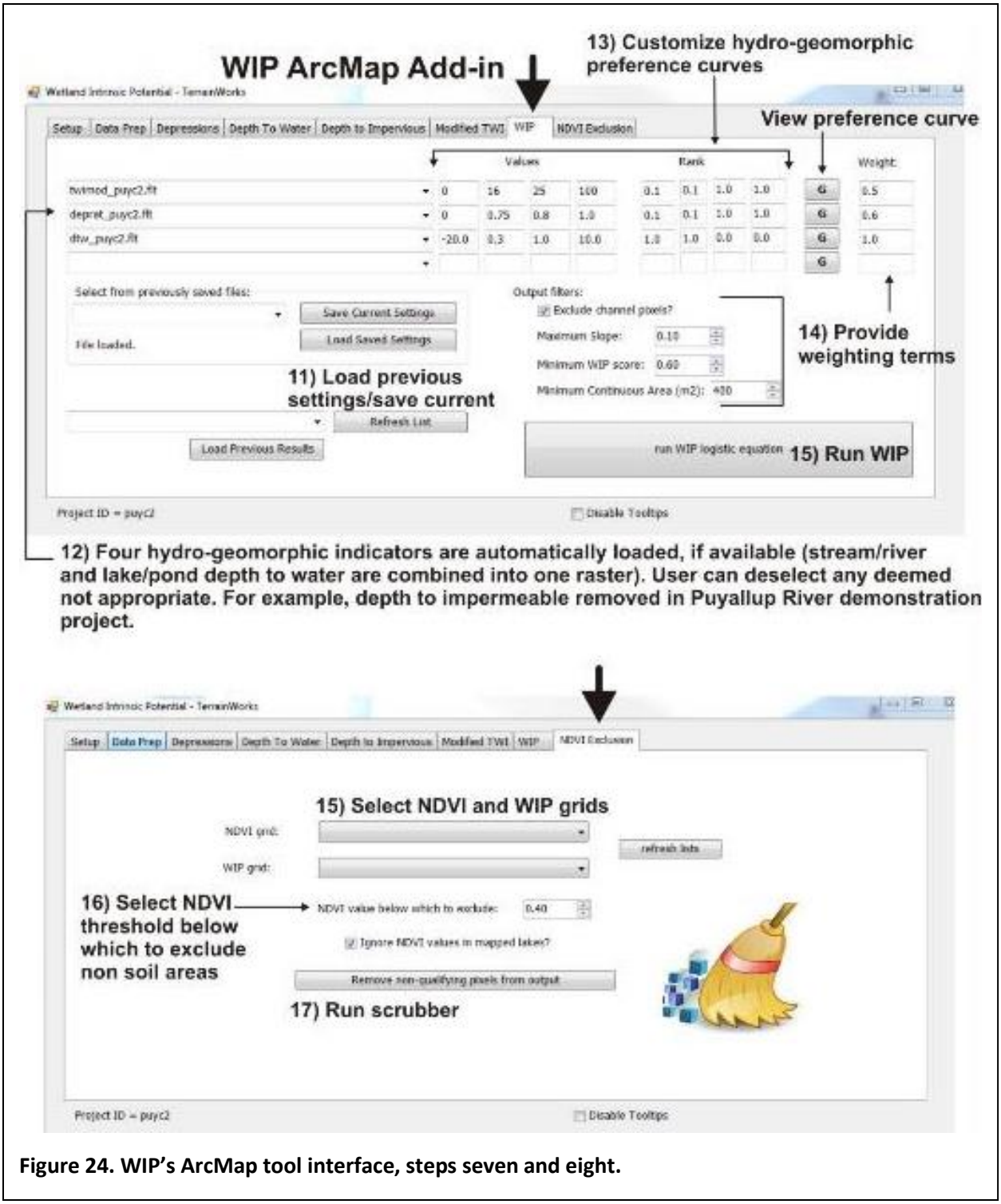

Figure 24. WIP's ArcMap tool interface, steps seven and eight.

WIP datafiles are in three groups of files: 1) WIP input rasters for stream/river depth-to-water, lake/pond depth-to-water, closed depressions, depth to impermeable layer, and climate-topographic wetness index, 2) WIP suitability curve index scores, and 3) WIP outputs (Figures 25 – 27).

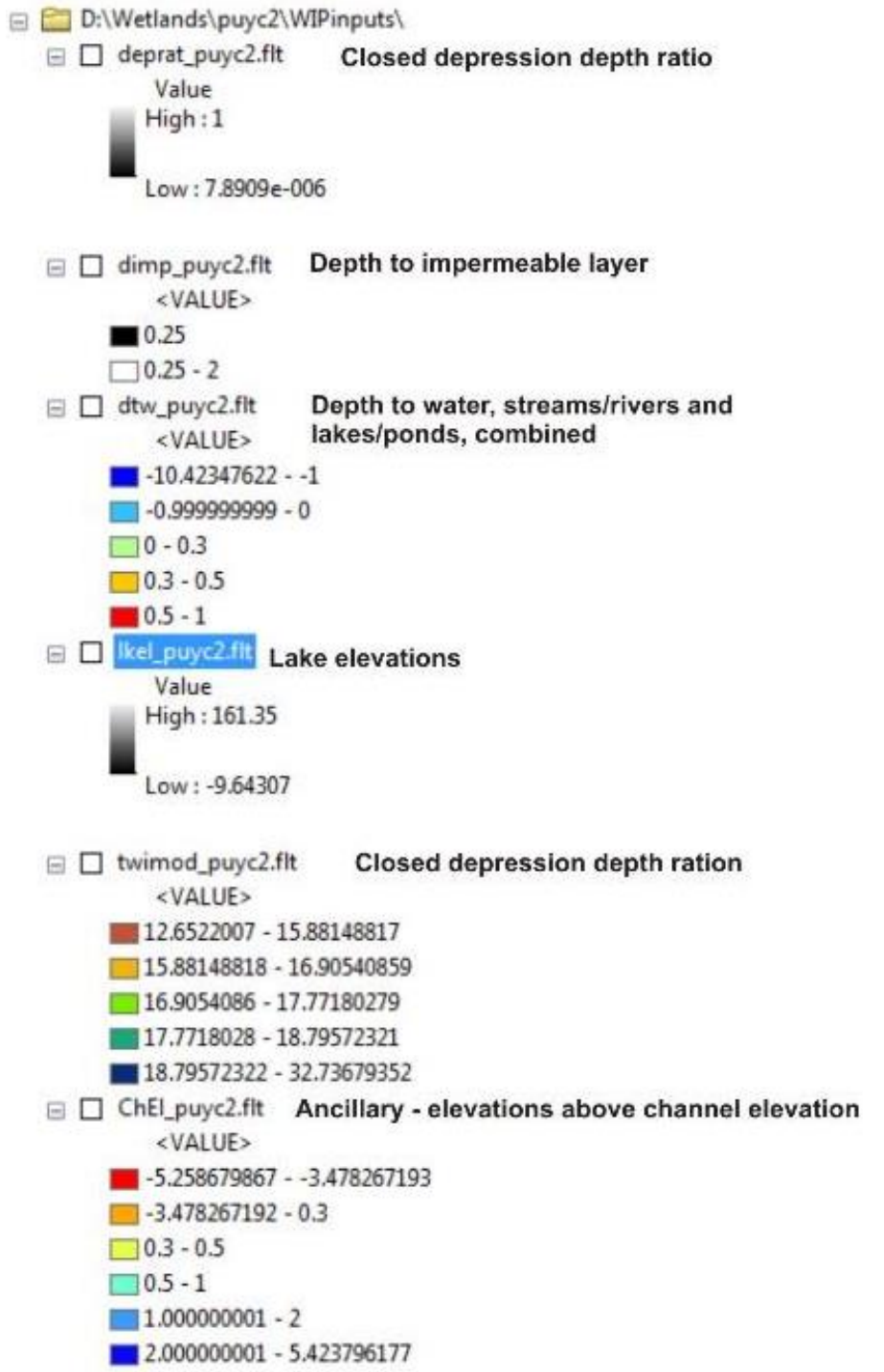

Figure 25. WIP hydrogeomorphic indicator values in ArcMap table of contents.

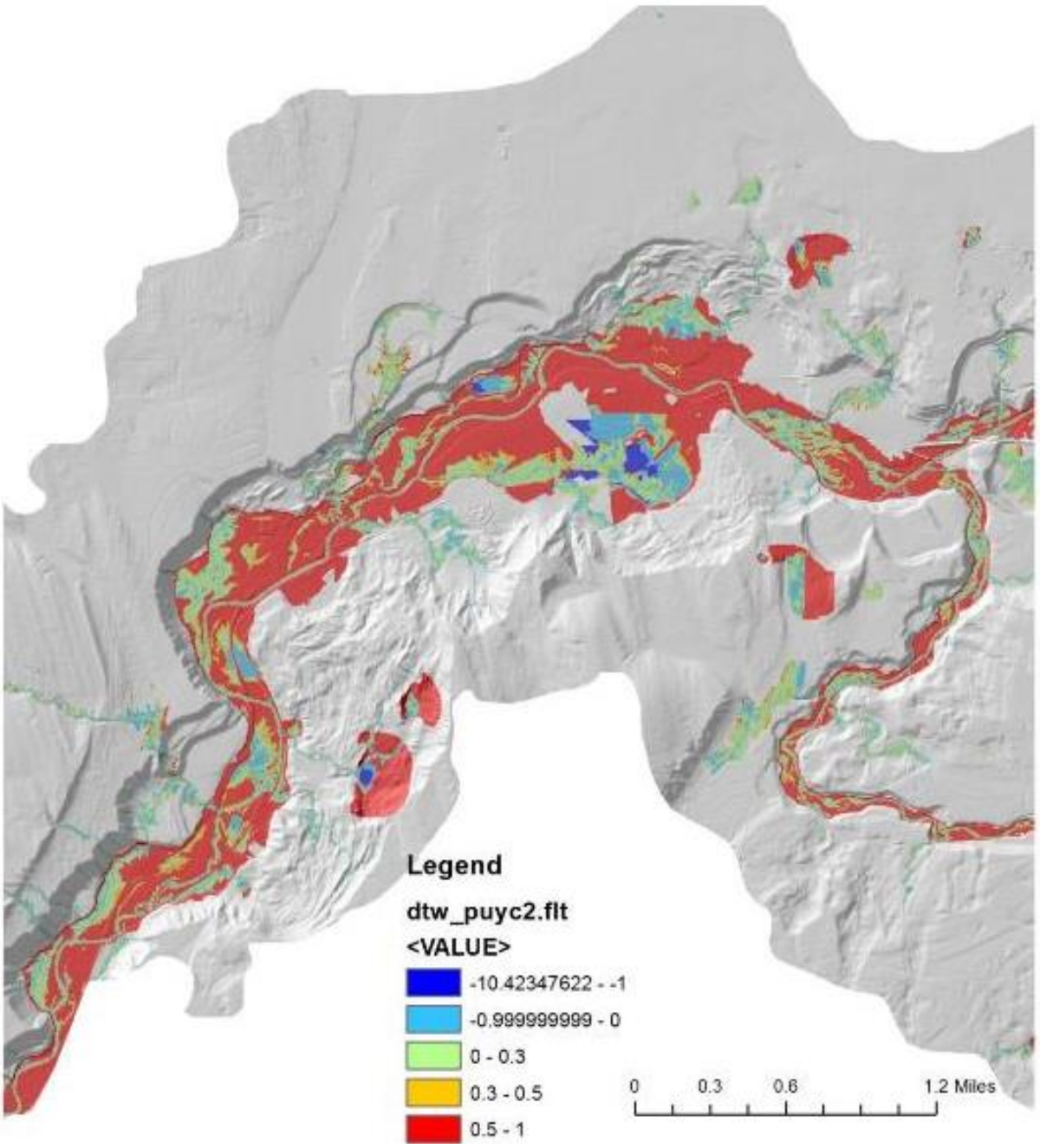

Figure 26. An example of stream/river and lake/pond depth to water (combined).

1

2

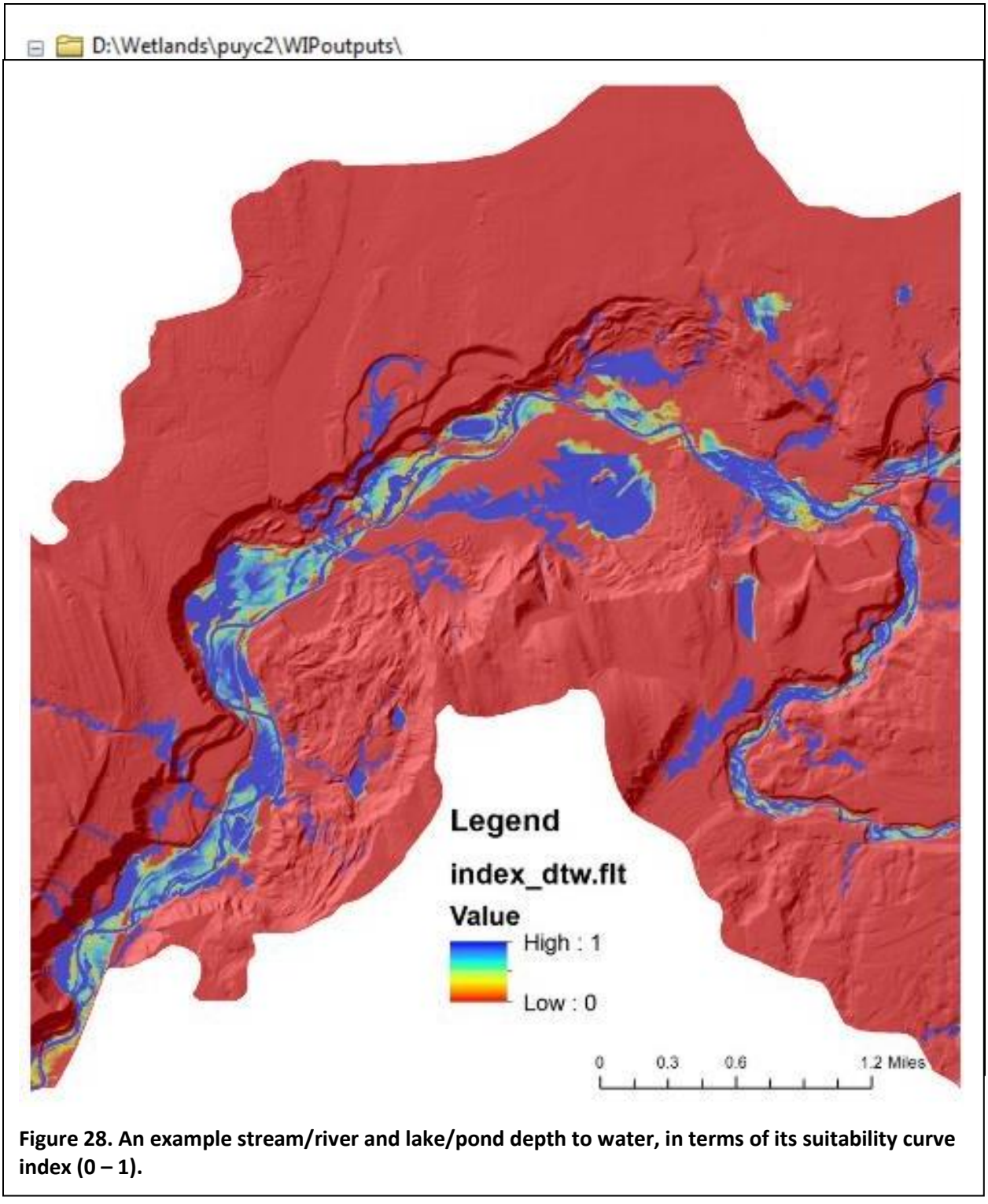

1

Figure 28. An example stream/river and lake/pond depth to water, in terms of its suitability curve index (0 – 1).

5. Demonstration of WIP in the Puyallup River Watershed

5.1. Study Area

The northwest – southeast trending Puyallup River watershed (2,694 km^2) drains to the southern portion of the Puget Sound in Washington state (**Figure 29**). Its larger tributaries (Mowich, White and Carbon Rivers) extend into Mt. Rainier National Park, draining glaciated terrain. Clearwater and Greenwater forks are non-glacier tributaries. The Puyallup River runs through the cities of Tacoma, Fife, Puyallup, Sumner, and Orting. The lower reaches of the Puyallup River were straightened with levees and revetments for flood control. Mud Mountain Dam is located on the White River at RM 29.6. The Puyallup River and its tributaries support native Chinook salmon (Oncorhynchus tshawytscha), coho salmon (O. kisutch), chum (O. Keta) and pink (O. gorbuscha) salmon. Steelhead (O. mykiss) and coastal cutthroat trout (O. clarkii clarkii) also occur in the basin.

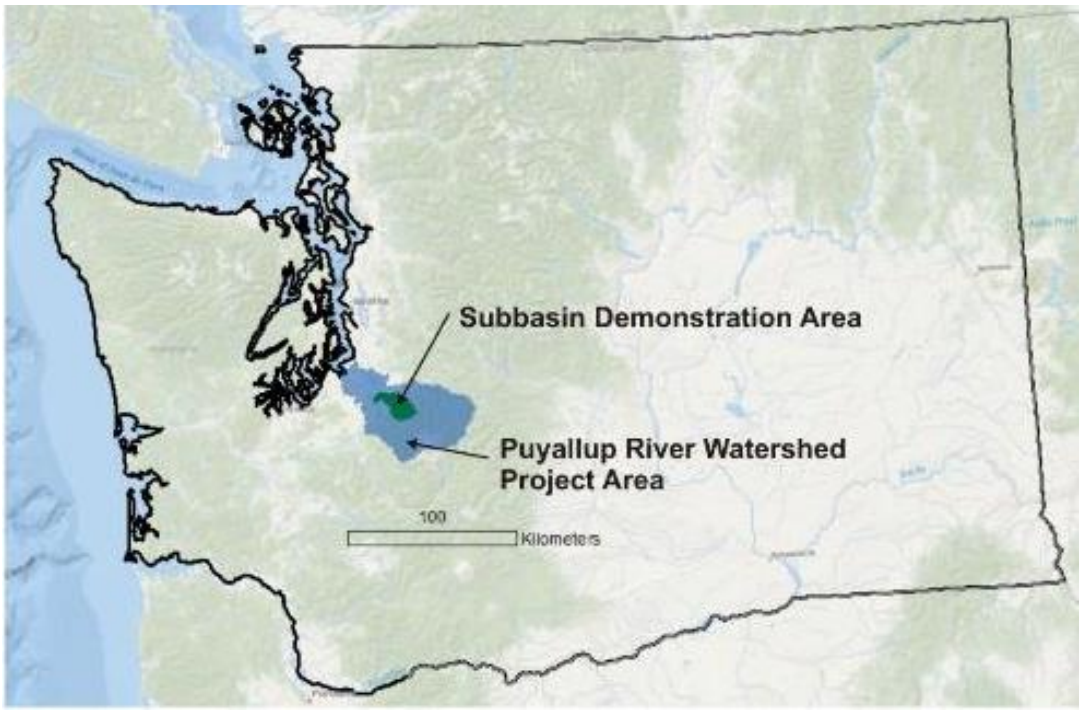

Figure 29. The Puyallup River watershed study area and the smaller subbasin used in the development of WIP and its demonstration application.

Annual precipitation ranges from 76 to 100 cm near the river outlet by Tacoma to 300 cm in the upper reaches on and near Mt. Rainier (4,392 m). The lower one-third of the Puyallup River watershed is underlain by a northwest-thickening sequence of unconsolidated glacial (till and outwash) and interglacial (fluvial, lacustrine, and mudflow) deposits. Sedimentary and volcanic bedrock underlie the unconsolidated deposits and crop out in the foothills along the southern and eastern margins of the study area. The upper parts of the watershed near Mt. Rainier are comprised of volcanic rocks (andesite) and volcanic mudflow deposits.

Groundwater in unconsolidated glacial and interglacial aquifers generally flows to the northwest towards Puget Sound, and to the north and northeast towards the Puyallup River, White River, and Green River valleys. These generalized flow patterns are complicated by the presence of low-permeability confining units and bedrock that separate discontinuous bodies of aquifer material and act as local groundwater-flow barriers (Welch et al. 2015). Major lakes include Sawyer, Tapps, Spanaway and Kapowsin. There are numerous smaller lakes formed by glaciation (kettle and moraine) and mudflow deposition.

Two HUC 6th subbasins (225 km^2) were selected within the Puyallup River watershed for the demonstration analysis contained in this report (**Figure 29**).

5.2. Puyallup River Virtual Watershed and Other Data Layers

A virtual watershed was developed for the Puyallup River basin inclusive of a synthetic river network. Approximately 70% of the lower Puyallup River watershed is covered with 4-m LiDAR (obtained from the University of Washington). The LiDAR DEM is merged with the 10 m National Elevation Dataset (DEM) to build a seamless, watershed-wide DEM[15]. The entire project subbasin (**Figure 29**), South Prairie Creek, is covered with LiDAR. The pixel size is 2m.

Other GIS data layers included: 1) mean annual precipitation (PRISM), 2) NHD waterbodies, 3) National Wetland Inventory polygons, 4) NAIP 1-meter imagery and 5) U.S.G.S. hydro-geologic mapping of aquifers and impeding layers in the lower third of the watershed (Welch et al. 2015).

Bankfull-channel geometry is calculated using regional regressions (Magirl and Olsen 2009):

- width (m) = 7.35 * mean annual flow ($m^3\ s^{-1}$) $^{0.45}$;
- depth (m) = 0.262 * mean annual flow ($m^3\ s^{-1}$) $^{0.37}$

Mean annual flow is from a regional regression by Kresch (1998):

- Mean annual flow ($m^3\ s^{-1}$) = 0.022*(drainage area $^{0.933}$)*(mean annual precipitation $^{1.48}$).

Mean annual precipitation is obtained from PRISM.

5.3. Application and Result

We evaluate the WIP predictions for each of three principle wetland geographies: 1) closed depressions, 2) riverine corridor, and 3) lacustrine fringe. Seep wetlands, driven by outcrops of impermeable layers, were omitted because of the low resolution of the permeability input data. High-WIP-score (> 0.6) contiguous groups of pixels with a combined area less than 0.1 acre were also removed[16]. Pixels within channels based on predicted channel width are set to 'no data'. Additional channel-adjacent areas are

[15] DEM merging was done using the Merge program from the open source Netstream suite. It creates a seamless DEM that accounts for elevation differences where merged DEMs meet or overlap. It is available from Dan Miller (dan@terrainworks.com).

[16] This processing is done in the WIP Fortran program, which delineates polygons based on contiguous groups of cells exceeding threshold WIP values.

also eliminated, if the delineated area is less than 6 m (3 pixels) wide (per channel side). NDVI is used to remove non-soil areas from WIP predictions. Only WIP scores > 0.6 are shown in the illustrative figures below.

5.3.1. *Closed Depression Wetland Potential*

Closed depressions occur in riverine corridor and lacustrine areas, and in associated with earthflows and glaciated areas (**Figure 9**). In the study area, there are 47,000 closed depressions. Half of these are one pixel in area (4 m x 4 m = 16 m^2); another 25% are two pixels in area. In accordance with the general minimum size of wetlands for management and conservation policies in the Pacific Northwest (0.1 ha, Janisch et al. 2011), we applied a minimum-size threshold for closed depressions of 1,000 m^2 (62.5 pixels). There were 853 closed depressions greater than 1,000 m^2 used in the WIP analysis. Ninety percent of closed depressions were less than 10,000 m^2 (2.5 acres); the largest was 500,000 m^2 (123 acres) (**Figure 30**). Depths of closed depressions ranged from 0.1 m to 22 m with 80% less than 2 m deep (**Figure 30**). Thirty nine of the 853 depressions (4.5%) coincided with lakes in the NHD waterbody layer.

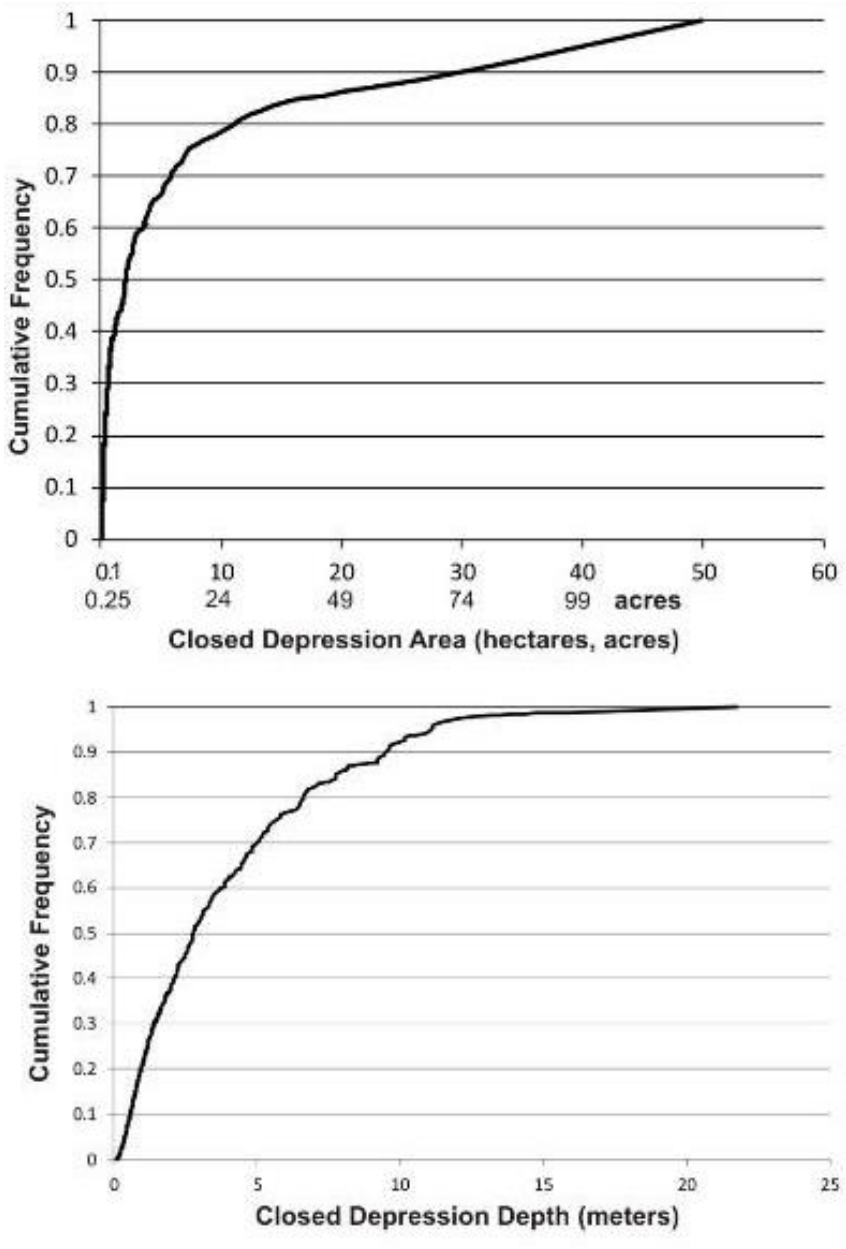

Figure 30. CDFs of closed depression areas and depths.

Closed depressions that occur near stream channels can have high WIP scores (**Figure 31**). In this example, the wetland with pixel scores of 0.7 to 0.8 is located on an actual wetland (visible in Google Earth), but is not included in the NHD Waterbodies (swamp/marsh) nor the NWI database.

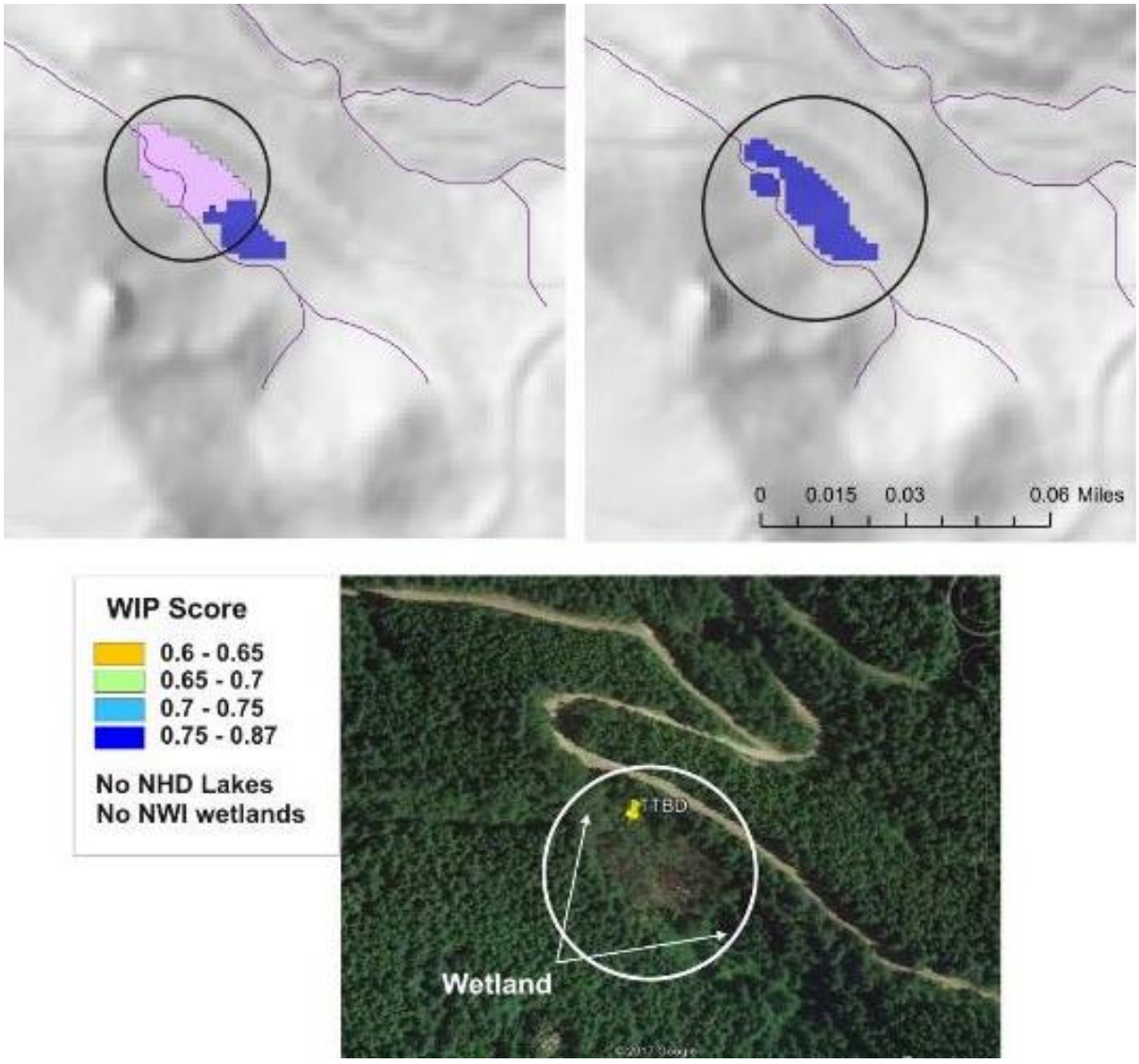

Figure 31. WIP scores associated with a closed depression influenced by a small stream.

5.3.2. *Riverine Corridor Wetland Potential*

WIP predicts relatively high scores along river corridors (including those abandoned) that have shallow depths to water (< 1 m) (**Figure 32**). Higher values occur within the riverine zone also due to depressions, which may be closed or partially open (side channels).

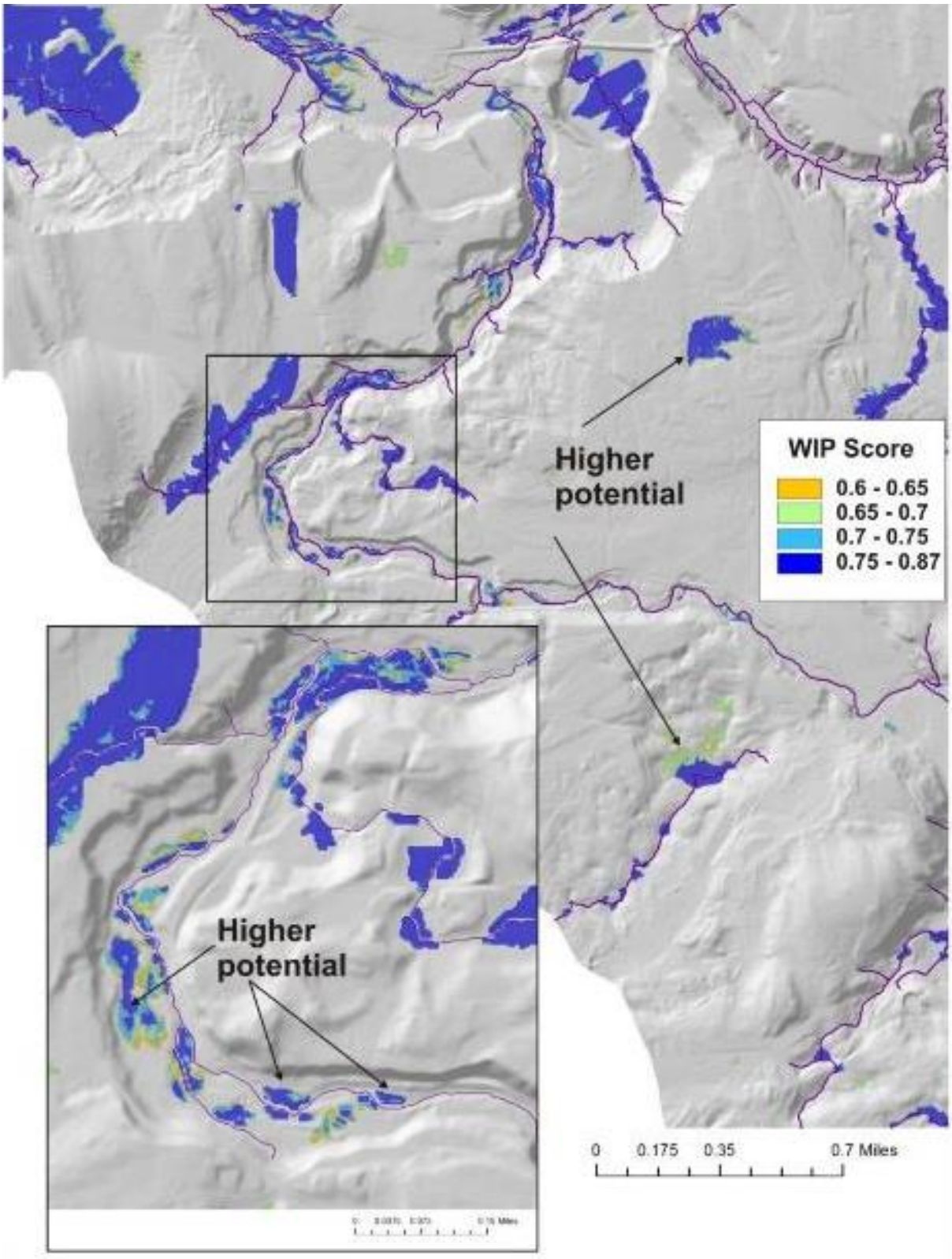

Figure 32. High WIP scores along riverine corridors indicate topography where side channels and natural levees create local low areas with higher water tables.

1

The same area along the river corridor can be examined in the context of the NWI polygons (**Figure 33**). Numerous concentrations of high value WIP pixels (**Figure 33**) overlap with NWI polygons.

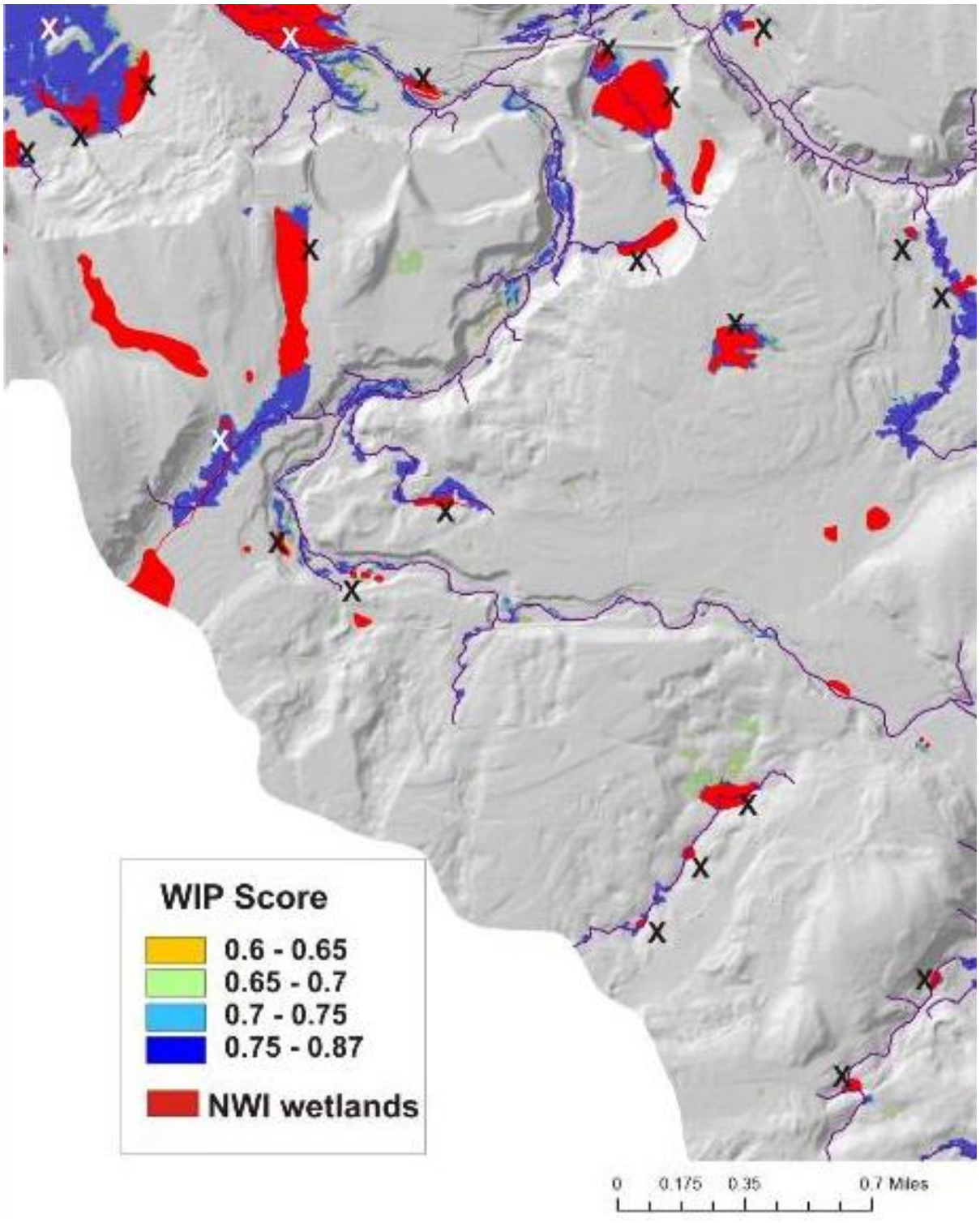

Figure 33. WIP scores along river overlaid with NWI polygons. X = areas of overlaps.

5.3.3. *Lacustrine Fringe Wetlands*

The third type of wetland in WIP represented in the Puyallup River watershed (subbasin study area) is the lacustrine fringe. Areas adjacent to lake or pond bodies have shallow depth to water and thus are areas that receive a high WIP score (**Figure 34**). Some lakes will also be contained within closed depressions that increase the WIP score. **Figure 34** shows how WIP captured an extensive wetland that was only partially included in the NWI database.

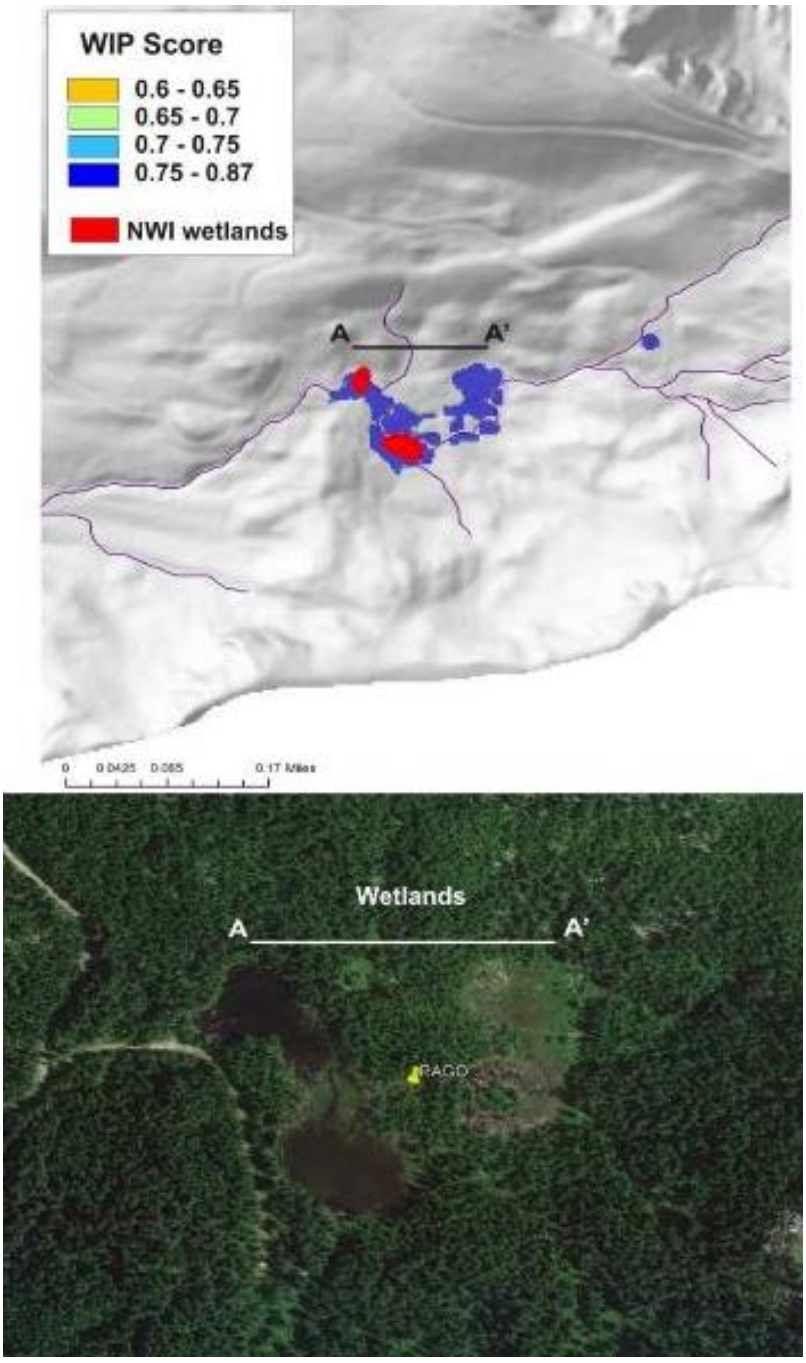

Figure 34. Lake-adjacent areas can have high WIP scores because of shallow depth to water.

The role of multiple hydrogeomorphic indicators in potential wetland development is apparent in WIP predictions. For example, a depression may be located within a riverine corridor, and located immediately adjacent to a hillside producing a high CTI index, three hydro-geomorphic indicators that produce a high WIP score (**Figure 35**).

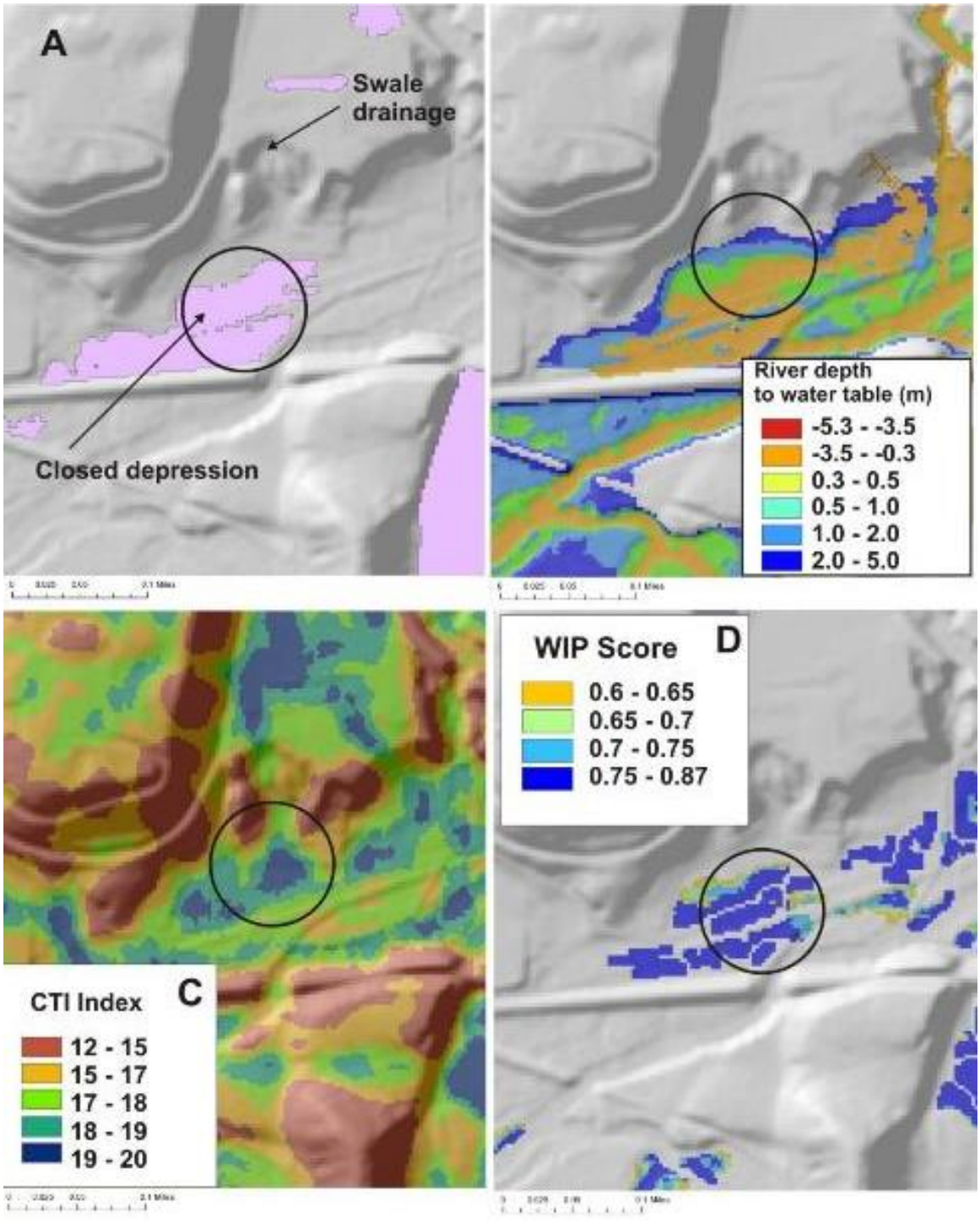

Figure 35. Three hydrogeomorphic indicators combine to create a high WIP score.

5.3.4. *WIP Wetland Screening and NHD/NWI Comparison*

To effectively apply WIP, an analyst may need to define a threshold WIP score from which to identify potential wetland areas. In this demonstration of WIP, we estimated the shape of the hydrogeomorphic indicator suitability curves (**Figure 16**) and the indicator weightings (b in Eq. 4, in Table 5). In Phase 2 of the wetland study, field data on forested wetland locations will be used to train or calibrate the WIP model to make more accurate predictions. To evaluate WIP scores, we compared them to wetlands within the NWI database and to areas outside of those wetlands in areas that likely have few or no wetlands (hillslopes, ridges) (**Figure 36**). The NWI database is no doubt incomplete, particularly under forest canopy. First, we calculated an average WIP score among all pixels that were located within individual NWI wetland polygons. We then calculated the average WIP score in the non-wetland areas. We also removed riverine corridors from the non-wetland polygons.

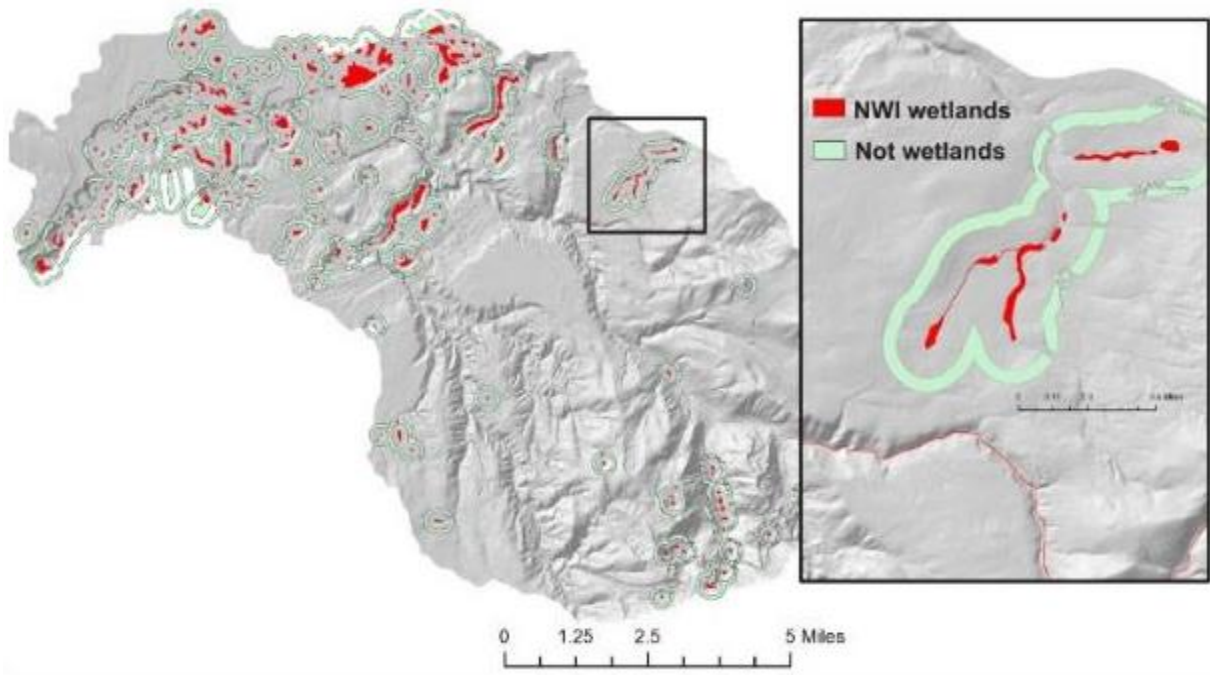

Figure 36. The NWI wetland and the non-wetland polygons that were used to calculate average WIP scores in NWI polygons and non-wetland polygons in the study basin.

Cumulative distributions of WIP scores within and outside of wetlands indicate very different populations (**Figure 37**). The comparative analysis revealed that the mean WIP score in the NWI wetlands and outside of the wetland areas is 0.76 and 0.68 respectively. The standard deviation of the WIP score in the NWI wetlands and outside is 0.03 (same for both). The pixel sample sizes for each were 102,482 and 1,036,052 respectively. T-tests for equal or unequal variance and unequal sample sizes indicated the two populations of WIP scores are significantly statistically different.

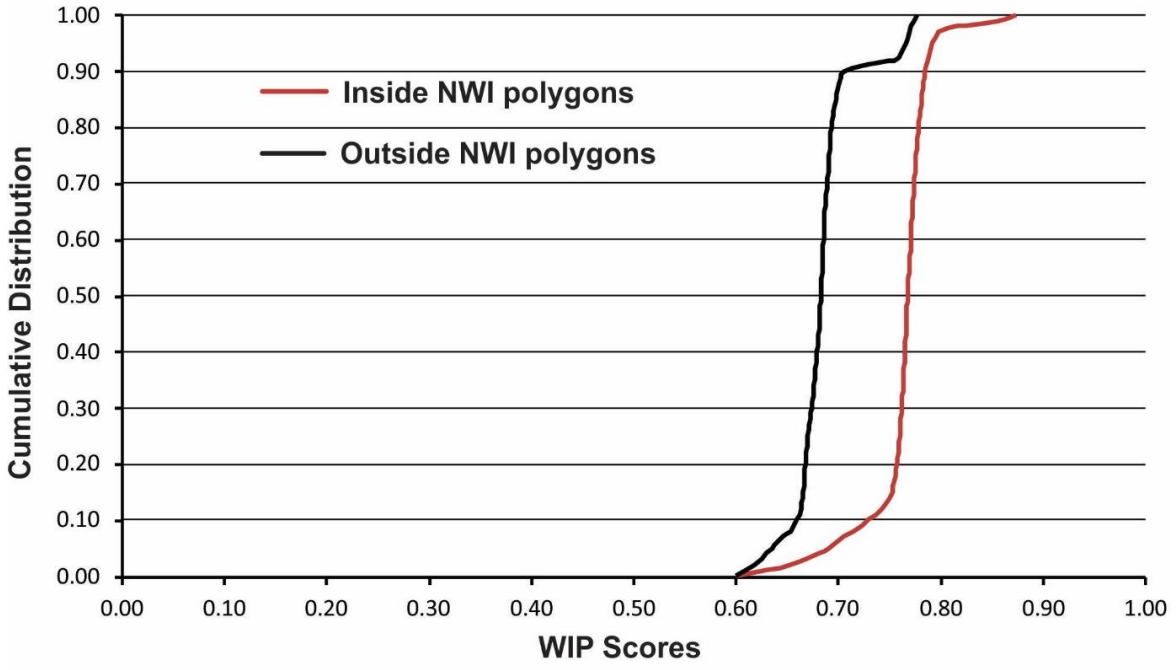

Figure 37. CDF of WIP scores inside and outside of NWI polygons.

The CDF of WIP scores indicates how they are distributed across the watershed. There is a marked inflection at a WIP score of about 0.74. Eighty-eight percent of scores are greater than 0.7 (**Figure 38**).

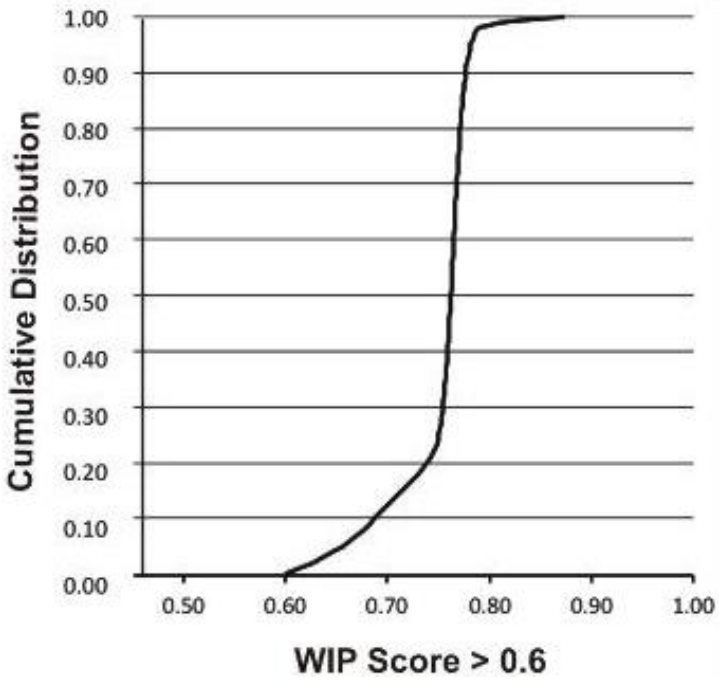

Figure 38. CDF of WIP scores.

Conducting a comprehensive statistical analysis of WIP scores compared to NWI polygons is beyond project scope and is planned for Phase 2. However, it is informative to visually compare WIP scores to mapped wetlands (NWI). In the upper watershed, every NWI polygon overlaps a clump of WIP pixels with scores greater than 0.7 (**Figure 39**). Fifteen of the 20 NWI polygons overlap NHD lakes/ponds, indicating that they are representing lacustrine fringe

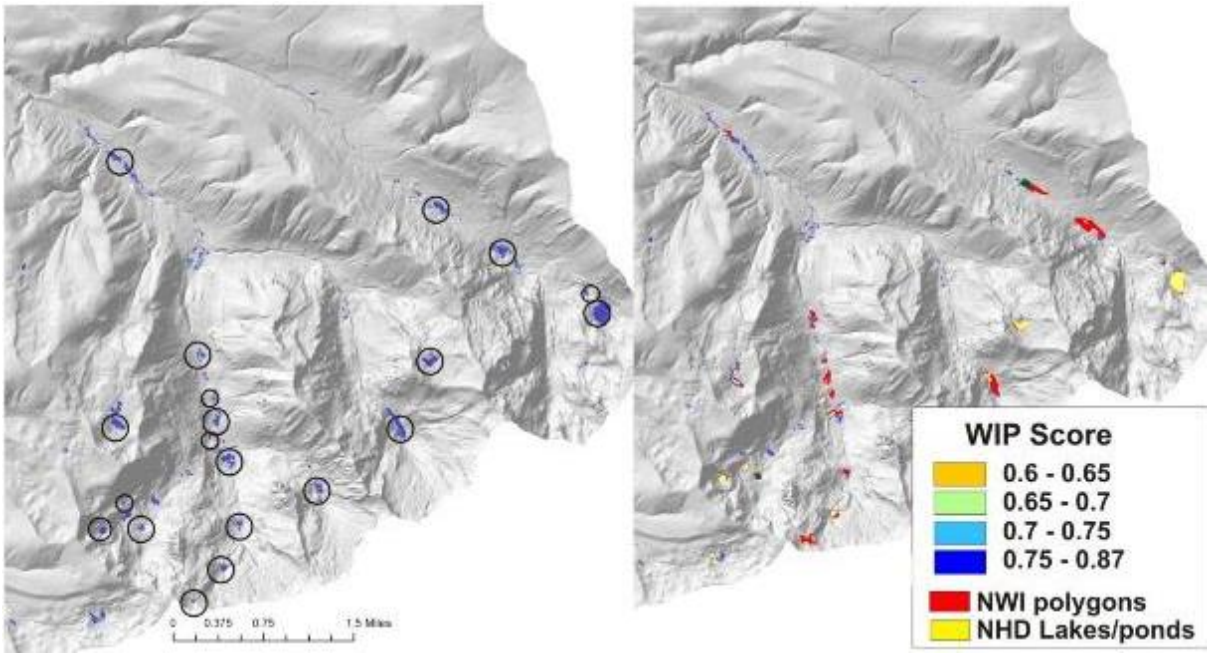

Figure 38. NWI polygons, NHD lakes, and WIP scores. Circles show where high WIP scores (> 0.7) overlap with NWI polygons, with almost a 100% match.

wetlands. A similar visual overlay in the lower watershed also revealed widespread agreement between clumps of WIP pixels with scores greater than 0.7 and the larger NWI polygons (**Figure 40** and see **Figure 33**). In the lower basin, only a small percentage of NWI polygons are coincident with NHD lakes. Figures 39, 40 and 33 indicate good agreement between WIP screening and actual wetlands on the ground.

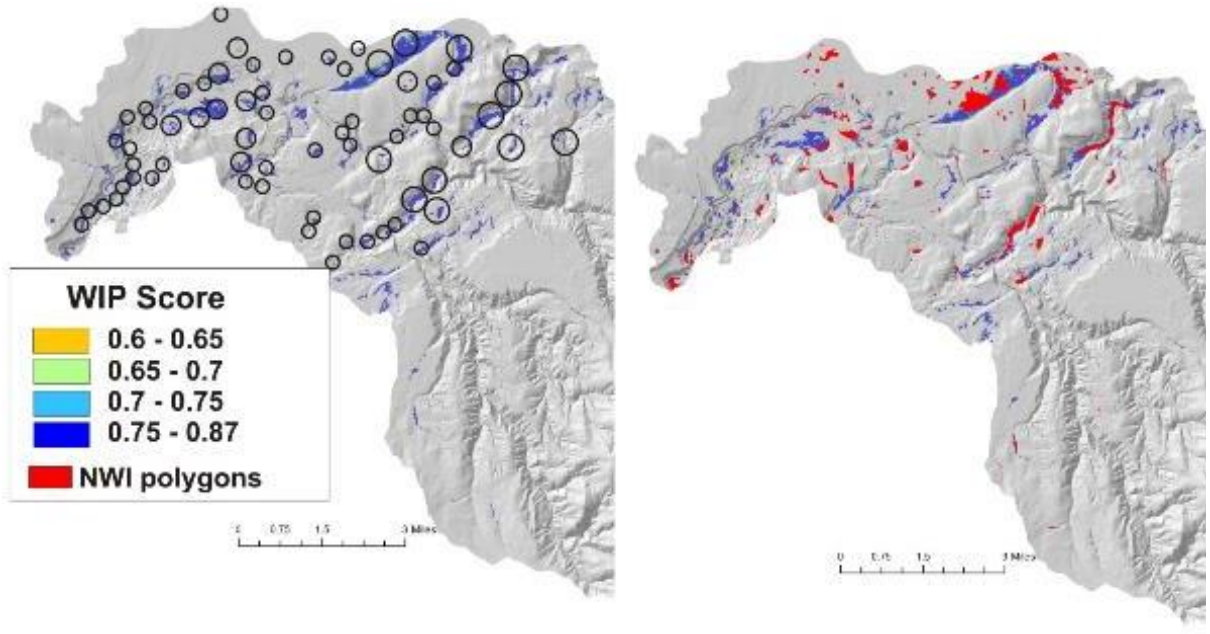

Figure 39. Comparing WIP scores to NWI database polygons reveals many overlaps (circles indicate coincidence between the two).

The WIP threshold of greater than 0.6 covered 3.5% of the watershed. For comparison, the NWI polygons encompass 1.6% of the watershed area. WIP scores greater than 0.7 and 0.8 encompass 3.1% and 0.04% respectively.

There are NWI polygons that do not overlap WIP scores greater than 0.7 (**Figure 40**). However, an analysis of those NWI polygons that do not overlap high WIP scores in the lower basins (there are virtually none in the upper basin, **Figure 39**) reveal that many of them, in the absence of forest canopy, do not appear to be wetlands (**Figures 41 and 42**). Perhaps the NWI includes areas of former wetlands, lost due to land use.

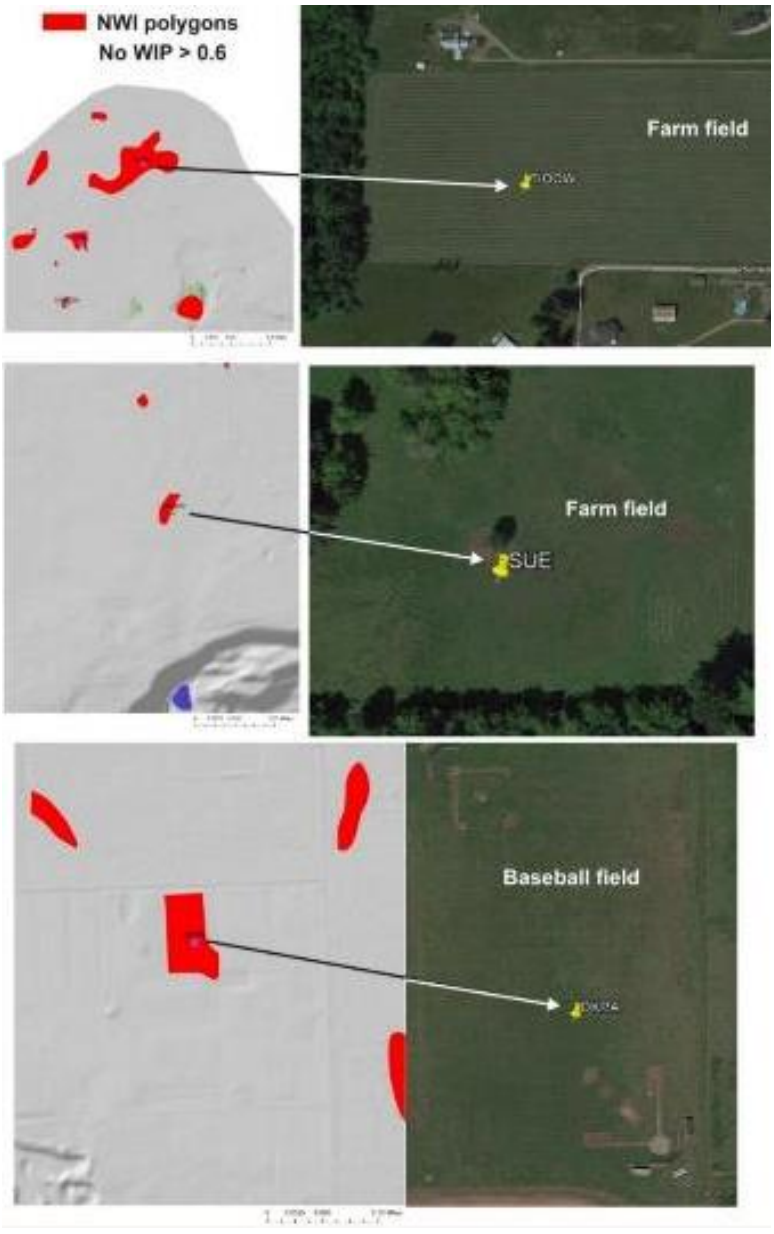

Figure 40. NWI polygons with no overlapping high WIP scores (> 0.6) are in areas with no visible wetlands.

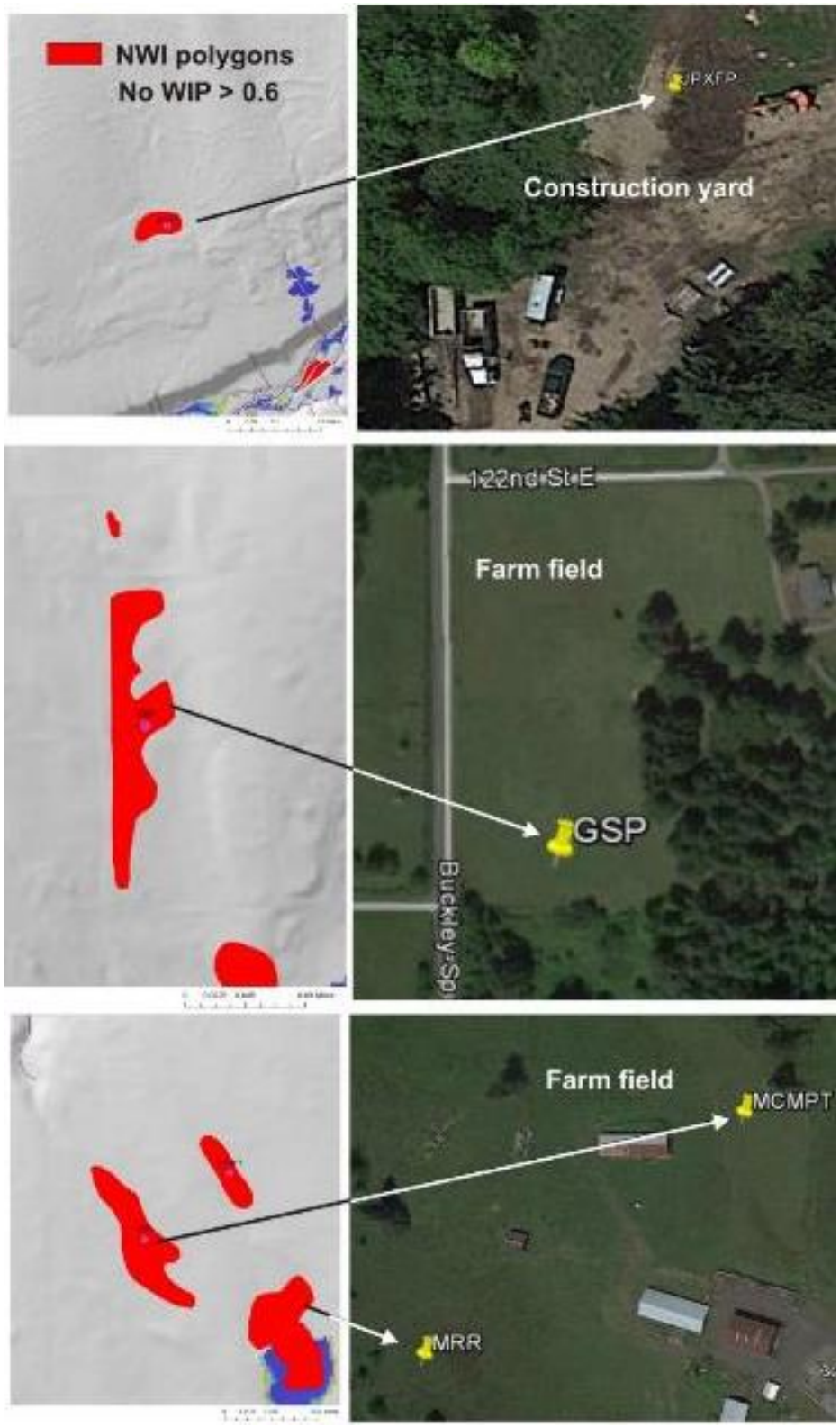

Figure 42. . NWI polygons with no overlapping high WIP scores (> 0.6) are in areas with no visible wetlands.

1

In forested areas, NWI wetlands are likely discovered opportunistically and not a result of a systematic search for wetlands. Consequently, it is likely that the NWI dataset under predicts the number of wetlands within forested river corridors and in other vegetated areas as well.

Wetland formation in forested settings should be sensitive to geomorphic controls, including valley morphology and tributary confluences. Unconfined valley floors and active tributary confluences (where sediment influxes from the tributary affect local valley morphology) are associated with higher WIP scores in the study basin **(Figure 43**).

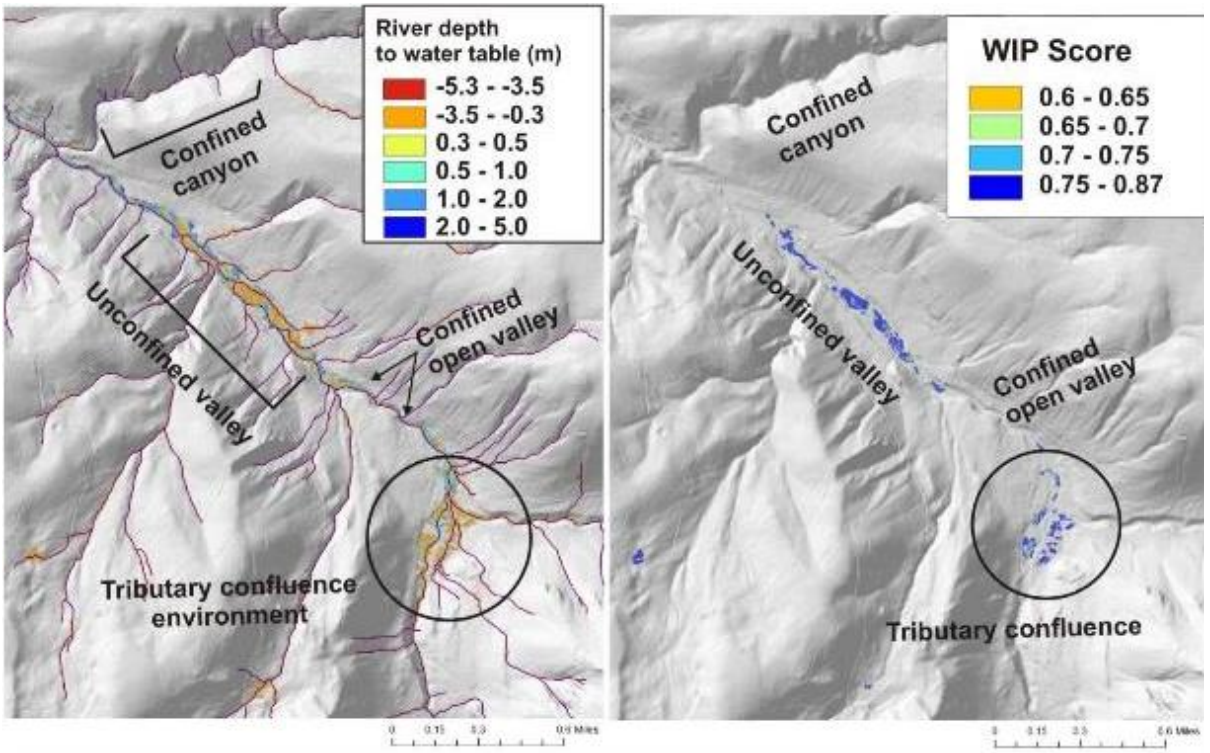

Figure 43. WIP scores and potential wetland extent are influenced by valley morphology and tributary confluences.

Viewing the entire study watershed provides an overview of the spatial distribution of potential wetlands as indicated by WIP. There is a much higher density of WIP scores that are associated with wetlands (NWI) in the lower watershed. In the uplands, wetlands are primarily lake related, although there may be many others located along river corridors but obscured by forest canopy (**Figure 44**). In addition, there is a much higher density of closed depressions in the lower watershed, that also contributes to the higher density of higher WIP scores in the lower basin and the higher incidence of NWI polygons there also (**Figure 40**).

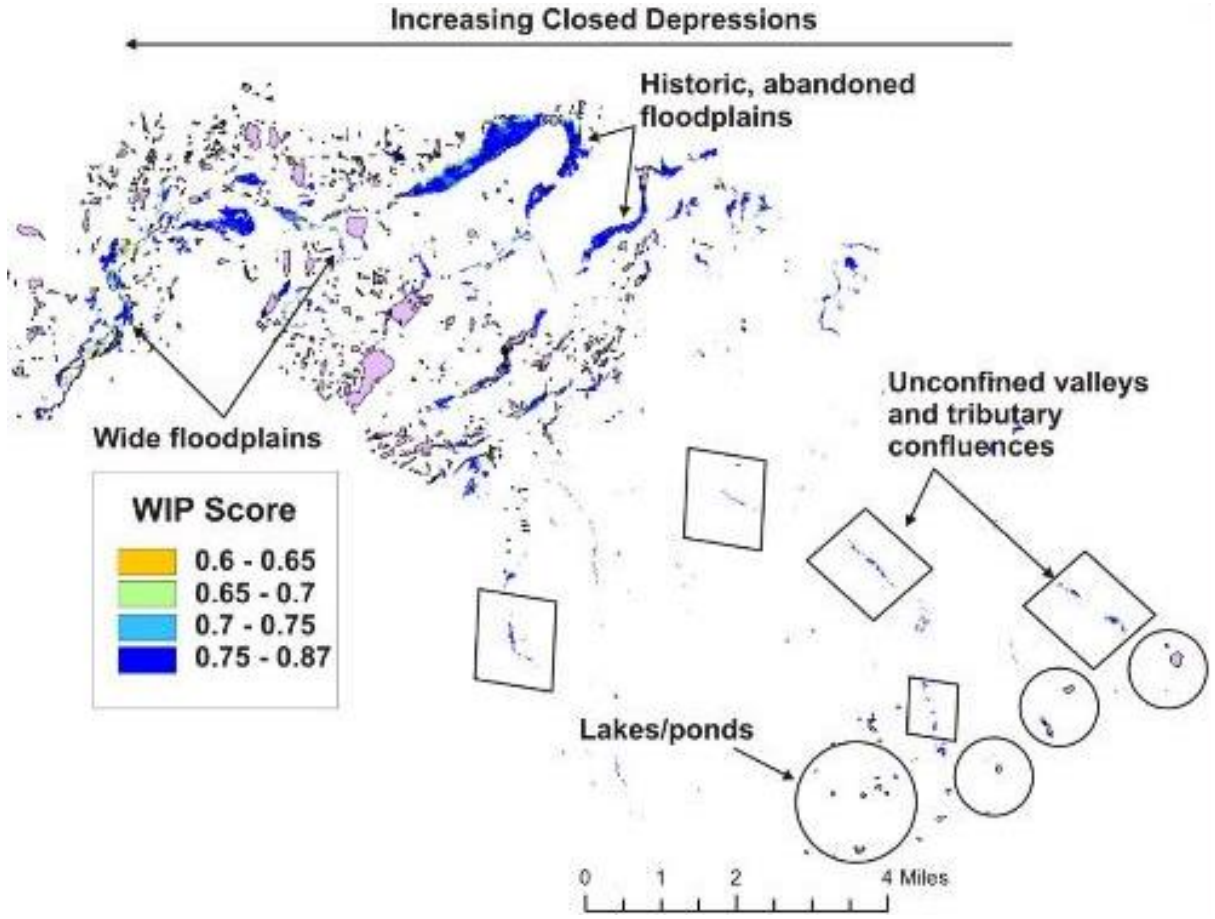

Figure 44. Areas of concentrated high WIP scores occuring in association with lakes/ponds, unconfined valleys, tributary confluences, and closed depressions increase in abundance downstream.

The NWI, a manually derived product using visual detection from optical imagery, appears to miss the full extent of some wetlands. In one example, the NWI included a wetland, but missed wetland areas around it, associated with a pond (**Figure 45**). The WIP scores identified a larger wetland area associated with actual wetlands, as verified in Google Earth.

Another example in the lower watershed shows an NWI wetland polygon that only covers part of an actual wetland as viewed from Google Earth (**Figure 46**). The actual wetland running for about two miles NE to SW (D). A high WIP score covers the entire wetland area (A). The NHD identifies two lakes where there are no lakes currently (B). The NWI misses the actual extent of the wetland (C).

The size threshold selected for closed depressions in the illustrative analysis may mean missing certain types and sizes of wetlands. For example, a mapped closed depression has an area of 800 m^2 and the lake is 384 m^2 (**Figure 47**). It was not included in the WIP analysis because the closed basin area was less than the specified depression area threshold of 1,000 m^2. The only way to capture this likely lacustrine

fringe wetland is to lower the area threshold for wetlands to 0.01 ha rather than 0.1 ha (100 m^2), include it in a more accurate lake layer, and then not exclude it by the NDVI during the analysis.

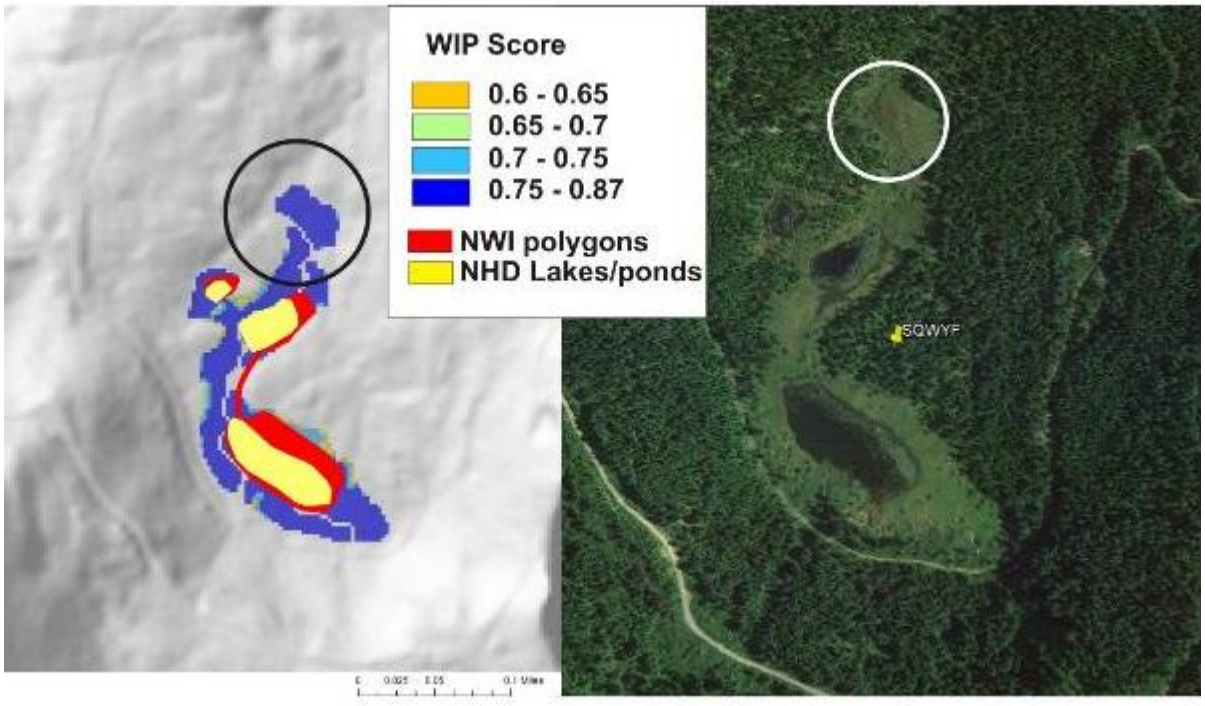

Figure 45. A comparison among WIP, NHD waterbodies and the NWI reveal inconsistencies in the identification and mapping of wetlands, including missing wetland areas in the NWI.

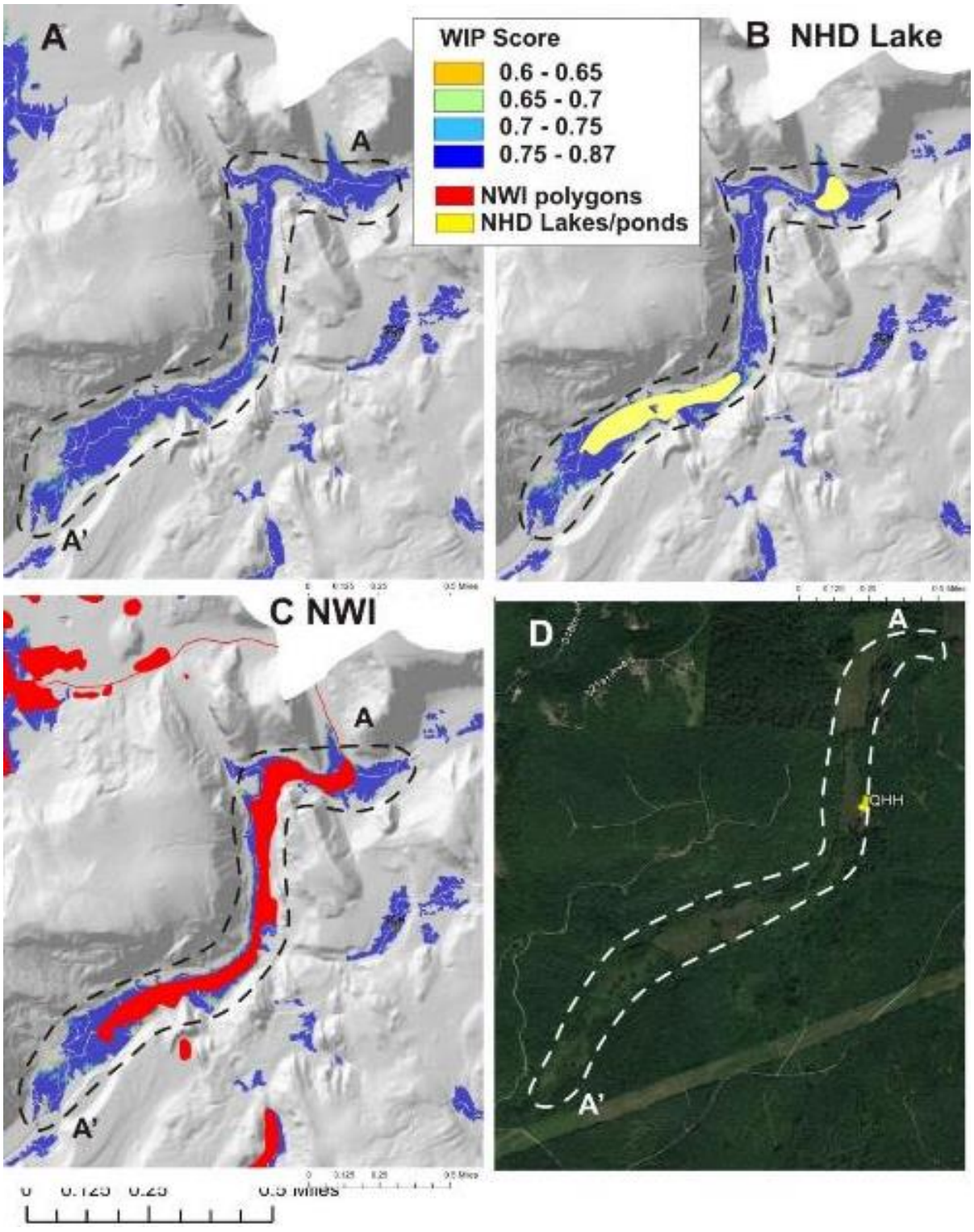

Figure 46. Example location where WIP identifies significant wetland areas that are missing from the NWI dataset and the NHD waterbodies layer.

1

Figure 47. Excluded lacustrine fringe wetland during the WIP analysis, because it failed to meet the minimum closed basin threshold and because it was not included in the NHD waterbody layer.

6. Summary and Recommendations

6.1. Summary Points

1. Phase 1 of a two-phase project, sponsored by CMER-WETSAG, focused on development of a hydrogeomorphic wetland screening tool for forested environments.
2. WIP requires simulation of river networks and landforms, and connectivity between them and among other landforms.
3. WIP uses suitability curves to relate individual hydrogeomorphic parameter values to wetland likelihood using a zero-to-one scalar. Hydrogeomorphic suitability-curve values are combined in a logistic model. Individual index-curve values for each hydrogeomorphic indicator can be optionally weighted based on their posited relative importance. Several types of filtering remove ancillary WIP pixels from the WIP map. These included channel pixels and contiguous groups of pixels with high WIP scores that were deemed to small to count as a wetland by regulatory definition.
4. The Wetland Intrinsic Potential (WIP) screening tool currently employs five hydrogeomorphic indicators of wetland development: 1) stream/river - depth to water, 2) lake/pond - depth to water, 3) closed depressions, 4) climate-topographic wetness index, and 5) depth to impermeable layer. The tool was demonstrated in the 225 km^2 study basin in the Puyallup River watershed.
5. Other hydrogeomorphic indicators could be integrated in future version of WIP, including local relief, microtopography in flat-lying terrain, and models of surface erosion and deposition to detect local low-permeability areas associated with sediment deposition.

6. WIP can be applied to forested and non-forested landscapes.
7. High WIP scores (> 0.6) covered 3.5% of the study basin compared to 1.6% covered with National Wetland Inventory polygons.
8. WIP scores within NWI polygons and outside of the polygons were significantly different, indicating that WIP's hydrogeomorphic indicators, suitability curve shapes, and indicator weights in the logistic model successfully captured the conditions associated with many mapped NWI wetlands.
9. WIP identified five geographic hotspots for wetland development in the study area, including: 1) adjacent to lakes and ponds, 2) along wide, unconstrained valley floors, 3) within wide forested riverine corridors, 4) at and near large tributary confluences and 5) within abandoned, historical river valleys.
10. High WIP scores (> 0.6) identified wetlands (confirmed with imagery) that are not included in the NWI nor the NHD Waterbodies. In addition, there were NWI polygons that were not mapped by WIP as potential wetlands.
11. In many cases, WIP identified wetlands larger in lateral extent compared to NWI polygons, particularly those in association with river corridors and lakes/ponds.
12. There are many locations where high WIP scores overlapped NWI polygons, but a statistically robust test and calibration of the model requires a comprehensive dataset of confirmed wetlands under forest canopy.
13. Numerous NWI polygons in the lower portion of the study watershed in areas of urban and semi-urban development, and farm fields, did not appear to be associated with wetlands on the ground based on imagery.
14. WIP is comprised of eight analytical steps that are contained within a stand-along ArcMap Add-In. Required input data layers include: i) DEMs (LiDAR recommended), ii) NHD waterbodies, iii) precipitation (PRISM), iv) NAIP-NDVI and v) soils/geology, specifically impermeable layers (optional). Adjustable parameters include hydrogeomorphic suitability curve shapes, weighting terms, NDVI filter thresholds, closed basin area threshold and minimum wetland size.
15. WIP could be used as a partial validation and to refine NWI polygons, particularly their lateral extent. NWI is based on field and photo detection of wetlands, and hence is inherently limited under forest canopy. Whereas, WIP is not limited by forest canopy, but can be limited by model design and application, and absence of digital data to run the models.
16. WIP could be used within individual watersheds to develop a better understanding of the potential locations and amount of wetlands in forested and non-forested settings for regulatory purposes, including review of proposed land uses, such as forestry activities.
17. WIP could be applied across multiple watersheds at the landscape or regional level. Comparison of WIP results to field-surveyed wetland inventories could then be used to develop a better understanding of geomorphic controls on wetland development related to spatially varying valley

morphology, lake abundance and morphology, basin shape and tributary confluences, complexity of riverine corridors and historical (abandoned) river valleys.

18. Although WIP can be calibrated using a comprehensive database of wetlands (including under forest canopy) it can be applied without it as a course screen.

19. The pixel based WIP scores could be aggregated into polygons using software such as ArcMap or ecognition (object based image segmentation and classification software).

20. The five hydrogeomorphic indicator data layers using in WIP could be integrated within eCognition, in the absence of the logistic model.

6.2. Recommendations

1. Other hydrogeomorphic indictors could be included in future versions of WIP, such as local relief models (e.g., Leonard et al., 2012) and models of hillslope erosion and deposition that could identify micro-topographic features, including depressions, where soil permeability is lower, and wetland formation likelihood is higher.

2. WIP's suitability curves, weightings for individual hydrogeomorphic indicators, and method for combining suitability scores to calculate an intrinsic-potential value could be adjusted based on model calibration to field-mapped wetland locations. Statistical methods to minimize discrepancies between predicted (by high WIP scores) and observed wetland locations could be applied to calibrate a WIP model.

   This might be useful if the model is used for screening purposes in areas without field data, but it may prove just as useful to calibrate the model through user-based adjustments. Every aspect of the WIP approach is built on our understanding of how wetlands work: the choice of hydrogeomorphic indicators, the suitability curves for each indicator, the method for combining suitability scores into an estimate of intrinsic potential – choices for each step are based on the model builder's conceptual model and understanding of wetland formation. Discrepancies between predicted and observed wetland locations allow a model builder or user to evaluate and improve their understanding of how wetlands work.

   Additionally, calibration of the WIP model to observed wetland locations may be counterproductive. Absence of a wetland does not necessarily indicate absence of conditions conducive for a wetland. Many former wetlands have been drained or modified; calibration of the model to those that remain may therefore be misleading.

3. Further evaluation of WIP, including its calibration, will require comprehensive wetland inventories, particularly under forest canopy. Such data do not presently exist. The NWI is one resource, but it lacks comprehensive coverage under forest canopy. In addition, it appears to include wetlands that do not exist. Moreover, NWI polygons appear to miss wetlands and under represent them spatially in certain locations.
4. In Phase 2 of this project, when field data are available, a GIS toolset could be developed to build and apply statistical models seeking correlations between remotely sensed data, including hydrogeomorphic indicators, and wetland locations. Statistical models would likely include logistic

regression and decision tree techniques, although the final choice of models to use would be determined as the GIS toolkit is built. WIP would be included in the suite of tools. These tools could include pixel-based methods, as described for the hydrogeologic indicators discussed in this report, and may also include classified polygon data types, as created with object-based analyses.

5. Other numerical approaches for combining individual hydrogeomorphic indicators could be applied in search of the best performing model, including the use of eCognition.

6. Field surveys of wetlands, particularly those under canopy, used to test and refine different wetland models would optimally map entire wetland footprints. However, in the absence of full wetland surface area mapping, point information could be used. If point data are collected, an estimate of relative wetland size per wetland point would be helpful.

7. Even without further testing and calibration, it would be beneficial to apply WIP in other watersheds to develop a better understanding (and develop hypotheses) about how wetland formation varies across entire landscapes (Olympic Peninsula versus Cascade draining watersheds).

8. WIP could be used, as a prototype, to screen for potential wetlands for informing and field surveys during land developments, including forestry activities, or during research activities.

7. References

Adamus, Paul. 2014. Effects of Forest Roads and Tree Removal In or Near Wetlands of the Pacific Northwest: A Literature Synthesis. Prepared for Washington Department of Natural Resources, Olympia, WA. Report Number: CMER #12-1202.

Ågren, A.M., W. Lidberg, M. Strömgren,, J. Ogilvie, and P.A. Arp*. 2014.* Evaluating digital terrain indices for soil wetness mapping—A Swedish case study. *Hydrol. Earth Syst. Sci.18:* 1–12.

Ågren, A.M., W. Lidberg, M. Strömgren, and E. Ring, 2015. Mapping temporal dynamics in a forest stream network-implications for forest management. Forests 6, 2982-3001, doi:10.3390/f6092982.

Anderson, R. R., R. G. Brown, and R. D. Rappleye. 1968. Water quality and plant distribution along the upper Patuxent River, Maryland. Chesapeake Sci. 9:145-156.

Benda, L., D. J. Miller, K. Andras, P. Bigelow, G. Reeves, and D. Michael. 2007. NetMap: A new tool in support of watershed science and resource management. Forest Science 52:206-219.

Benda L, D. Miller, J. Barquın. 2011. Creating a catchment-scale perspective for river restoration. Hydrol Earth Syst Sci 15:2995–3015.

Benda, L.E., D. Miller, J. Barquin, R. McCleary, T. J Cai and Y. Ji. 2015. Building virtual watersheds: a global opportunity to strengthen resource management and conservation. Environmental Management 57:772-739.

Barquin, J., L.E. Benda, F. Villa (8 more authors). 2015. Coupling virtual watersheds with ecosystem services assessment: a 21st century platform to support river research and management. WIREs Water 2(6):609-621.

Benda, L. and S. Litchert. in progress. Combining bathymetry, LiDAR and tidal cycles to predict probability of marine inundation for the reconstruction of Puget Sound estuary environments.

Beven, K. J. and M. J. Kirkby. 1979. A Physically Based Variable Contributing Area Model of Basin Hydrology. Hydrological Sciences Bulletin, 24(1): 43-69.

Bidlack, A. L., Benda, L. E., Miewald, T., Reeves, G. H., and McMahan, G., 2014. Identifying suitable habitat for Chinook salmon across a large, glaciated watershed: Transaction of the American Fisheries Society, v. 143, no. 3, p. 689-699.

Brinson, M.M. 1993. A hydrogeomorphic classification for wetlands, Technical Report WRP–DE–4, U.S. Army Corps of Engineers Engineer Waterways Experiment Station, Vicksburg, MS. http://el.erdc.usace.army.mil/wetlands/pdfs/wrpde4.pdf

Brinson, M.M. 1993. A hydrogeomorphic classification for wetlands, Technical Report WRP–DE–4, U.S. Army Corps of Engineers Engineer Waterways Experiment Station, Vicksburg, MS.

Brinson, M.M., L.C. Lee, R.D. Rheinhardt, G.G. Hollands, D.F. Whigham, and W.D. Nuttler. 1997. A summary of common questions, misconceptions, and some answers concerning the hydrogeomorphic approach to functional assessment of wetland ecosystems: scientific and technical issues. Draft of paper published as a Bulletin of the Society of Wetland Scientists 17(2):16–21.

Buchanan, B.P., M. Fleming, R. L. Schneider, B. K. Richards, J. Archibald, Z. Qiu, and M. T. Walter. 2014. Evaluating topographic wetness indices across central New York agricultural landscapes. Hydrolo. Earth Syst. Sci. 18, 3279-3299.

Burnett, K.M., Reeves, G.H., Miller, D.J., Clarke, S., Vance-Borland, K., and Christiansen, K. 2007. Distribution of salmon-habitat potential relative to landscape characteristics and implications for conservation. Ecol. Appl. 17(1): 66-80.

Busch, D.E., N.L. Ingraham, and S.D. Smith. 1992. Water uptake in woody riparian phreatophytes of the southwestern United States: a stable isotope study. Ecological Applications 2:450-459.

Busch, D. S., M. Sheer, K. Burnett, P. Mcelhany and T. Cooney. 2011. Landscape-level model to predict spawning habitat for lower Columbia Fall Chinook Salmon (ONCORHYNCHUS TSHAWYTSCHA). River Research and Applications.

Chambers, J. C., Ro. J. Tausch, J. L. Korfmacher, D. Germanoski, J. R. Miller and D. Jewett. 2004. Effects of Geomorphic Processes on Riparian Vegetation. Chapter 7 in Great Basin Riparian Ecosystems: Ecology, Management and Restoration. Edited by Jeanne C. Chambers and Jerry R. Miller. Society for Ecological Restoration International. Island Press.

Collins, B.D., Montgomery, D.R., and Sheikh, A.J., 2003, Reconstructing the historical riverine landscape of the Puget lowland: Restoration of Puget Sound Rivers. University of Washington Press, Seattle, WA,, p. 79–128.

Cooke Scientific Services, Inc. 2005. Pacific Northwest Forested Wetland Literature Survey Synthesis Paper. Cooperative Monitoring Evaluation and Research Committee/Wetland Scientific Advisory Group, Washington Dept. of Natural Resources, Olympia, WA.Cowardin, L. M., V. Carter, F. C. Golet and E. T. LaRoe. 1976. Interim classification of wetlands and aquatic habitats of the United States. U.S. Fish and Wildlife Service, Office of Biological Services, Washington, DC.

Cowardin, L. M., V. Carter, F. C. Golet, and E. T. LaRoe. 1979. Classification of wetlands and deepwater habitats of the United States. U.S. Fish and Wildlife Service. FWS/OBS-79/31. Washington, DC.

Creed, I.F., S.E. Sanford, F.D. Beall, L.A. Molot and P.J. Dillon. Cryptic wetlands: integrating hidden wetlands in regression models of the export of dissolved organic carbon from forested landscapes. Hydrological Processes 17: 3629-3648.

Curie, F., S. Gaillard, A. Ducharne, and J. Bendjoudi. 2007. Geomorphological methods to characterize wetlands at the scale of the Seine watershed. Science of the Total Environment 375, 59-68.

Dahl , T.E. 1990. Wetland losses in the United States 1780s to 1980s. US Department of Interior, Fish and Wildlife Service, Washington, D.C. 2100.

Janisch, J.E., A.D. Foster and W. J. Ehinger. 2011. Characteristics of small headwater wetlands in second growth forests of Washington, USA. Forest Ecology and Management 261:1265-1274.

Karan, S, P. Engesgaard, M. Looms, T. Laier and J. Kazmierczak. 2013. Groundwater flow and mixing in a wetland-stream system: field study and numerical modeling. Journal of Hydrology, V. 488: 73-83.

Knight, J.F., J.M. Corcoran, L.P. Rampi and K.C. Pelletier. 2015. Theory and applications of object-based image analyis and emerging methods in wetland mapping. In: Remote Sensing of Wetlands: Applications and Advances. Ed. by: R. W. Tiner, M.W. Lang, and V.V. Klemas. 179-194.

Kresch, D.L. 1998. Upstream boundaries for western Washington streams and rivers under the requirements of the Shoreline Management Act of 1971: U.S. Geological Survey Water-Resource Investigations Report 96-4208. 46 p.

Lang, M.W. and G.W. McCarty. 2009. LiDAR intensity for improved detection of inundation below the forest canopy. Wetlands 29(4):1166-1178.

Lang, M., G. McCarty and R. Oesterling. 2013. Topographic metrics for improved mapping of forested wetlands. Wetlands 33, 141-155.

Leonard, P. B., R. F. Baldwin, J. A. Homyack and T. B. Wigley. 2012. Remote detection of small wetlands in the Atlantic coastal plain of North America: local relief models, ground validation and high-throughput computing. Forest Ecology and Management 284: 1-7-115.

Lyon, S.W., P. M.T. Gerard-Marcant, T.S. Walter, and Steenhuis. 2004. Using a topographic index to distribute variable source area runoff predicted with the SCS-Curve Number equation, Hydrological Processes, 18 (2004), pp. 2757-2771.

Magirl, C. S., and T. D. Olsen 2009. Navigability Potential of Washington Rivers and Streams Determined with Hydraulic Geometry and a Geographic Information System. US Geological Survey. Retrieved from http://pubs.usgs.gov/sir/2009/5122/.

Merot, P.H., B. Ezzahar, C. Walter and P. Aurousseau. 1995. Mapping waterlogging of soils using digital terrain models. Hydrological Processes, V9: 27-34.

Merot, P.H. H. Squividant, P. Aurousseau, M. Hefting, T. Burt, V. Maitre, M. Kruk, A. Butturinif, C. Thenail, and V. Viaud. 2002. Testing a climato-topographic index for predicting wetlands distribution along an European climate gradient. Ecological modeling 163, 51-71.

Miller, G.T. 1990. Living in the environment: an introduction to environmental science. 6th ed. Wadsworth Publishing Company, Belmont, California.

Miller, D. J., 2003, Programs for DEM Analysis, Landscape Dynamics and Forest Management, General Technical Report RMRS-GTR-101CD: Fort Collins, CO, USA, USDA Forest Service, Rocky Mountain Research Station.

Miller, D., L. Benda, J. DePasquale and D. Albert. 2015. Creation of a digital flowline network from IfSAR 5-m DEMs for the Matanuska-Susitna Basins: a resource for NHD updates in Alaska. Report to The Nature Conservancy, Juneau, Alaska. 32pp.

Morrison, M. L., B. G. Marcot, and R. W. Mannan. 1998. Wildlife habitat relationships: concepts and applications. Second edition. The University of Wisconsin Press, Madison, Wisconsin, USA.

Murphy, P.N.C., Ogilvie, J., Connor, K., Arpl, P.A., 2007. Mapping wetlands: a comparison of two different approaches for New Brunswick. Can. Wetlands 27, 846–854.

Murphy, P.N.C., Ogilvie, J., Castonguay, M., Zhang, C.-F., Meng, F.-R., Arp, P.A., 2008. Improving forest operations planning through high-resolution flow-channel and wet-areas mapping. The Forest. Chron. 84, 568–574.

Murphy, P.N.C., Ogilvie, J., Meng, F.R., White, B., Bhatti, J.S., Arp, P.A., 2011. Modelling and mapping topographic variations in forest soils at high resolution: a case study. Ecol. Model. 222, 2314–2332.

National Research Council. 1995. Wetlands: Characteristics and Boundaris. Committee on Characterization of Wetlands, National Research Council. 328pp.

Olson, D.P. 1964. The use of aerial photographs in studies of marsh vegetation. Bulletin 13, Orono, Maine: Maine Agricultural Experiment Station. 62pp.

Poggio, L., and Soille, P., 2012, Influence of pit removal methods on river network position: Hydrological Processes, v. 26, p. 1984-1990.

Rodhe, A., Seibert, J., 1999. Wetland occurrence in relation to topography: a test of topographic indices as moisture indicators. Agric. For. Meteorol. 98–9, 325–340.

Silva, T.S.E., M.P. Costa, J.M. Melack and E.M. Novo. 2008. Remote sensing of aquatic vegetation: theory and applications. Environmental Monitoring and Assessment 140: 131-145.

Skaggs, R. W., D. Amatya, R. O. Evans, and J. E. Parsons. 1994. Characterization and evaluation of proposed hydrologic criteria for wetlands. J. Soil and Water Conser. 49(5): 501-510.

Stromberg, J.C. and D.T. Patten. 1996. Instream flow and cottonwood growth in the eastern Sierra Nevada of California USA. Regul. River, 1: -12

Tarboton, D. G., 1997. A new method for the determination of lfow directions and upslope areas in grid digital elevation models. Water Resources Research, v33:309-319.

Tiner, R. W., M. W. Lang and V. V. Klemas. 2015. Remote sensing of wetlands: applications and advances. CRC Press, Taylor and Francis Group, Boca Raton, Florida.

Tiner, R. W. 2015. Early applictions of remote sensing for mapping wetlands. In: Remote Sensing of Wetlands: Applications and Advances. Ed. by: R. W. Tiner, M.W. Lang, and V.V. Klemas. 67 – 78.

Vadas, R. L., and D. J. Orth. 2001. Formulation of habitat suitability models for stream fish guilds: do the standard methods work? Transactions of the American Fisheries Society 130:217–235.

VanHorne, B., and J. A. Wiens. 1991. Forest bird habitat suitability models and the development of general habitat models. U.S. Fish and Wildlife Service, Fish and Wildlife Research 8, Washington, D.C.

Voldseth, R. A., W. C. Johnson, T. Gilmanov, G. R. Guntenspergen and B. V. Millett. 2007. Model estimation of land use effects on water levels of northern prairie wetlands. Ecological Applications, 17(2), pp. 527-540.

USACE. 1987. Corp of Engineers: Wetland Delineation Manual, United States Army Corp of Engineers. Wetland Research Program, Vicksburg, MS.

U.S. Fish and Wildlife Service. 1981. Standards for the development of habitat suitability index models. Division of Ecological Services US. Fish and Wildlife Service, Department of the Interior, Washington D. C. 103 ESM.

Walter M.T., T.S. Steenhuis, V.K. Mehta, D. Thongs, M. Zion, and E. Schneiderman. 2002. Refined conceptualization of TOPMODEL for shallow subsurface flows. Hydrological Process, 16: 2041-2046.

Welch, W.B., Johnson, K.H., Savoca, M.E., Lane, R.C., Fasser, E.T., Gendaszek, A.S., Marshall, C., Clothier, B.G., and Knoedler, E.N., 2015, Hydrogeologic framework, groundwater movement, and water budget in the Puyallup River Watershed and vicinity, Pierce and King Counties, Washington: U.S. Geological Survey Scientific Investigations Report 2015–5068, 54 p., 4 pls., http://dx.doi.org/10.3133/sir20155068.

White, B., Ogilvie, J., Campbell, D. M. H., Hiltz, D., Gauthier, B., Chisholm, H. K., Wen, H. K., Murphy, P. N. C., and Arp, P. A.: Using the Cartographic Depth-to-Water Index to Locate Small Streams and Associated Wet Areas across Landscapes, Can. Water Resour. J., 37, 333–347, doi:10.4296/cwrj2011-909, 2012.

8. Appendix A. WIP Model Background

The 'Netstream' suite of Fortran programs (Miller 2003, Miller et al. 2015) is used to develop the WIP tool. Netstream is licensed under the open-source GNU General Public License v3 (GPLv3). The Fortran programming language is used, because the current language standard (Fortran 2008, http://www.j3-fortran.org/) implements usage and protocols for numerical analysis of very large datasets, current Fortran compilers provide options for fully optimized, vector and parallel processing on current CPUs, and Fortran libraries are interchangeable with C-language libraries. The programs operate using command-line interfaces, but have been incorporated into user interfaces in support of watershed analysis in ArcGIS 10.x using vb.net and python scripts (NetMap, Benda et al., 2007, 2015). Netstream programs have been used to explore temporal and spatial patterns of landscape dynamics (Benda and Dunne, 1997a, b; Benda et al., 1998; USDA Forest Service, 2003), including creating digital hydrography from DEMs (Agrawal et al., 2005; Bruno et al., 2014; Busch et al., 2011; Clarke et al., 2008; Flitcroft et al., 2014; McCleary et al., 2011; Peñas et al., 2014; Sheer and Steel, 2006; Steel et al., 2004; Steel et al., 2008), assessing aquatic habitat potential (Bidlack et al., 2014; Burnett et al., 2007), delineating floodplains (Benda et al., 2011) and riparian zones (Fernández et al., 2012b), mapping landslide hazards (Burnett and Miller, 2007; Hofmeister and Miller, 2003; Hofmeister et al., 2002; Miller and Burnett, 2008), and assessing potential for wood recruitment to streams (Atha, 2013; Benda et al., 2003). These methods have evolved and continue to grow through extensive, collaborative use, and they have demonstrated superior performance in comparisons with other options for extraction of channel networks (Peñas et al., 2011) and riparian zones (Fernández et al., 2012a) using DEMs.

8.1. Gradient, Plan Curvature and Contour Length Rasters (Makegrids)

Gradient and curvature at each DEM point are calculated by fitting a partial quartic equation to elevations at the point and eight surrounding points, as described by Zevenbergen and Thorne (1987). The 8 surrounding points are located on a circle centered at the DEM point, as described by Shi et al. (2007). Radius of the circle determines the spatial grain at which gradient and curvature are estimated. The smallest length scale over which these values can be resolved is twice the grid spacing of the DEM. Elevation at points on the circle that do not fall directly on a DEM grid point are determined using bilinear interpolation.

Using the partial quartic solution of Zevenbergen and Thorne (1987), gradient requires elevation values only along the cardinal directions (e.g., N-S and E-W). To reduce bias from the orientation of the DEM grid, gradient is calculated twice, first using elevations along the cardinal DEM orientation, and then again at an orientation rotated 45 degrees. Gradient at the point is determined as the average of the two values (the modified Zevenbergen -Thorne method of Shi et al., 2007).

To estimate specific contributing area (contributing area per unit contour length) for each DEM pixel, we need the contour length crossed by flow exiting each pixel. Ideally, this contour length is estimated by integrating the projection of flow direction (for outgoing flow only) over a circle centered at the DEM point, with the circle radius the same as that used for calculating gradient and curvature. For length scales spanning several DEM grid pixels, however, this method is slow. As an alternative, we used the surface representation applied for the D-infinity flow-direction algorithm (Tarboton, 1997): that of eight

triangular facets defined for a pixel centered over the grid point, with edge length equal to the specified length scale, and with corner elevations obtained with bilinear interpolation. The projection of flow direction out of each facet is then integrated along each facet edge and summed over all facets. For planar flow, this gives a contour length of one pixel length. For divergent flow, the contour length is greater than the pixel length, and for convergent flow, it is less. Specific contributing area is then obtained by dividing the flow accumulation calculated for a DEM pixel (using D-infinity) by the contour length crossed by flow exiting the pixel, both normalized by pixel length. Note that these topographic attributes are all calculated for the original DEM, not the hydrologically conditioned DEM. Our intent is to base analyses on data that has been altered as little as possible.

The appropriate length scale to use for calculating topographic attributes depends on the ability of the DEM to resolve surface features, on the amount of noise in the DEM (which can create spurious high curvature values), and on the spatial scale of the topography controlling the physical processes being modeled (e.g., Pirotti and Tarolli, 2010).

8.1.1. *Flow Direction*

Once the DEM has been hydrologically conditioned, all pixels have an adjacent pixel of equal or lower elevation. For pixels with an adjacent pixel of lower elevation, the D-infinity method (Tarboton, 1997) is used to define the primary direction of flow out of the pixel. D-infinity is one of a family of flow-direction algorithms that can account for dispersion of flow over divergent topography by proportioning flow out of one pixel into more than one downslope pixel, unlike the D-8 algorithm, which sends all flow into one of the eight adjacent pixels (Wilson et al., 2008). D-infinity limits the amount of dispersion by allowing flow into no more than two downslope pixels. It is computationally efficient and is found to provide estimates of flow accumulation considerably more accurate than D-8 (Wilson et al., 2007) and of comparable accuracy as other dispersive algorithms for mathematically constructed surfaces with known contributing area (Qin et al., 2013) and to also perform well for prediction of field-observed soil wetness (Sorensen et al., 2006).

Pixels surrounded by areas of equal or higher elevation form flat areas within the DEM, for which flow directions are undetermined. To define flow directions through flat zones, we use the algorithm described by Garbrecht and Martz (1997), as modified by Barnes et al., (2014a). This algorithm directs flow away from higher terrain and towards lower terrain; this produces flow paths that tend to traverse through the center-line of flat zones.

8.1.2. *Flow Accumulation*

After flow directions are defined for all DEM pixels, flow accumulation to each pixel is calculated using the iterative approach described by Tarboton (1997). Initially, prior to channel initiation, D-infinity flow directions are used for all pixels. D-8 flow directions are used once the criteria for channel initiation are met. This prevents dispersion of channelized flow.

To determine the D-8 flow direction for a pixel, the method of steepest descent is commonly used, in which flow is directed to the adjacent pixel for which the downhill slope (calculated as the elevation difference between DEM points divided by the distance between DEM points) is greatest. We have

found, however, that in areas with relatively planar slopes, small channel courses are not well traced with this method, particularly if the channel does not align with one of the D-8 directions. We find that small channels are better traced using a combination of steepest descent and largest plan curvature. Use of plan curvature is similar to use of contour crenulations to trace channel courses (Strahler, 1957); we want to direct channel flow both downslope and along the course with topographic characteristics most indicative of a channel.

To choose the appropriate D-8 direction for channelized flow from a pixel, we use the D-infinity method of proportioning flow between downslope pixels. If any adjacent pixel receives more than a greater proportion of flow (e.g., 75%), as estimated with D-infinity, then the D-8 flow direction is set to that pixel. However, if flow is more equally divided between two downslope pixels, then the D-8 flow direction is set to the pixel with the largest plan curvature. The threshold proportion of flow is a user-specified value, which we have set through trial and error to 75%.

It is also useful to define D-8 flow directions for all pixels. Watershed boundaries and local contributing areas to any point can be readily estimated by tracing D-8 flow paths until pixels with no inflow are encountered. D-8 flow directions are used, for example, to delineate catchments in creation of NHDplus datasets. To translate D-infinity flow directions to D-8 flow directions, we set the D-8 direction to the adjacent downslope pixel that receives most of flow (as estimated using D-infinity). Again, if flow is partitioned equally between two pixels, the one with the greatest plan curvature is chosen, and if both pixels also have the same plan curvature, the one along a cardinal direction is chosen.

In certain cases, D-8 flow directions, whether determined using the methods described here or based solely on steepest descent, result in a flow direction diagonally across a DEM pixel that crosses a traced channel traversing the pixel along the other diagonal. Then, if the D-8 flow directions are used to delineate the local contributing area to one side of a channel segment, it will appear as though drainage from both sides is flowing into the channel from only one bank. After channel courses are traced, we check for this condition and redirect channel-crossing flow into the channel.

8.2. Synthetic River Network (Bldgrds.exe/Netrace.exe)

8.2.1. *Channel Initiation*

Channel initiation locations are based on a set of three thresholds (Miller et al., 2015): a minimum value of the product of slope squared and specific contributing area, minimum plan curvature, and a minimum flow length along which the other two thresholds must be met. Thresholds are defined separately for low- and high-gradient areas, and are determined by plotting drainage density versus threshold value: an inflection in the log-log plot shows where channels start to extend onto planar hillslopes (Clarke et al., 2008).

8.2.2. *Channel Network as Linked Nodes*

We want to maintain information at the finest spatial grain available, with the ability to summarize over any larger spatial scale. For the traced channel network, the finest spatial grain is that of the DEM points

that the flow lines follow. We therefore use a linked-node data structure, which maintains information at this spatial scale.

Each DEM point along the traced flow lines defines one channel node. Each channel node is connected to its adjacent upstream nodes and downstream nodes, so that the network can be traversed moving up or downstream. There may be multiple adjacent up or downstream nodes, to accommodate branching in both up and downstream directions. Each node has an associated DEM point, and a displacement from that point to indicate its location on the smoothed flow line.

Each node is associated with a record in an associated database. This record may contain any number of data fields, depending on what attributes have been calculated for that location in the channel network and on what other data sources are available.

Channel nodes can be assembled into line segments and data attributes summarized for nodes in each segment. This approach provides flexibility in specifying flow-line segment lengths and data attributes for creation of line vector files for import to GIS. Flow line networks can thereby be created to meet NHD topology, geometry, and formatting standards.

8.2.3. *Building the Vector Channel Network*

Flow lines defined by following D-8 flow directions consist of a series of straight-line segments following DEM pixel edges or diagonals. This gives flow lines a jagged appearance and results in over-estimated channel lengths and under-estimated channel gradients. We therefore smooth the traced channel courses by fitting a polynomial of specified order over a centered window along the traced channel flow lines. The polynomial is over fitted, in that the window includes more DEM points than needed to define the polynomial. This gives a smooth curve traversing points within the window. This is done from each DEM point along the flow line and the vertex of the flow line at that point is shifted to the location along the fit polynomial curve.

8.2.4. *Floodplain Delineation*

To characterize valley-floor surfaces DEM pixels are classified according to elevation above the channel. Each pixel within a specified radius (1500 m) of a channel is associated to the closest channel pixel, with distance to the channel weighted by intervening relief. Valley-floor DEM pixels are associated with channels that are closest in Euclidean distance and have the fewest and smallest intervening high points. The elevation difference between each valley-floor pixel and the associated channel location is reported as absolute elevations. Elevations are also normalized by bankfull depth with floodplains and terraces characterized in terms of number of bankfull depths above the channel. This procedure is repeated for every channel segment in the synthetic river network.

Floodplains typically lie at, or somewhat above, bankfull stage (Dunne and Leopold, 1978). In practice, zones of frequent inundation are defined by an elevation above the channel equivalent to two bankfull depths (Rosgen, 1996, Castro, 1977). To illustrate a wide range of flow inundation-valley topography relations in the Pas River, we delineated surfaces above the DEM-inferred channel using elevation equivalents of one, two, and three bankfull depths.

8.2.5. *Closed Depressions (Closed.exe)*

To identify closed depressions (and to calculate the topographic wetness index, see below), a DEM is used to model surface flow direction and accumulation. A closed depression, also called a 'sink', is a pixel or set of spatially connected pixels that cannot be assigned a flow direction out of the pixels. The closed depression is then filled up to an elevation that will allow flow out of the pixel. The areal extent of the filling to the required elevation defines the area of the depression. When building a synthetic river network from flow direction and accumulation grids, closed depressions that are filled, or alternatively cut through, allows for a continuous stream network, a process often referred to 'hydro-flattening' or 'hydro-conditioning'.

Various algorithms are available to model flow direction and accumulation, including one that restricts flow from any grid pixel to one of its eight neighboring pixels, referred to as D-8 (Jensen and Domingue 1988) and another that allows grid pixels to be subdivided into triangular facets, thus allowing numerous flow directions and hence greater accuracy, referred to as D-infinity (Tarboton 1997). In the modeling platform 'NetMap' (Miller et al. 2002, Benda et al. 2007) used in WIP, the D-infinity algorithm is used in non-channelized environments and after channel heads are defined, the D-8 algorithm is used (Miller et al. 2015). Channel heads in NetMap are defined using four physical parameters including drainage area per unit contour length (Montgomery and Dietrich 1989), hillslope gradient, planform curvature, and a minimum flow length for which all criteria are met (Clarke et al. 2008).

The raw DEM is subtracted from the filled DEM to create the closed depression grids. Elevation of the original DEM pixels (prior to filling) is subtracted from the elevation of the filled DEM, yielding the absolute depth of the depression, per grid pixel. We assume that the deeper the depression, the higher likelihood that it is closer to the local or regional ground water table, all other things being equal.

To determine locations within a depression that might be the most likely to have higher wetness or wet soils, each grid pixel depth in a depression is divided by the maximum depression pixel depth, resulting in a relative depth of the depression, per pixel (0 to 1). Larger relative depths are equivalent to being deeper and lower in a closed depression. Hence, the suitability index for closed depressions is designed so the largest relative depths (>0.8) are associated with the largest potential for wet soils and wetland formation.

8.3. References

Agrawal, A., Schick, R. S., Bjorkstedt, E. P., Szerlong, R. G., Goslin, M. N., Spence, B. C., Williams, T. H., and Burnett, K. M., 2005, Predicting the potential for historical coho, chinook and steelhead habitat in northern California, NOAA Technical Memorandum NMFS: National Oceanic and Atmospheric Administration.

Atha, J. B., 2013, Fluvial wood presence and dynamics over a thirty year interval in forested watersheds [PhD: University of Oregon, 161 p.

Barnes, R., Lehman, C., and Mulla, D., 2014a, An efficient assignment of drainage direction over flat surfaces in raster digital elevation models: Computers & Geosciences, v. 62, p. 128-135.

-, 2014b, Priority-flood: An optimal deprression-filling and watershed-labeling algorithm for digital elevation models: Computers & Geosciences, v. 62, p. 117-127.

Benda, L., Miller, D. J., Andras, K., Bigelow, P., Reeves, G. H., and Michael, D., 2007, NetMap: A new tool in support of watershed science and resource management: Forest Science, v. 53, no. 2, p. 206-219.

Benda, L., Miller, D. J., Sias, J., Martin, D., Bilby, R. E., Veldhuisen, C., and Dunne, T., 2003, Wood recruitment processes and wood budgeting, in Gregory, S. V., Boyer, K. L., and Gurnell, A. M., eds., the Ecology and Management of Wood in World Rivers, Volume Symposium 37: Bethesda, Maryland, American Fisheries Society, p. 49-73.

Benda, L. E., and Dunne, T., 1997a, Stochastic forcing of sediment routing and storage in channel networks: Water Resources Research, v. 33, no. 12, p. 2865-2880.

-, 1997b, Stochastic forcing of sediment supply to channel networks from landsliding and debris flow: Water Resources Research, v. 33, no. 12, p. 2849-2863.

Benda, L. E., Miller, D. J., and Barquin, J., 2011, Creating a catchment scale perspective for river restoration: Hydrology and Earth System Science, v. 15.

Benda, L. E., Miller, D. J., Dunne, T., Reeves, G. H., and Agee, J. K., 1998, Dynamic landscape systems, in Naiman, R. J., and Bilby, R. E., eds., River Ecology and Management: New York, Springer-Verlag, p. 261-288.

Bidlack, A. L., Benda, L. E., Miewald, T., Reeves, G. H., and McMahan, G., 2014, Identifying suitable habitat for Chinook salmon across a large, glaciated watershed: Transaction of the American Fisheries Society, v. 143, no. 3, p. 689-699.

Bruno, D., Belmar, O., Sánchez-Fernández, D., and Velasco, J., 2014, Environmental determinants of woody and herbaceous riparian vegetation patterns in a semi-arid mediterranean basin: Hydrobiologia.

Burnett, K. M., and Miller, D. J., 2007, Streamside policies for headwater channels: an example considering debris flows in the Oregon Coastal Province: Forest Science, v. 53, no. 2, p. 239-253.

Burnett, K. M., Miller, D. J., Guritz, R., Meleason, M. A., Vance-Borland, K., Flitcroft, R., Nemeth, M. J., Priest, J., Som, N. A., and Zimmerman, C. E., 2013, 2011 Arctic-Yukon-Kuskokwim Sustainable Salmon Initiative, Landscape Predictors of Coho Salmon.

Burnett, K. M., Reeves, G. H., Miller, D. J., Clarke, S., Vance-Borland, K., and Christiansen, K., 2007, Distribution of salmon-habitat potential relative to landscape characteristics and implications for conservation: Ecological Applications, v. 17, no. 1, p. 66-80.

Busch, D. S., Sheer, M., Burnett, K., McElhany, P., and Cooney, T., 2011, Landscape-level model to predict spawning habitat for Lower Columbia River Fall Chinook Salmon (Oncorhynchus tshawytscha): River Research and Applications.

Byun, J., and Seong, Y. B., 2015, An algorithm to extract more accurate stream longitudianl profiles from unfilled DEMs: Geomorphology, v. 242, p. 38-48.

Chang, S., 2007, Extracting skeletons from distance maps: International Journal of Computer Science and Network Security, v. 7, no. 7, p. 213-219.

Clarke, S. E., Burnett, K. M., and Miller, D. J., 2008, Modeling streams and hydrogeomorphic attributes in Oregon from digital and field data: Journal of the American Water Resources Association, v. 44, no. 2, p. 459-477.

Dunne, T., 1980, Formation and controls of channel networks: Progress in Physical Geography, v. 4, p. 211.

Fernández, D., Barquín, J., Álvarez-Cabria, and Peñas, F. J., 2012a, Quantifying the performance of automated GIS-based geomorphological approaches for riparian zone delineation using digital elevation models: Hydrology and Earth System Sciences, v. 16, p. 3951-3862.

Fernández, D., Barquín, J., Álvarez-Cabria, M., and Peñas, F. J., 2012b, Delineating riparian zones for entire river networks using geomorphological criteria: Hydrology and Earth System Sciences, v. 9, p. 4045-4071.

Flitcroft, R., Burnett, K., Snyder, J., Reeves, G., and Ganio, L., 2014, Riverscape patterns among years of juvenile coho salmon in midcoastal Oregon: implications for conservation: Transaction of the American Fisheries Society, v. 143, no. 1, p. 26-38.

Garbrecht, J., and Martz, L. W., 1997, The assignment of drainage direction over flat surfaces in raster digital elevation models: Journal of Hydrology, v. 193, p. 204-213.

Heidemann, H. K., 2014, Lidar base specification (ver. 1.2, November 2014), U.S. Geological Survey Techniques and Methods, Book 11, p. 67.

Hofmeister, R. J., and Miller, D. J., 2003, GIS-based modeling of debris-flow initiation, transport and deposition zones for regional hazard assessments in western, Oregon, USA, in Reickenmann, and Chen, eds., Debris-Flow Hazards Mitigation: Mechanics, Prediction, and Assessment: Rotterdam, Millpress, p. 1141-1149.

Hofmeister, R. J., Miller, D. J., Mills, K. A., Hinkle, J. C., and Beier, A. E., 2002, Hazard map of potential rapidly moving landslides in western Oregon, Interpretive Map Series - 22: Oregon Department of Geology and Mineral Industries.

Imaizumi, F., Hattanji, T., and Hayakawa, Y. S., 2010, Channel initiation by surface and subsurface flows in a steep catchment of the Akaishi Mountains, Japan: Geomorphology, v. 115, p. 32-42.

Jenson, S. K., and Domingue, J. O., 1988, Extracting topographic structure from digital elevation data for geographic information system analysis: Photogrammetric Engineering and Remote Sensing, v. 54, no. 11, p. 1593-1600.

Kaiser, B., Ducey, C., and Wickwire, D., 2010, The Oregon LiDAR Hydrography Pilot Project, Evaluation of Existing GIS Hydrological Toolsets for Modeling Stream Networks with LiDAR and Updating the National Hydrography Datset (NHD).

McCleary, R. J., Hassan, M. A., Miller, D., and Moore, R. D., 2011, Spatial organization of process domains in headwater drainage basins of a glaciated foothills region with complex longitudinal profiles: Water Resources Research, v. 47, no. W05505.

Miller, D. J., 2003, Programs for DEM Analysis, Landscape Dynamics and Forest Management, General Technical Report RMRS-GTR-101CD: Fort Collins, CO, USA, USDA Forest Service, Rocky Mountain Research Station.

Miller, D. J., and Burnett, K. M., 2008, A probabilistic model of debris-flow delivery to stream channels, demonstrated for the Coast Range of Oregon, USA: Geomorphology, v. 94, p. 184-205.

Miller, D., L. Benda, J. DePasquale and D. Albert. 2015. Creation of a digital flowline network from IfSAR 5-m DEMs for the Matanuska-Susitna Basins: a resource for NHD updates in Alaska. Report to The Nature Conservancy, Juneau, Alaska. 32pp.

Montgomery, D. R., and Foufoula-Georgiou, E., 1993, Channel network source representation using digital elevation models: Water Resources Research, v. 29, no. 12, p. 3925-3934.

Pelletier, J. D., 2013, A robust, two-parameter method for the extraction of drainage networks from high-resolution digital elevation models (DEMS): Evaluation using synthetic and real-world DEMS: Water Resources Research, v. 49, p. 15.

Peñas, F. J., Barquín, J., Snelder, T. H., Booker, D. J., and Álvarez, C., 2014, The influence of methodological procedures on hydrological classification performance: Hydrol. Earth Syst. Sci., v. 18, p. 3393-3409.

Peñas, F. J., Fernández, F., Calvo, M., Barquín, J., and Pedraz, L., 2011, Influence of data sources and processing methods on theoretical river network quality: Limnetica, v. 30, no. 2, p. 197-216.

Pirotti, F., and Tarolli, P., 2010, Suitability of LiDAR point density and derived landform curvature maps for channel network extraction: Hydrological Processes, v. 24, p. 1187-1197.

Poggio, L., and Soille, P., 2012, Influence of pit removal methods on river network position: Hydrological Processes, v. 26, p. 1984-1990.

Poppenga, S. K., Gesch, D. B., and Worstell, B. B., 2013, Hydrography change detection: the usefulness of surface channels derived from lidar dems for updating mapped hydrography: Journal of the American Water Resources Association, v. 49, no. 2, p. 371-389.

Qin, C.-Z., Bao, L.-L., Zhu, A.-X., Hu, X.-M., and Qin, B., 2013, Artificial surfaces simulating complex terrain types for evaluating grid-based flow direction algorithms: International Journal Geographical Information Science, v. 27, no. 6, p. 1055-1072.

Sheer, M. B., and Steel, E. A., 2006, Lost watersheds: barriers, aquatic habitat connectivity, and salmon persistence in the Willamette and Lower Columbia river basins: Transactions of the American Fisheries Society, v. 135, p. 1645-1669.

Shi, X., Zhu, A.-X., Burt, J., Choi, W., Wang, R., Pei, T., Li, B., and Qin, C., 2007, An experiment using a circular neighborhood to calculate slope gradient from a DEM: Photogrammetric Engineering & Remote Sensing, v. 73, no. 2, p. 143-154.

Sofia, G., Tarolli, P., Cazorzi, F., and Fontana, G. D., 2011, An objective approach for feature extractions: distribution analysis and statistical descriptors for scale choice and channel network identification: Hydrol. Earth Syst. Sci., v. 15, p. 1387-1402.

Soille, P., Vogt, J., and Colombo, R., 2003, Carving and adaptive drainage enforcement of grid digital elevation models: Water Resources Research, v. 39, no. 12.

Sorensen, R., Zinko, U., and Seibert, J., 2006, On the calculation of the topographic wetness index: evaluation of different methods based on field observations: Hydrology and Earth System Sciences, v. 10, p. 101-112.

Steel, E. A., Feist, B. E., Jensen, D. W., Pess, G. R., Sheer, M. B., Brauner, J. B., and Bilby, R. E., 2004, Landscape models to understand steelhead (Oncorhynchusmykiss) distribution and help prioritize barrier removals in the Willamette basin, Oregon, USA: Canadian Journal of Fisheries and Aquatic Science, v. 61, p. 999-1011.

Steel, E. A., Fullerton, A., Caras, Y., Sheer, M. B., Olson, P., Jensen, D. W., Burke, J., Maher, M., and McElhany, P., 2008, A spatially explicit decision support system for watershed-scale management of salmon: Ecology and Society, v. 13, no. 2, p. 50.

Strahler, A. N., 1957, Quantitative analysis of watershed geomorphology: Transactions, American Geophysical Union, v. 38, no. 6, p. 913-920.

Tarboton, D. G., 1997, A new method for the determination of flow directions and upslope areas in grid digital elevation models: Water Resources Research, v. 33, no. 2, p. 309-319.

USDA Forest Service, 2003, Landscape dynamics and forest management: U.S. Department of Agriculture, Forest Service, Rocky Mountain Research Station, General Technical Report RMRS-GTR-101CD.

Wilson, J. P., Aggett, G., Yongxin, D., and Lam, C. S., 2008, Water in the landscape: a review of contemporay flow routing algorithms, in Zhou, Q., Lees, B., and Tang, G.-a., eds., Advances in digital terrain analysis: Berlin, Springer, p. 213-236.

Wilson, J. P., Lam, C. S., and Deng, Y., 2007, Comparison of the performance fo flow-routing algorithms used in GIS-based hydrologic analysis: Hydrological Processes, v. 21, p. 1026-1044.

Zevenbergen, L. W., and Thorne, C. R., 1987, Quantitative analysis of land surface topography: Earth Surface Processes and Landforms, v. 12, p. 47-56.